Texture Classification on Uneven Surfaces Using Deep Learning Techniques

by

Maliheh Marzani

A Dissertation Presented to the

DEPARTMENT OF COMPUTER SCIENCE

and the

FACULTY OF GRADUATE STUDIES OF LAKEHEAD UNIVERSITY

In Partial Fulfillment of the

Requirements for the Degree of

MASTER OF COMPUTER SCIENCE

(SPECIALIZATION IN ARTIFICIAL INTELLIGENCE)

Aug 2024

Abstract

Robots are increasingly essential in various fields, excelling in tasks from routine operations to hazardous situations. Enhancing robots with human-like capabilities, such as tactile sensing, broadens their potential applications. Tactile sensors enable robots to perceive and interact with their environment similarly to humans. This research focuses on leveraging tactile sensors to classify textures on uneven surfaces, an area previously unexplored in the literature. By collecting data points along predefined paths on object surfaces, we minimized assumptions about the object's geometry, making the system more flexible and adaptable. These data points guided the robot's trajectory, during which tactile data were systematically gathered on the surface of uneven objects, marking a pioneering effort in this area.

To improve texture classification and reduce processing time, we employed a sliding window approach, segmenting the dataset into smaller overlapping windows for multi-scale analysis. In addition to data from uneven surfaces, we supplemented our dataset with tactile data from even surfaces from another study. We applied advanced deep learning models, including convolutional neural networks (1D CNN), recurrent neural networks (bidirectional LSTM), and hybrid architectures, to classify tactile textures using time-series data. The models achieved average accuracy, precision, and recall rates of 92.3%, 92.4%, and 92.3% for uneven surfaces, and 96.9%, 97.0%, and 97.0% for even surfaces.

This study demonstrates the importance of tactile sensing in robotic systems, particularly for texture classification on uneven surfaces. By incorporating MARG and barometer sensors into the Open Manipulator X, this research advances tactile perception in robotics, equipping robots to interact more effectively with diverse environments. The findings set the stage for future applications where precise tactile perception is essential.

Acknowledgments

I would like to express my heartfelt gratitude to those who have supported and guided me throughout the journey of this thesis.

Firstly, I am deeply appreciative of my supervisor, Dr. Thiago E. Alves de Oliveira, whose exceptional academic support and insightful guidance have been instrumental in the completion of this work. Dr. Thiago's profound understanding of my research and his unwavering encouragement have not only shaped the direction of this study but have also been a source of inspiration throughout this process.

I am profoundly grateful to my beloved husband, Benyamin, for his boundless patience, encouragement, and belief in my abilities. His steadfast support has been a pillar of strength and motivation, making this journey all the more manageable. To my parents, sister, and brother, I extend my heartfelt thanks for their boundless support and understanding. Although they are far away, their love and encouragement have been a constant source of motivation. Their sacrifices and support have played a vital role in my achievements, and I am forever grateful for their presence in my life.

I also wish to acknowledge the faculty and staff of Lakehead University, particularly those in the Computer Science department, for their invaluable contributions to my academic journey. Their dedication and support have significantly enhanced my educational experience. Finally, I am grateful to the Vector Institute for selecting me from a highly competitive pool of candidates and providing crucial support and generous scholarship for my research.

The successful completion of this thesis is a testament to the collective support and encouragement from all these remarkable individuals. I am deeply thankful for each of their contributions.

With deepest gratitude,

Maliheh

Table of Contents

List of Tables

List of Figures

List of Abbreviations

3D	Three-Dimensional
3DGS	Three-Dimensional-Geometric-Scanning
1D CNN	One-Dimensional Convolutional Neural Network
Acc	Accuracy
AL	Active Learning
BiLSTM	Bidirectional Long Short-Term Memory
CNN	Convolutional Neural Network
CSV	Comma-Separated Values
D-CNN	Deep Convolutional Neural Network
EEG	Electroencephalography
FEM	Finite Element Method
GAN	Generative Adversarial Network
GPU	Graphics Processing Unit
ICP	Iterative Closest Point
IMU	Inertial Measurement Unit
LiDAR	Light Detection and Ranging
LSTM	Long Short-Term Memory
MARG	Magnetic, Angular Rate, and Gravity
MEMS	Micro-Electro-Mechanical Systems
MLP	Multilayer Perceptron
ReLU	Rectified Linear Unit
RGB	Red, Green, Blue
TouchSDF	Touch Surface Distance Field

Chapter 1

Introduction

Robotic interaction with the environment plays a pivotal role in enabling robots to perform various tasks autonomously and effectively [1]. For robots to operate effectively and safely, they need a sophisticated understanding of their surroundings. Also, When it comes to tackling complex tasks, the collaboration between humans and robots is indispensable. This collaboration combines the precision and repeatability of automation with the adaptability and decision-making capabilities of human operators [2], [3]. For robots to interact with humans safely, it is vital that they perform actions securely, which heavily relies on their keen perception of the environment. This capability underscores the critical importance of ensuring safety and efficiency in various industries [4].

The safe and efficient operation of robots heavily depends on the perception capabilities enabled by the sensors. Sensors act as the robot's "eyes, ears and tactile sensation," [5], [6], [7] providing crucial data about the environment, including object properties, spatial relationships, and external conditions hat guides robots in navigating, manipulating objects, and interacting with their environment.

One specific type of sensor, the tactile sensor, plays a particularly critical role in robot manipulation tasks [8]. Tactile sensors mimic the human sense of touch, enabling robots to perceive object properties like texture, shape, temperature, and compliance through physical contact [9]. This information is invaluable for robots to perform tasks requiring delicate manipulation, such as assembling intricate components or handling fragile objects.

However, while vision sensors are widely used for environmental perception, they have limitations. Factors like lighting variations, occlusions, and limited depth perception can significantly hinder the effectiveness of vision-based approaches. For instance, a robot relying solely on vision might struggle to distinguish a dark object from a shadow in a poorly lit environment. Moreover, vision-based approaches may struggle with occluded or cluttered environments, where objects are partially or fully obstructed from view.

Unlike vision-based approaches, tactile sensing is less susceptible to environmental factors such as lighting conditions, making it particularly useful in diverse and unpredictable environments. Therefore, while vision plays a significant role in robot-environment interaction [10], its limitations necessitate the exploration of complementary solutions. Tactile sensors offer a valuable alternative, providing information about the physical properties of objects that vision alone cannot capture. for example, By analyzing tactile signals, robots equipped with tactile sensors can discern subtle differences between textures that may not be easily distinguishable through vision alone [11]. Additionally, tactile sensing can enhance vision-based approaches, as both modalities can be combined to achieve a more comprehensive understanding of the environment [12].

One notable advantage of tactile sensors is their ability to gather data essential for texture classification, which is pivotal for dexterous robot manipulation [13]. This capability enables robots to distinguish between different surface textures for various applications such as object recognition, manipulation, and navigation. As robots are increasingly tasked with manipulating objects in real-world environments, one crucial aspect of successful manipulation is the ability to distinguish between different textures [14]. This information plays a vital role in tasks like grasping objects securely, differentiating delicate items from sturdy ones, or even identifying objects based solely on their surface feel.

Tactile sensors capture information about surface roughness, friction, and other tactile properties through contact with objects, offering rich data that can be utilized for texture classification tasks [15], [16]. Mimicking the human sense of touch, tactile sensors provide

robots with the ability to perceive object properties through physical contact. These sensors measure various physical parameters like pressure, vibration, and temperature, creating a rich dataset that allows robots to "feel" the texture of an object.

Recognizing textures on uneven surfaces remains a significant challenge in the field of tactile perception. Despite advancements in robotic sensing technologies, accurately classifying textures on irregular surfaces is still an open problem. This challenge serves as the primary motivation for this work. In the following sections, I will discuss my approach to utilizing tactile sensors to address this issue and outline the structure of the research framework. The approach involves innovative techniques for collecting and processing tactile data, enabling more precise texture classification even on complex surfaces. Subsequently, I will delve deeper into each aspect of this methodology in the subsequent chapters, providing a comprehensive overview of the research conducted and the solutions proposed to overcome the identified challenges.

1.1 Objectives

Addressing the ongoing challenge in tactile perception, particularly the accurate recognition of textures on uneven surfaces, this research introduces a novel method for classifying tactile textures by meticulously collecting tactile data from such surfaces. The objective is to empower the robot to classify textures on uneven surfaces encountered without prior knowledge of their shapes, mirroring human tactile exploration performed with eyes closed. By collecting data points along predefined paths, the robot sequentially probes different points on the object's surface, dynamically adapting to its complex geometry. This approach minimizes assumptions about the object's shape, allowing the robot to establish a trajectory based on the collected data points. Tactile data is then gathered systematically during these trajectories, providing the comprehensive and detailed information needed for accurate texture recognition.

To achieve our primary goal of texture recognition on uneven surfaces, we first needed to address the absence of tactile texture datasets for such surfaces. To this end, we focused on collecting and analyzing tactile data specifically from uneven surfaces and then developing tactile texture classification models based on that data. Our structured approach is outlined below:

1. **Developing a Strategy for Robotic Tactile Data Acquisition:**

   The first challenge addressed in this work was the lack of existing methods in the literature for effectively collecting tactile data on uneven surfaces. Traditional approaches primarily focused on even surfaces, leaving a significant gap in robotic tactile perception for more complex, uneven environments. Our approach is therefore crucial as it enables the collection of tactile data from such challenging surfaces, paving the way for more sophisticated robotic exploration and interaction. We began by designing a method to capture tactile data from the surfaces of various uneven objects. This process involved recording both the position and the normal vector at each point of contact during robotic exploration. These data points serve as waypoints, which are essential for planning exploratory trajectories that guide the robot across the object's surface. By following these trajectories, the robot ensures comprehensive and accurate data collection, critical for subsequent texture analysis. To ensure the reliability of our approach before real-world implementation, we developed a simulation environment. This simulated testing phase allowed us to validate and refine our strategies in a controlled setting, thereby minimizing the risks and inefficiencies associated with direct physical testing. The advantages of this approach include saving time, reducing resource consumption, and providing a safer platform for initial experiments.

2. **Establishing a Tactile Texture Dataset for Uneven Surfaces:**

   In the second phase of this research, we addressed another significant gap in the literature—the absence of tactile texture datasets for uneven surfaces. While datasets

for even surfaces exist, there was no prior work on systematically collecting and curating data for uneven surfaces. Our contribution in this area marks a pioneering effort in the field. For data acquisition, we utilized a combination of MARG (Magnetic, Angular-Rate, Gravity) and barometer sensors. These sensors provided a comprehensive dataset with 10 distinct features, including 3-axis magnetic, 3-axis angular velocity, 3-axis gravity readings, and one barometer reading. We collected data across 25 trajectories for each of the 12 different textures, resulting in a total of 300 samples. The raw data underwent a preprocessing pipeline that included an overlapping sliding window technique with a configurable window size. This method was carefully chosen to balance the need for diversity in the dataset with the computational efficiency required for machine learning. The resulting preprocessed data were scaled using a Min-Max scaler, preparing it for input into machine learning models.

3. **Developing Deep Learning Models for Tactile Texture Classification on Uneven Surfaces:**

   In the final phase, we focused on developing deep learning models capable of classifying tactile textures on uneven surfaces. We employed advanced architectures including convolutional neural networks (CNNs), recurrent neural networks (RNNs), and hybrid models that integrate both CNNs and RNNs. These models are specifically tailored to capture local features and temporal dependencies inherent in time-series tactile data. The deep learning models were trained on the tactile texture dataset collected from uneven surfaces, with the expectation that their robustness would extend to even surfaces as well. This dual application not only demonstrates the versatility of the models but also ensures their effectiveness across different surface conditions.

We began by designing a simulation environment to rigorously test and refine our data collection strategies, ensuring robustness and efficiency before applying them in real-world scenarios. Following successful validation in simulation, these strategies were implemented

on a robotic system to gather tactile data, resulting in the creation of a new dataset specifically for tactile textures on uneven surfaces. The simulated environment allows for safe and controlled testing of data collection and trajectory methods. However, it is important to note that simulation has limitations, particularly in texture classification. This is because simulations cannot perfectly replicate the intricate physical properties and variability of real-world textures, such as subtle surface roughness and material differences. Consequently, while simulations are used to develop and test the waypoints collection processes and trajectory methods, the actual texture classification model will be based on data collected from real-world experiments.

Overall, The capacity for a robot to discern the texture of objects holds significant utility across diverse applications and industries, mirroring the perceptual capabilities of humans. By enabling robots to recognize object textures akin to human tactile discernment, their integration within workplaces and various environments can be substantially broadened. My research endeavors focus on the texture classification of uneven surfaces by employing a robot, specifically the Open Manipulator X in this instance, in conjunction with a tactile sensing module. This module comprises a Multi-Axis Gyroscope Accelerometer (MARG) sensor and a barometer sensor.

In conclusion, this work represents a significant advancement in tactile perception for robotics, addressing critical gaps in both data collection and texture classification on uneven surfaces. Through the development of novel strategies to execute carefully planned trajectories to collect tactile data, the creation of a new tactile dataset on uneven surfaces, and the implementation of sophisticated deep learning models for such dataset, we have laid the groundwork for more effective and versatile robotic systems capable of navigating and interacting with complex environments.

1.2 Dissertation Structure

The dissertation is structured with the following chapters:

- **Chapter 1: Introduction** - This chapter serves as a foundational cornerstone for the entire dissertation. It begins by articulating the problem statement, offering clarity on the research objectives, and providing a comprehensive overview of how the dissertation is structured and organized.

- **Chapter 2: Literature review** - This chapter surveys recent advancements in areas such as robotic tactile sensing, manipulation, surface reconstruction, and texture classification. It also discusses the role of robotics in simulation.

- **Chapter 3: Methodology** - This chapter details the research methods employed, including techniques for blind tactile data collection for texture classification, along with other experimental procedures conducted in both simulation and real-world environments.

- **Chapter 5: Results and Discussions** - In this section, the culmination of the research endeavors is unveiled, showcasing the outcomes stemming from the detailed process of tactile data collection for texture classification. Through meticulous analysis of this specialized dataset, significant insights and patterns have been unearthed, providing valuable contributions to the field of robotics.

- **Chapter 6: Conclusion** - This section encapsulates the key findings and implications of the study, offering a comprehensive synthesis of the research outcomes. It highlights the significance of the approach in advancing texture classification in robotics and underscores avenues for future exploration and innovation in this area.

Chapter 2

Literature Review

Robotic tactile sensing, mimicking the human sense of touch, has emerged as a critical area of research in robotics, enabling robots to interact intelligently with their environment. Recent developments in tactile sensing have seen significant progress, driven by advancements in sensor technology. Traditional tactile sensors, such as pressure sensors and force/torque sensors [17], [18], have evolved to encompass more sophisticated capabilities, including multimodal sensing and compliance. Bio-inspired tactile sensors [19], drawing inspiration from biological systems, offer enhanced sensitivity and adaptability, enabling robots to perceive and manipulate objects with greater dexterity.

Recent research in the field of robotic perception has highlighted several key areas of focus, including the integration of tactile sensing into robotic systems, its diverse applications, and the challenges and future directions it presents. These explorations uncover a vibrant panorama of advancements and innovations driving the field onward, each area briefly touched upon to provide a comprehensive overview.

Researchers have employed various methodologies and techniques to integrate tactile sensing into robotic systems effectively. One common approach involves embedding tactile sensors on robotic end effectors or grippers, allowing robots to perceive and manipulate objects with precision [20], [21]. Additionally, advances in sensor fusion techniques, combining data from multiple sensor modalities, have enhanced the richness and reliability of tactile information [22]. Furthermore, tactile sensor data can be merged with visual sensor data,

enabling robots to gain a more comprehensive understanding of their surroundings and further enhancing their manipulation capabilities [23]. A notable technique in this context is the use of a tactile probe equipped with a 9-DOF MEMS MARG (Magnetic, Angular Rate, and Gravity) system and a MEMS pressure sensor, as described in [24]. This setup allows for the collection of tactile data through a sliding motion performed by a robotic finger. The data is then analyzed using multiscale principal components analysis and classified with a multilayer neural network.

Another innovative approach involves a data-driven analysis for sensor selection in contour following for shape discrimination tasks, as discussed in [25]. This method involves a 4-DOF robotic finger performing sliding movements over synthetic shapes with different fingertip materials. Data from the motors, inertial measurement unit, and magnetometer is analyzed using principal component analysis (PCA) and a multilayer perceptron (MLP) neural network. The study demonstrates how different sensors perform under varying conditions, noting the robustness of the magnetometer in both rigid and soft fingertip scenarios. Additionally, a comprehensive approach to tactile object recognition involving signal processing and mechatronics solutions is discussed in [26]. This paper presents methods for recognizing objects from tactile displacement profiles using force-sensing transducers and for recognizing textures through a rubbing motion executed by a robotic finger equipped with a dynamic tactile fingertip. Neural network solutions are employed for intelligent recognition of symbols, such as embossed numbers and letters, and different texture profiles. The techniques described demonstrate significant advances in the integration of tactile sensing with robotic systems for enhanced object and texture recognition.

Robotic tactile sensing finds applications across a wide range of domains, from manufacturing and healthcare to search and rescue operations.

In manufacturing, tactile sensing enables robots to perform delicate assembly tasks with high precision and reliability. Force and tactile sensors gauge pressure, force, or vibrations, aiding robots in assessing the intensity of their grip or pressure exertion on an object. In

intricate tasks, these sensors enable robots to apply precise pressure, ensuring components remain undamaged throughout the process. In [27] the authors introduce a tactile sensing solution utilizing a MEMS pressure sensor array. This innovative sensor provides precise measurements of force and contact pressure, resembling a soft and human-like touch. It finds applications in handling delicate objects, enhancing prosthetic tactile perception, and improving human-robot interactions, as demonstrated in a collaborative robot work scenario.

In healthcare, tactile sensors are used in robotic prosthetics and exoskeletons to provide feedback to users, enhancing mobility and dexterity. In this article, [28] underscores the significance of tactile sensors in healthcare robotics. These sensors offer crucial feedback on touch, force, and contact interactions, empowering robots to operate safely and efficiently in medical environments. Additionally, [29] presents a study on using a multimodal tactile sensor for heart rate detection. The sensor, combined with a Z-score based peak detection algorithm, demonstrated accurate heart rate measurements comparable to commercial wrist monitors, highlighting the potential of tactile sensors in monitoring vital signs. Furthermore, [30] introduces a miniaturized multimodal tactile sensor emulating the four main mechanoreceptors of human skin for heart rate detection. The study showed that the tactile sensors provided similar heart rate measurements to a wrist monitor in 80% of cases, emphasizing the sensor's reliability and the growing importance of tactile systems in bio-inspired robotics and prosthetics.

In search and rescue operations, robots equipped with tactile sensors can navigate complex environments and detect objects or survivors in hazardous conditions. This article [31] discusses the importance of safe physical interaction between humans and robots in shared workspaces, highlighting the necessity of monitoring contact forces. It introduces a pressure-sensitive skin technology that can be customized to fit complex robot geometries and provides accurate contact measurements across the robot's entire body. This sensitive skin is designed with integrated cushioning elements to mitigate the risk of injuries during physical human-robot interactions. In addition to safety functions, the sensitive skin enables

touch-based robot motion control, thereby simplifying human-robot interaction.

The study described in [24] further exemplifies the application of tactile sensing in robotics. It focuses on surface profile recognition through a sliding motion of a robot finger equipped with a tactile probe. By employing multiscale principal components analysis and a multilayer neural network for classification, the method achieves high accuracy in distinguishing between different surface profiles. This approach is particularly useful for tasks that require precise surface recognition, such as quality control in manufacturing and robotic exploration in unstructured environments. Another significant application is in the selection of sensors for contour following in shape discrimination tasks, as outlined in [25]. This research demonstrates the effectiveness of using a robotic finger with different fingertip materials to explore synthetic shapes. The data collected from various sensors, including the magnetometer, is analyzed to determine the best sensor configuration for different conditions. This approach can be particularly beneficial in applications where precise shape recognition is crucial, such as in automated quality control systems and robotic surgery. the integration of signal processing and mechatronics solutions for tactile object recognition, as discussed in [26], shows the potential of advanced tactile sensing systems in various applications. The paper describes the use of neural networks for recognizing symbols and textures through dynamic exploration by a robotic finger. These techniques can significantly enhance the capability of robots to identify and manipulate objects in unstructured environments, making them suitable for a wide range of industrial and domestic applications. Robots are expected to recognize object properties for safe and efficient handling in various applications such as healthcare, manufacturing, and high-risk environments. A novel bio-inspired tactile probe has been developed, comprising a 9-DOF MEMS MARG system and a deep MEMS pressure sensor embedded in a compliant structure mimicking human skin's mechanoreceptors and hardness [32].

Two experiments evaluated the module: first, using a linear motion carriage to slide over grating patterns, demonstrating the module's frequency detection accuracy. Second, employ-

ing a robotic finger to perform sliding motions over the same patterns, mimicking human exploratory movements. Data from the robotic finger setup enabled surface classification using multiscale principal components analysis and a multilayer neural network, achieving accuracies from 85.1% to 98.9%. This demonstrates the effectiveness of traditional MEMS sensors embedded in flexible substrates for tactile sensing applications.

Despite significant advancements, several challenges remain in the field of robotic tactile sensing. One key challenge is the integration of tactile sensing with other sensory modalities, such as vision and proprioception, to enable robots to perceive and interact with their environment holistically. Additionally, improving the robustness and adaptability of tactile sensing systems to varying environmental conditions and surface textures is essential for real-world applications. Future research directions may focus on developing novel sensor materials, innovative sensing modalities, and advanced data processing techniques to address these challenges and unlock the full potential of robotic tactile sensing.

Tactile perception involves the intricate process of interpreting and representing touch sensing information to discern object properties. Indeed, in the realm of sensory perception, touch often proves superior to vision and hearing in analyzing object characteristics [33]. This superiority mirrors the capabilities observed in human sensory experiences. While vision has traditionally been a favored method for recognizing object materials [34], it has limitations; it can only identify previously known surface materials and lacks the capability to estimate physical parameters independently. Consequently, the integration of touch sensing becomes imperative for effectively identifying material properties [35].

Tactile information is rich and multifaceted, providing valuable insights into various aspects of an object's nature. Alongside shape and material properties [36], tactile sensors can capture additional data such as object pose [37], temperature [38], and vibration patterns [39].

This wealth of information can be harnessed for a myriad of purposes in robotics, including but not limited to:

1. **Grasp Control and Stability:** Tactile feedback plays a crucial role in optimizing both grasp control and stability. By continuously monitoring tactile data, the robot can adjust its grip strength and positioning in real-time, ensuring precise and adaptive grasping actions. This capability is particularly important for handling delicate or irregularly shaped objects. Tactile sensors provide essential information on the force distribution across the contact points, allowing the robot to assess and refine its grip to prevent slippage and maintain object integrity. The integration of tactile feedback into grasp stability assessments enables the robot to dynamically adapt its hold based on the surface contours and material properties of the object. This ensures that the robot can securely manipulate objects without compromising stability, thereby enhancing overall task performance.

2. **Slippage detection and prevention:** Effective manipulation requires the ability to detect and respond to slippage during tasks. Tactile sensors enable the robot to monitor variations in feedback from the object's surface, identifying early signs of slippage. By analyzing these changes, the robot can implement corrective actions, such as adjusting the grip force or repositioning its grasp, to prevent objects from slipping or falling. This proactive approach ensures secure handling, which is crucial for tasks involving fragile or valuable items.

3. **Object manipulation and manipulation planning:** Tactile feedback also plays a significant role in guiding complex manipulation tasks. It informs the robot's planning algorithms by providing real-time data on how objects interact with its end-effector. This information enables the robot to execute tasks with greater dexterity and precision, adapting its actions based on the dynamic conditions of the environment. Enhanced manipulation planning, driven by tactile feedback, allows the robot to perform intricate operations effectively, improving its ability to operate in diverse and changing conditions.

4. **Surface Reconstruction:** The capability to reconstruct uneven surfaces is essential for effective tactile sensing and manipulation. Surface reconstruction involves mapping the geometric and topological features of an object, which facilitates accurate tactile data collection and subsequent texture classification. This process is crucial for dealing with irregular or complex surfaces where traditional methods fall short. By employing advanced reconstruction techniques, the robot can gain a detailed understanding of an object's surface, enabling more precise manipulation and interaction.

5. **Texture recognition:** Advanced tactile sensors are capable of discerning subtle surface textures, which allows the robot to identify and differentiate between various materials or surface finishes. This ability to recognize and classify textures based on tactile input is vital for applications requiring material-specific interactions or quality control. By integrating texture recognition with other sensory data, the robot can make more informed decisions about how to handle and interact with different surfaces.

By leveraging the wealth of tactile information available, robots can achieve greater autonomy, adaptability, and efficiency in interacting with their surroundings, ultimately advancing the field of robotics and expanding the scope of applications for robotic systems.

In conclusion, the literature on advancements in robotic tactile sensing reflects a rich tapestry of research endeavors aimed at expanding robots' perceptual and manipulative capabilities. From the integration of traditional tactile sensors to the exploration of cutting-edge multimodal and bio-inspired sensing techniques, researchers have demonstrated a commitment to pushing the boundaries of what is possible in robotic interaction with the physical world. Through meticulous experimentation and innovative design, these studies have laid a solid foundation for future advancements in the field, promising even greater strides in robotic manipulation and interaction in the years to come.

2.1 Robotic Manipulation

Robot manipulation encompasses a broad spectrum of tasks where robots interact with objects in their environment. These tasks can range from simple pick-and-place operations [40] to more complex actions requiring dexterous manipulation [41], fine motor control [42], and precise insertion maneuvers [43]. In robot manipulation, the robot's end-effector, such as a gripper or robotic arm, is used to grasp, move, and manipulate objects according to predefined instructions or autonomously learned behaviors.

Robot manipulation has applications across industries, including manufacturing, logistics, healthcare, and household assistance, where robots can perform repetitive or dangerous tasks with precision and efficiency.

To execute tasks effectively, particularly those involving handling unfamiliar objects, robots must assess the state and characteristics of the objects they manipulate. Tactile sensors play a crucial role in acquiring diverse object-level information, either through direct sensor readings or by amalgamating data gathered during physical interactions [44]. Recent studies highlight the benefits of using temporal data from tactile sensors for estimating the orientation of grasped objects, showing that sliding-window sampling and LSTM neural networks significantly improve pose estimation accuracy [44]. Additionally, research emphasizes the integration of tactile sensing with visual systems, akin to the human "What and Where" subsystem, to enhance object pose estimation [45].

Drawing inspiration from human exploration behaviors aimed at discerning object properties [46], robots often rely on sensors to facilitate similar exploratory actions during tasks. Combining tactile sensors and machine learning models can provide valuable information about manipulated objects, particularly in scenarios involving underactuated hands, which adapt to unknown surfaces but introduce challenges in object recognition due to their flexibility and unexpected movements [47].

Incorporating tactile sensing into robot manipulation tasks enhances their capabilities in

various ways, such as object grasping, robotic stabilization, and edge following. Through tactile feedback, robots can better understand their interactions with objects and their environment, leading to more robust and adaptable manipulation behaviors. For example, tactile sensors can provide valuable information about the contact forces and object properties during grasping tasks, enabling the robot to adjust its grip and ensure a secure hold [48], [49], [50]. Additionally, tactile feedback can aid in robotic stabilization, helping the robot maintain balance and stability while interacting with objects or navigating uneven terrain [51]. Moreover, tactile sensing facilitates edge following tasks by enabling the robot to detect and track edges accurately, allowing for precise manipulation and navigation [52].

A new approach to in-hand manipulation using fuzzy controlled teleoperation and a recently proposed multimodal tactile sensor is presented in this article. Real-time grasping experiments were conducted with a fuzzy controlled gripper equipped with a compliant tactile sensor. This approach focused on compliance, stable grasping, and tactile sensing, with a teleoperated thumb performing object rotation while the gripper maintained stability. The consistency of the data from these experiments highlights their utility for in-hand control algorithms [53].

In the realm of robotic manipulation research, visual grasp detection algorithms have proven invaluable for predicting stable grips based on color, shape, and object location, leveraging deep learning techniques [54], [55], [56]. While visual methods excel in rapid object recognition, tactile sensors enhance manipulation precision and deepen the understanding of object properties [48], [57]. Their ability to provide detailed insights into texture, temperature, and geometry complements the rapid object recognition strengths of visual methods. The use of tactile sensors, either on their own or in combination with visual methods, holds promise for significant advancements in robotic manipulation capabilities.

The literature highlights five prominent types of robotic manipulation, each representing advancements in the field and offering distinct advantages and challenges in achieving autonomous, efficient, and reliable manipulation capabilities.

1. **Manipulator Arms with Grippers:** These traditional robotic arms are equipped with specialized grippers designed to grasp and manipulate objects. Tactile sensors can be integrated into these grippers to provide feedback on contact forces, object properties, and grasp stability. Vision systems mounted on the arm or in the environment can aid in object detection, localization, and tracking [58], [59].

2. **Dexterous Robotic Hands:** Advanced robotic hands mimic the dexterity and flexibility of the human hand, allowing for intricate manipulation tasks. Tactile sensing can be extensively distributed over the hand's surface, enabling fine-grained feedback on object properties and facilitating delicate manipulation tasks such as grasping fragile objects or manipulating irregular shapes. Vision systems can complement tactile sensing by providing high-resolution visual feedback for precise object localization and recognition [60], [61], [62].

3. **Soft Robotics:** Soft robotic systems employ flexible materials and compliant structures to achieve versatile and adaptive manipulation capabilities. Tactile sensing in soft robots can be achieved through embedded sensors or deformable materials that change shape upon contact with objects, providing information about object compliance, texture, and shape. Vision systems can be integrated with soft robots to provide environmental awareness and enhance manipulation accuracy [63], [64].

4. **Whole-Body Manipulation:** In addition to arm and hand-based manipulation, some robotic systems employ whole-body manipulation strategies. These systems use the robot's entire body to interact with objects and the environment, often relying on tactile sensing distributed across the robot's surface to provide feedback during manipulation tasks [65].

The integration of tactile sensing with various manipulation approaches, including manipulator arms, dexterous hands, soft robotics, hybrid systems, and whole-body manipulation,

opens up new avenues for advancing robotic manipulation capabilities in diverse applications and environments. Advancements in robotic manipulation extend beyond mechanical enhancements to encompass sophisticated sensory technologies that enable robots to perceive and interact with their environment more effectively. Central to this evolution is the integration of tactile sensing. This sensory feedback is essential for executing precise manipulation tasks, as it allows robots to adjust their actions based on the immediate context of the object they are handling. By incorporating tactile sensors, robots gain a nuanced understanding of the surfaces they interact with, facilitating more accurate and adaptable responses. This enhanced sensory capability is pivotal in bridging the gap between mere mechanical function and intelligent interaction, setting the stage for advanced manipulation techniques that rely on a deep comprehension of both object geometry and texture.

Overall, surface reconstruction and texture recognition are critical for robotic manipulation, as they provide the necessary information for precise interaction with objects in complex environments. Surface reconstruction allows robots to understand and model an object's geometry, essential for tasks requiring accurate navigation and delicate manipulation, such as grasping or applying force without causing damage. Texture recognition, on the other hand, enables robots to differentiate between various surface materials, optimizing grip and movement by adjusting to the nature of the surfaces encountered. In certain scenarios, this capability allows the robot to determine the most reliable surface from which to grasp an object, minimizing the risk of slippage or dropping during manipulation. These processes collectively improve the robot's ability to interact with complex environments, making them indispensable in advanced robotic systems.

2.2 Robotic Surface Reconstruction

Surface reconstruction in robotics involves creating three-dimensional models of object surfaces or environments using sensor data. Surface reconstruction is vital for tasks like object

manipulation, scene understanding and terrains exploration. Traditional methods, like point cloud registration and surface mesh generation, are widely used. Recent advances in depth sensing and machine learning have improved accuracy and efficiency. Current research directions in surface reconstruction is focused on the following areas:

Surface reconstruction techniques draw upon various types of data, including tactile and vision-based sensing modalities, along with other sensory inputs. Vision-based data, such as RGB-D data from sensors like Microsoft Kinect [66], combines color and depth information to provide both visual and geometric data, facilitating surface reconstruction tasks. Tactile sensing offers direct physical interaction with surfaces, capturing detailed information about texture, shape, and material properties, which can complement vision-based data and enhance reconstruction accuracy [67]. Additionally, tactile sensing alone demonstrates significant progress in achieving object reconstruction tasks without additional modalities [68]. LiDAR data generates point clouds representing 3D structures, while pressure sensors measure applied force, aiding in reconstructing deformable surfaces or objects under pressure [69]. Thermal imaging captures temperature information, and acoustic sensors capture sound waves reflecting off surfaces, each providing supplementary data to enrich surface reconstruction processes [70]. By integrating these diverse data sources, surface reconstruction techniques can achieve more accurate and robust reconstructions, benefiting various applications in robotics, computer vision, and beyond.

While visual-tactile fusion offers distinct advantages, methods solely relying on tactile sensors have shown remarkable progress towards achieving accurate surface reconstruction. In [71], the authors discuss the significance of tactile data in reconstructing 3D object shapes and its complementary role alongside vision-based methods. Vision sensors typically offer frontal surface shape representation, while tactile sensors provide detailed shape information essential for stable grasps and interaction tasks. However, tactile reconstruction is sequential and requires aligning acquired contact points to form a consistent tactile point cloud. Challenges include low spatial resolution and managing large data volumes. Exist-

ing methods focus on offline reconstruction using active exploration or probabilistic haptic maps, aiming for real-time applications like grasp planning and object classification. The proposed method combines space partitioning, Kalman filtering, and the iterative closest point (ICP) algorithm for efficient shape reconstruction, demonstrated through autonomous data acquisition with a robotic hand. Tactile sensor-based surface reconstruction holds immense potential for enhancing robotic capabilities, particularly in scenarios where vision limitations exist. Additionally, [72] discusses the utility of tactile sensing arrays in providing detailed surface information, even without vision-based data, underscoring the adequacy of tactile perception in complex environments. The study emphasizes that tactile sensors can accurately capture surface details, essential for robotic manipulation tasks in vision-impaired settings. Moreover, [73] highlights the importance of flexible tactile sensing modules that can adapt to various surface inclinations, enhancing the ability of robots to navigate and interact with unstructured environments. The authors of [74] present a novel method for blind surface reconstruction using a robotic manipulator equipped with the same sensing module of [73]. The approach leverages kinematic data and sensors to estimate contact positions and surface normals, allowing for the reconstruction of larger surfaces with fewer probing attempts. This method outperforms traditional vision systems, especially in unstructured environments where vision systems struggle with transparency, reflections, and occlusions. The experimental validation demonstrates higher accuracy and efficiency, making it suitable for complex, non-flat surfaces.

Development of fast and computationally efficient algorithms is critical for real-time robotic tasks requiring dynamic surface reconstruction based on sensor feedback. Surface reconstruction techniques encompass various methods categorized by their underlying principles and methodologies. Point cloud-based methods [75] utilize 3D point data acquired from sensors like LiDAR or stereo cameras [76], employing algorithms such as Poisson surface reconstruction. Mesh-based techniques [77] represent surfaces through interconnected triangles or polygons, involving processes like surface simplification and refinement. Volumetric

methods [78] depict surfaces as volumetric grids or implicit functions, adept at handling complex geometries and noisy data. Implicit surface reconstruction [79] represents surfaces as zero-level sets of implicit functions, defining them as points where function values remain constant. Deep learning-based methods [80] leverage neural networks, like CNNs or GANs, to directly generate surfaces from input data, showcasing recent advancements. Hybrid approaches [81] integrate multiple techniques, such as combining vision and tactile sensing, to enhance reconstruction accuracy, exploiting the strengths of different methodologies for more robust outcomes. Furthermore, [82] presents a novel approach to haptic surface reconstruction using a compliant tactile sensing module and robotic manipulator. The study demonstrates the effectiveness of this method in accurately reconstructing non-flat surfaces by estimating contact positions and surface normals, thereby addressing challenges posed by traditional vision systems in unstructured environments. Additionally, [73] emphasizes the flexibility of bioinspired tactile sensing modules, which can detect surface inclinations even when the end-effector's orientation is fixed, thus improving the robustness and efficiency of surface reconstruction tasks.

Hybrid approaches combine multiple techniques or modalities, such as combining vision-based and tactile-based sensing for improved reconstruction accuracy. These methods leverage the strengths of different approaches to overcome limitations and achieve more robust reconstructions.

Indeed, while vision-based methods are common in surface reconstruction, tactile sensing has demonstrated superior accuracy across numerous scenarios. Many articles have explored the combination of both modalities, highlighting the complementary nature of tactile sensing in capturing fine surface details and improving reconstruction accuracy. This article [83] proposes Tactile-Informed 3DGS, a method that integrates touch data with multi-view vision to enhance surface reconstruction and novel view synthesis. By optimizing 3D Gaussian primitives at touch points and reducing transmittance, it achieves refined surface reconstruction, particularly beneficial for non-Lambertian objects. Evaluation on glossy and reflective

surfaces shows significant improvements in reconstruction quality, demonstrating the effectiveness of the approach. The other article [69] introduces TouchSDF 2, a novel surface reconstruction algorithm inspired by human tactile perception. It utilizes a new vision-based tactile sensor to reconstruct the surface structure of unfamiliar objects with millimeter-level accuracy. Key techniques include point cloud registration, loop-closure detection with deep learning, and pose graph optimization. TouchSDF 2 enables robots to understand and reconstruct 3D shapes using their sense of touch, both in simulations and the real world. This approach enhances robot manipulation tasks, especially in scenarios where visual methods fail due to occlusion during physical contact.

In summary, current advancements in robotic surface reconstruction have led to more precise and efficient modeling of three-dimensional surfaces. These advancements enhance robotic perception and interaction, with broad applications in autonomous navigation, texture classification, object manipulation, and augmented reality.

2.3 Robotic Texture Classification

Texture classification by robotics involves using tactile sensing to categorize the textures of objects. Robots gather data about surface properties through physical contact, analyzing it with machine learning to differentiate textures like roughness or smoothness [84]. This capability has applications in manufacturing, healthcare, and agriculture, where robots can identify defects, assist in surgeries, or assess soil quality. Challenges include sensor calibration and developing robust classification algorithms. Nonetheless, texture classification enhances robots' abilities across diverse real-world tasks.

Accurately classifying the texture of objects plays a vital role in various robotic recognition and manipulation tasks. From robots sorting objects in warehouses to surgical robots grasping delicate tissues, the ability to perceive and differentiate textures through touch is crucial for safe and effective manipulation.

Recent advancements highlight the importance of combining tactile sensing with machine learning for improved texture classification. Tactile sensing provides essential information that enhances robotic manipulation in unstructured environments where visual feedback alone is insufficient. Research has demonstrated that combining tactile and visual information can address limitations such as occlusions or confined spaces [84]. Additionally, understanding human tactile perception, which involves manipulation, exploration, and response, is crucial for developing effective robotic systems [84].

Further research shows that reproducing human-like dexterous manipulation in robots requires sophisticated tactile sensors to identify textures. Studies have investigated the use of multimodal tactile sensing modules, incorporating pressure, gravity, angular rate, and magnetic field sensors, achieving high classification accuracy rates exceeding 90% [85]. This work emphasizes the need for tactile exploration strategies similar to human touch to enhance texture classification in dynamic settings. The integration of advanced tactile sensors and machine learning methods is essential for improving robotic dexterity and handling in various applications [85]. In recent years, significant advancements have been made in robotic texture classification, driven by the development of sophisticated tactile sensors, powerful machine learning algorithms, and innovative data acquisition techniques.

Advanced Tactile Sensors represent a significant leap in enhancing robotic sensory capabilities, fundamentally transforming how robots interact with their environments. The evolution of these sensors encompasses several key advancements:

1. **Biomimetic Sensors:** Researchers are drawing inspiration from biological systems to develop tactile sensors that mimic the human sense of touch. These sensors often incorporate multiple sensing modalities (e.g., pressure, vibration, temperature) to capture a richer set of texture features such as the work by [86] where the authors introduce a biomimetic tactile sensor inspired by human fingerprints, its integration with machine learning algorithms for texture recognition, and its potential applications in robotics and human-computer interaction.

2. **High-Resolution Sensors:** The development of high-resolution tactile sensors with a dense array of sensing elements allows for capturing detailed information about texture variations across an object's surface. This facilitates more accurate classification, particularly for differentiating between fine textures. In [87] the researchers explored integrating high resolution tactile sensors with robotic end-effectors for object recognition using pressure readings treated as standard images.

Machine Learning for Texture Classification plays a pivotal role in the interpretation and analysis of tactile data, significantly advancing the field of robotic texture recognition. Key developments in this area include:

1. **Deep Learning Techniques:** Deep learning algorithms, such as convolutional neural networks (CNNs), have shown remarkable success in texture classification tasks. These algorithms can automatically learn complex features from tactile sensor data, enabling them to accurately distinguish between different textures, as demonstrated in [88] where the authors propose a CNN-based approach for texture classification using tactile sensor data, achieving high accuracy on a diverse set of materials.

2. **Transfer Learning:** By leveraging pre-trained models on large datasets of labeled texture data, researchers can improve the performance of texture classification algorithms for robotic applications. In [87] two approaches are explored for tactile object recognition: transfer learning using pre-trained convolutional neural networks (CNNs) and a custom-made CNN called TactNet trained from scratch with tactile information. Transfer learning reduces the need for extensive training data specific to the robotic task.

Data Acquisition and Processing Techniques are fundamental to enhancing the effectiveness of tactile sensing in robotics, providing crucial methods for improving data quality and model performance. Notable advancements in this area include:

1. **Active Touch Exploration:** Robots can actively explore objects using their tactile sensors, acquiring data from different contact points and orientations. This allows for a more comprehensive understanding of the object's texture compared to static contact. For instance, In [89] the authors investigate the relationship between motor movements, sensory perception, and EEG signals during active tactile exploration of textured surfaces. Participants performed rubbing or tapping motions on surfaces with different levels of roughness while EEG data were recorded. Also, In [90], the authors explors how Active Learning (AL) strategies improve texture classification in robotic tactile sensing. AL helps robots select informative samples, cutting down on human labeling efforts. A new class-balancing algorithm is introduced, and various AL strategies are evaluated. Results show reduced training data needs with maintained or improved performance. This work advances robotic exploration by enhancing texture recognition with less human input.

2. **Data Augmentation Techniques:** Techniques like data augmentation can be used to artificially increase the amount and diversity of training data for texture classification algorithms. This helps to improve the robustness and generalization capabilities of the models. In [91], we can find data augmentation techniques in the context of tactile object classification using machine learning. The study involves expanding a dataset of 2000 samples across 20 classes through augmentation methods such as jitter, scaling, magnitude warp, time warp, and cropping. The effectiveness of these techniques is evaluated by comparing the classification performance of different neural network architectures, including MLP, LSTM, CNN, CNNLSTM, ConvLSTM, and deep CNN (D-CNN). Results indicate a significant improvement in classification accuracy, with the D-CNN achieving the highest success rate of 72.58%̇The findings underscore the importance of data augmentation in enhancing the capabilities of tactile sensing for robotics applications.

The primary objective of this thesis is to advance tactile perception in robotics, with a

particular focus on texture classification of uneven surfaces. A comprehensive review of existing literature reveals a notable gap in this domain. Previous research has struggled with the reconstruction of uneven surfaces, which has impeded their ability to collect tactile data and subsequently perform texture classification. This limitation has largely resulted in an underexplored area of robotic tactile sensing. In contrast, our work addresses these challenges head-on. By developing methodologies to reconstruct uneven surfaces and gather tactile data effectively, we are pioneering efforts in this crucial aspect of robotic perception.

Chapter 3

Methodology

In the upcoming sections, we delve into the methodologies employed to achieve the primary objectives of this study: advancing tactile perception in robotics, particularly texture recognition on uneven surfaces using deep learning techniques. Our approach encompasses developing a strategy for robotic systems to collect tactile data from uneven surfaces, creating a comprehensive simulation environment for preliminary testing, establishing a novel tactile texture dataset, and designing robust deep learning models capable of accurate classification across both uneven and even surfaces. Each step of this methodology is critical to addressing the existing challenges in the field and pushing the boundaries of tactile sensing in robotics.

3.1 Materials

In this study, the choice of sensor and manipulator is crucial for achieving precise tactile data collection and accurate texture classification. The selected sensor provides high-resolution tactile feedback, enabling detailed texture mapping of various surfaces. Meanwhile, the manipulator is designed to perform intricate exploratory motions, essential for thorough surface examination and data acquisition. Together, these components form the backbone of our experimental setup, facilitating reliable and reproducible results.

The robotic manipulator utilized in this study is the OpenMANIPULATOR-X RM-X52-

TNM [92]. This advanced manipulator features five actuators: four joints and one gripper. Joint 1 facilitates rotational movement around the base, allowing for a wide range of movement, while the remaining joints operate within the plane established by the position of Joint 1. Together, these joints provide 4 Degrees of Freedom (DOF), enabling the manipulator to perform complex tasks with precision. The gripper at the end of the manipulator securely holds the sensory module, which is mounted on a custom-designed 3D-printed structure to ensure enhanced stability and precision during operation (refer to Fig. 3.1 for the structure).

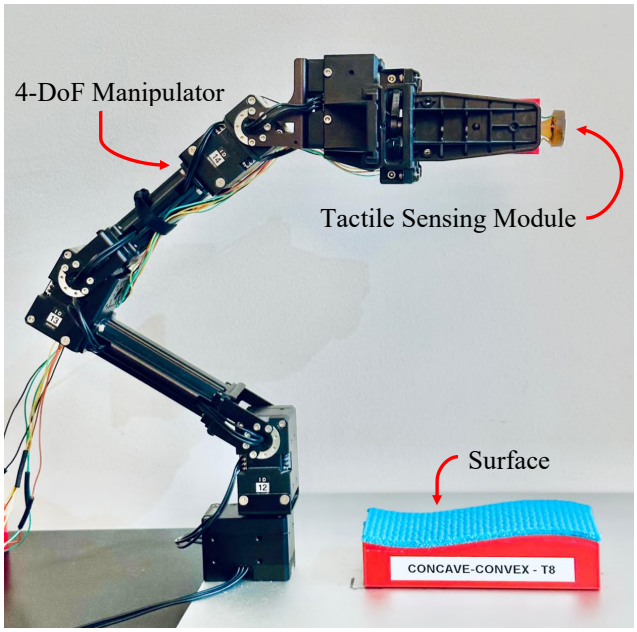

Figure 3.1: Setup featuring a 4-DoF manipulator, tactile sensing module, and surface.

For sensory input, this study employs a bio-inspired multi-modal sensing module as described in [19], [93]. The sensing module integrates a LSM9DS0 MARG (Magnetic, Angular Rate, Gravity) sensor and a MPL115A2 barometric pressure sensor. These sensors are embedded in a flexible polyurethane matrix, which provides both durability and adaptability to various tactile surfaces. Encased within a flexible polyurethane housing, the MARG sensor includes a tri-axis accelerometer, gyroscope, and magnetometer, which allow for accurate detection and characterization of spatial orientations and magnetic fields. In addition, the MPL115A2 Barometer delivers precise pressure measurements, crucial for altitude estima-

tion and environmental monitoring. This innovative integration allows the sensing module to accurately capture a wide range of tactile data, including magnetic fields, angular rates, gravity, and barometric pressure. The structural composition of this sensing module is illustrated in Figure 3.2. This multi-modal approach allows for the collection of comprehensive tactile data, facilitating robust texture classification and enhancing the manipulator's interaction with different materials.

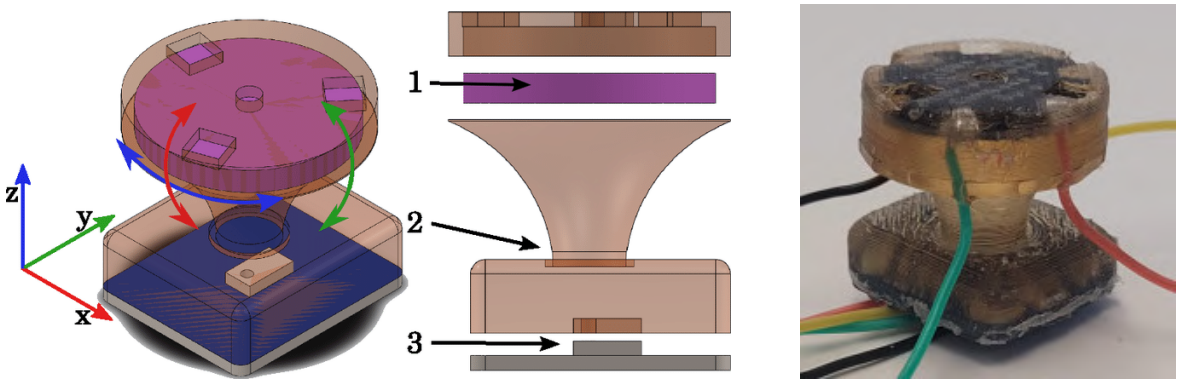

(a) (b)

Figure 3.2: a) Tactile sensing module components: 1—MARG (magnetic, angular rate, and gravity) system; 2—compliant structure; 3—barometer [19]; b) Sensing module encapsulated in flexible structure.

Command communication with the manipulator is managed through the Robot Operating System (ROS) [94], in conjunction with the OpenCR 1.0 embedded board, an open-source control module specifically designed for ROS integration. This setup ensures seamless operation and real-time responsiveness of the manipulator, enabling efficient execution of complex tasks. The ROS framework provides a flexible and modular environment for developing and deploying robotic applications, which is essential for handling the sophisticated control algorithms and sensor data processing required in this study.

To send the sensor readings in the appropriate format, we use a Teensy 3.2 microcontroller [95]. This microcontroller is programmed to transmit the sensory data via a ROS serial publisher node at a baud rate of 250000 to an Ubuntu 16.04 machine. The Teensy 3.2 is chosen for its high performance and reliability in handling high-speed data communication,

ensuring that the sensory data is accurately and efficiently relayed to the main control system.

By leveraging the capabilities of the OpenMANIPULATOR-X RM-X52-TNM and the advanced sensory module, this study aims to advance the field of tactile texture recognition. The integration of these technologies provides valuable insights and practical applications in robotic sensing and control, enabling the development of more sophisticated and capable robotic systems.

The use of simulation in robotic research offers numerous advantages, particularly in the early stages of experimentation. By employing a simulated environment, researchers can safely and efficiently test hypotheses, refine methodologies, and identify potential issues without the risks and costs associated with real-world testing. the simulation of the robot and tactile sensor, elucidating its pivotal role in conducting pre-real world testing. This involves creating a virtual environment where the robot and tactile sensors can interact with digital models of various objects. By simulating the tactile exploration process, we can refine the data collection techniques, identifying potential issues and making adjustments before real-world implementation, thus minimizing risks and optimizing performance.

With this setup, the simulation is conducted to emulate real-world interactions and validate the performance of the sensor and manipulator in a controlled environment. The simulation helps in fine-tuning the data collection techniques and ensures that the system can accurately navigate and gather tactile data from objects with diverse shapes. Once the simulation results are satisfactory, the same setup is applied in real-world scenarios to further validate the methods.

This methodological approach involved the meticulous simulation of both the bioinspired tactile sensor, encompassing its intricate MARG and barometer components, and the subsequent integration of this simulated sensor onto the simulated OpenManipulator-X platform, as shown in 3.3 . Simulation in URDF (Unified Robot Description Format) and Gazebo is accomplished by creating a detailed robot model and defining its physical and visual properties. URDF files describe the robot's joints, links, and sensors, which can then be loaded

into the Gazebo simulator. Gazebo provides a robust physics engine and graphical interface, allowing for realistic interaction with the simulated environment. The simulation can interact with ROS (Robot Operating System) applications, enabling seamless integration between the simulated robot and ROS-based control algorithms.

In this work, the simulation of the tactile sensory module and the OpenManipulator-X robotic arm was performed meticulously within the URDF and Gazebo framework. The simulated sensor, along with its corresponding probe, was precisely modeled and integrated with the OpenManipulator-X, a robotic arm readily accessible through [92].

Before integrating the simulated sensor with the OpenManipulator-X, careful attention was given to simulating the probe to ensure its accurate representation within the virtual environment. The STL file of the 3D sensor probe was seamlessly incorporated into the URDF file, enabling its attachment to the end effector of the robotic arm. Subsequently, the simulated sensor was affixed to this probe, establishing a cohesive integration between the sensor and the robotic platform.

By meticulously replicating the entire system encompassing the tactile sensor, its manipulative apparatus, and the corresponding control mechanisms within a carefully designed simulation environment, a comprehensive platform was established for rigorous testing and validation prior to real-world implementation (see 3.3). This simulation environment served as a critical intermediary step, enabling the identification and resolution of potential issues in a controlled, risk-free setting. Through this approach, each component of the system, from the sensor's data acquisition capabilities to the robotic arm's precision in executing exploratory trajectories, was thoroughly evaluated. The integration of the tactile sensor with the robotic manipulator within the simulation allowed for the fine-tuning of their interactions, ensuring optimal performance when deployed in practical applications. This setup allowed for testing diverse scenarios, ensuring the sensor and robotic arm worked effectively together. The simulation enabled detailed analysis and refinement of the tactile sensing system, improving its reliability before real-world deployment.

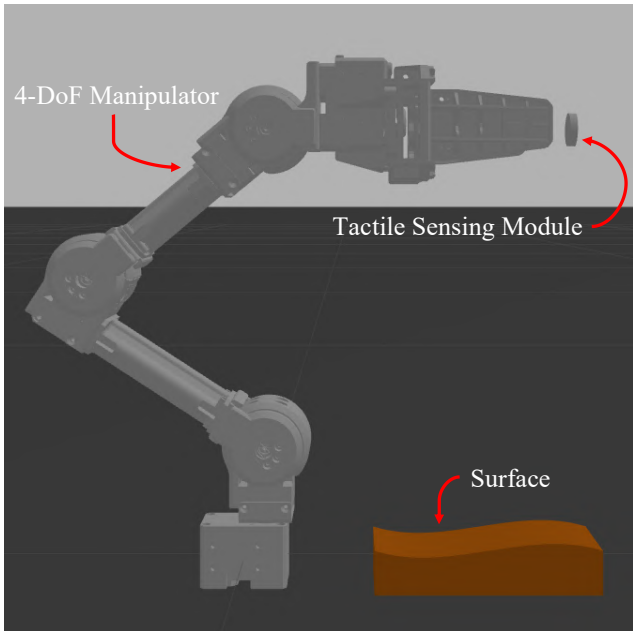

Figure 3.3: Simulated setup featuring a 4-DoF manipulator, tactile sensing module, and surface

In the process of simulating these sensors, meticulous attention was given to the development of a comprehensive URDF (Unified Robot Description Format) model. This model encompasses four distinct joints, each meticulously engineered to emulate the sensory capabilities of the physical sensors. Notably, revolute joints, aligned along the x, y, and z axes, facilitate the sensor's deformations and rotations (see part b of Figure 3.4), enabling it to dynamically adapt to spatial variations. Complementing these capabilities, a prismatic joint, initially aligned with the z-axis, enables controlled compression or expansion of the sensor (see part c of Figure 3.4).

The simulation of the tactile sensor module involved integrating these joints into the URDF model (refer to part a of Figure 3.4). Plugins within the simulation environment interpret the sensor's movements and deformations, translating them into actionable data streams such as orientation, angular velocity, magnetic field strength, and pressure variations. These data streams are essential for further analysis and application within the robotic system.

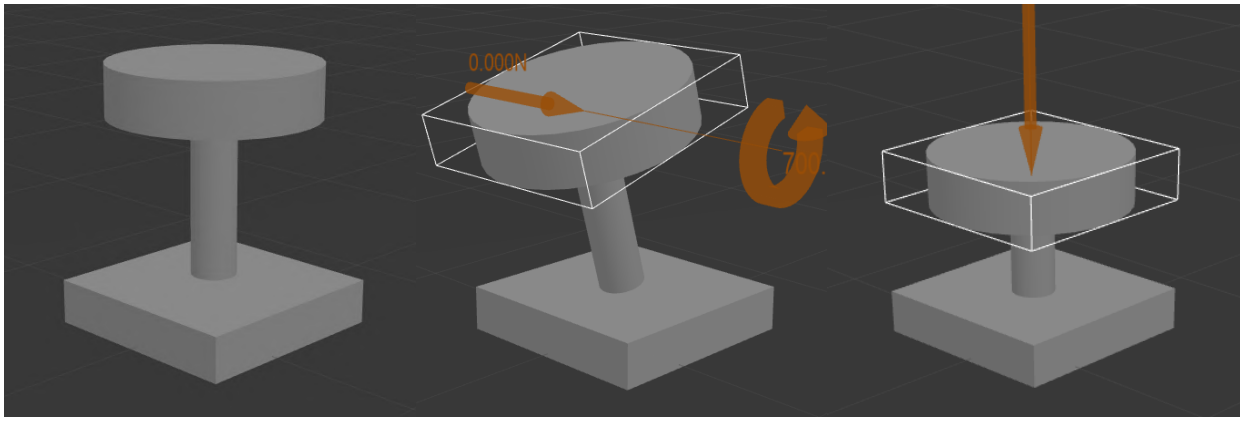

(a) (b) (c)

Figure 3.4: a) Simulated tactile sensing module; b) Demonstration of the simulated tactile sensing module's ability to deform in any direction of space; c) Demonstration of the simulated tactile sensing module's ability to be pressed and released.

While the research presented utilizes a specific type of tactile sensor and manipulator, the methodologies and developed approaches are designed to be broadly applicable across various tactile sensing technologies and robotic manipulators. The core principles and techniques employed, including advanced tactile feedback analysis, surface reconstruction, and texture recognition, are inherently adaptable to different sensor modalities and manipulative systems. This versatility ensures that our approach offers significant insights and effective solutions across a broad spectrum of tactile sensing scenarios, thereby enhancing the capability to address a wide array of tactile sensing challenges within the robotics field.

3.2 Methods

By first leveraging a simulated environment to perfect our techniques, we established a robust foundation for developing a system capable of accurate texture classification using tactile data collected by the robotic manipulator and tactile sensing module. This two-phased approach, encompassing both simulation and real-world implementation, was critical to ensuring the methods' efficacy and reliability.

The process begins in the simulated environment, where the robot, equipped with a tactile

sensor, performs exploratory motions across various surface types. This environment allowed us to refine the robot's motion strategies, sensor integration, and data collection methods under controlled conditions. The simulation provided a flexible platform to experiment with different trajectories and sensor placements, which would be challenging and time-consuming to test repeatedly in a physical setting. By optimizing these parameters in the virtual space, we reduced the risk of errors during real-world trials and ensured that the system could handle the complexities of uneven surfaces effectively.

Once the techniques were perfected in the simulated environment, the next phase involved transferring these strategies to a physical robot. The robot, now in a real-world setting, undertakes the tactile data collection process, meticulously tailored for texture classification. During this phase, the robot's tactile sensor interacts with the surfaces of objects, gathering critical data points, including the position and normal vector at each contact point. These data points serve as the foundation for generating precise trajectories that guide the robot across the object's surface, ensuring comprehensive tactile exploration.

As the robot executes these trajectories, it systematically collects tactile data, which is then processed and analyzed to develop a model capable of classifying the texture of the objects. This real-world data is crucial, as it accounts for the physical properties of textures that simulations cannot fully replicate. By relying on actual tactile data, the classification model is grounded in reality application.

Figure 3.5 provides a detailed overview of the entire workflow. It illustrates the estimation of pathway points, the execution of trajectories along the surface, the systematic collection of tactile data, and the application of advanced models to classify the textures of surfaces based on the acquired tactile information. Each step in this workflow is integral to the overall methodology, ensuring that the system is both comprehensive and adaptable to various tactile sensing tasks. These steps will be elaborated upon in the subsequent sections, providing a deeper understanding of the strategies and techniques employed to achieve accurate and reliable tactile texture classification.

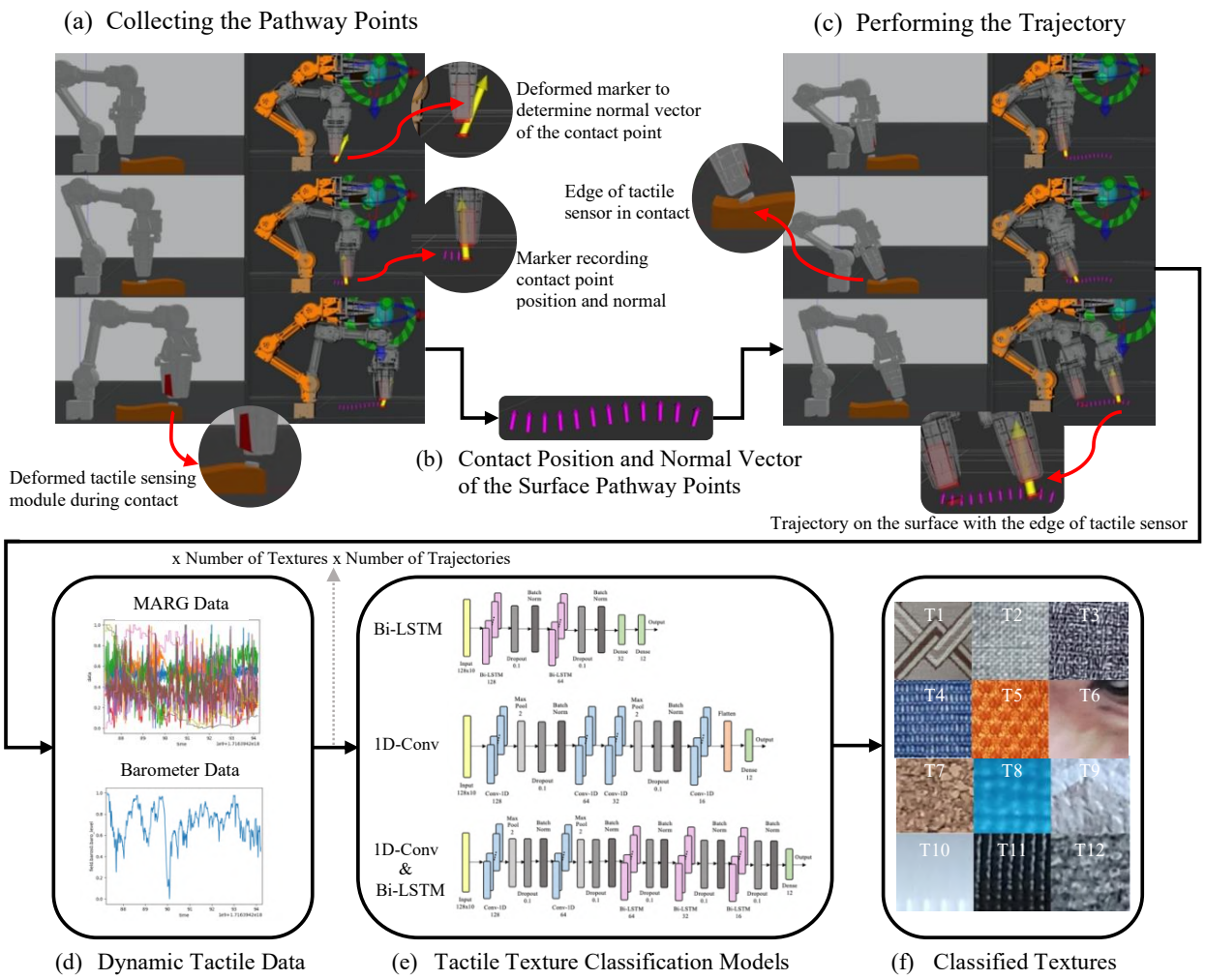

Figure 3.5: a) Estimation of pathway points on the surface; b) Achieving contact points' positions and normals to perform a trajectory with respect to them; c) Tracking the trajectory on the established pathway to collect tactile data; d) Dynamic tactile data collection, including MARG and barometric data; e) Classifiers that categorize textures based on the collected tactile data; f) 12 different textures on which data was collected and analyzed by the classifiers.

3.2.1 Pathway Generation

In the process of guiding the robot along a surface and utilizing tactile data, the primary objective is to gather comprehensive information about each contact point. This includes capturing the precise 3D position (x, y, z) where the robot interacts with the surface. Equally essential is determining the orientation of these contact points, specifically the normal vector (nx, ny, nz) that defines the direction of the surface at each contact location. This orientation

data is crucial as it guides the robot in understanding the spatial configuration of the surface and enables it to adjust its trajectory and interactions accordingly, utilizing tactile feedback to enhance its operational effectiveness and adaptability.

The position $\mathbf{p} = (p_x, p_y, p_z)$ represents the spatial coordinates of a contact point in 3D space, which can be determined using the robot interface. However, the normal orientation is derived directly from tactile data, which necessitates accurate estimation methods.

To represent rotations in 3D space, we can use axis-angle representation, where any rotation can be described by an axis of rotation $\mathbf{v} = (v_x, v_y, v_z)$ and an angle ϕ. This rotation can be encoded into a rotation matrix $\mathbf{R}$ as follows:

$$\mathbf{R} = \mathbf{I} + \sin(\phi)\mathbf{K} + (1 - \cos(\phi))\mathbf{K}^2 \tag{3.1}$$

where $\mathbf{I}$ is the identity matrix, and $\mathbf{K}$ is the skew-symmetric matrix of $\mathbf{v}$:

$$\mathbf{K} = \begin{pmatrix} 0 & -v_z & v_y \\ v_z & 0 & -v_x \\ -v_y & v_x & 0 \end{pmatrix} \tag{3.2}$$

This matrix $\mathbf{R}$ can be used to rotate vectors in 3D space.

Estimating the sensor's orientation relative to the Earth frame involves accelerometer readings $\mathbf{a} = (a_x, a_y, a_z)$ and assuming the gravity direction is $\mathbf{g} = (0, 0, 1)$. We can compute a rotation matrix $\mathbf{R}_{ag}$ that aligns $\mathbf{a}$ with $\mathbf{g}$:

$$\mathbf{R}_{ag} = \mathbf{I} + \sin(\theta)\mathbf{K}_{ag} + (1 - \cos(\theta))\mathbf{K}_{ag}^2 \tag{3.3}$$

where θ is the angle between $\mathbf{a}$ and $\mathbf{g}$, and $\mathbf{K}_{ag}$ is the skew-symmetric matrix of the cross product $\mathbf{a} \times \mathbf{g}$:

$$\mathbf{K}_{ag} = \begin{pmatrix} 0 & -a_z & a_y \\ a_z & 0 & -a_x \\ -a_y & a_x & 0 \end{pmatrix} \tag{3.4}$$

To account for the robot's base link rotation, we consider a rotation matrix $\mathbf{R}_z$ representing a rotation by an angle α around the z-axis:

$$\mathbf{R}_z = \begin{pmatrix} \cos(\alpha) & -\sin(\alpha) & 0 \\ \sin(\alpha) & \cos(\alpha) & 0 \\ 0 & 0 & 1 \end{pmatrix} \tag{3.5}$$

The final orientation matrix $\mathbf{R}_{\text{final}}$ is obtained by combining $\mathbf{R}_z$ and $\mathbf{R}_{ag}$:

$$\mathbf{R}_{\text{final}} = \mathbf{R}_z \mathbf{R}_{ag} \tag{3.6}$$

The Madgwick filter enhances orientation estimation using accelerometer $\mathbf{a}$ and gyroscope $\boldsymbol{\omega} = (\omega_x, \omega_y, \omega_z)$ readings. It iteratively updates the orientation matrix $\mathbf{R}_t$ to $\mathbf{R}_{t+1}$:

$$\mathbf{R}_{t+1} = \mathbf{R}_t + \Delta t \left(\mathbf{R}_t \boldsymbol{\Omega}_t - \beta \mathbf{E}_t \right) \tag{3.7}$$

where Δt is the time step, $\boldsymbol{\Omega}_t$ is the skew-symmetric matrix of $\boldsymbol{\omega}_t$, β is a parameter balancing the gyroscope and accelerometer data, and $\mathbf{E}_t$ is the error term matrix:

$$\boldsymbol{\Omega}_t = \begin{pmatrix} 0 & -\omega_z & \omega_y \\ \omega_z & 0 & -\omega_x \\ -\omega_y & \omega_x & 0 \end{pmatrix} \tag{3.8}$$

The error term $\mathbf{E}_t$ represents the difference between the measured and predicted accelerations. The predicted acceleration $\hat{\mathbf{a}}_t$ is obtained by rotating the gravity vector $\mathbf{g}$ using $\mathbf{R}_t$:

$$\hat{\mathbf{a}}_t = \mathbf{R}_t \mathbf{g} \tag{3.9}$$

The filter iteratively refines the rotation matrix $\mathbf{R}_t$ to minimize the error between the predicted and measured accelerations, ensuring accurate orientation estimation over time.

Once the sensor's final orientation is established, it is applied to the tactile sensor link, depicted by the yellow marker in Figure 3.6. A dedicated ROS node is responsible for updating the orientation of this yellow marker. This node continuously monitors the sensor's orientation and remains on standby for an obstacle detection signal. When an obstacle is detected by the robotic manipulator, a signal is sent to the ROS node, which then broadcasts the current position and orientation of the sensor, marked by small purple arrows at that specific time.

In parts (a) to (d) of Figure 3.6, the yellow marker's orientation corresponds to the deformation of the sensor on the surface, capturing the normal vector of each contact point. The position of the point is derived from the sensor frame coordinates, while the orientation is calculated using quaternion representations of the sensor's orientation relative to its initial state. This process enables the collection of a comprehensive pathway of robot motion, comprising information points detailing the position, normal vectors along the path.

By meticulously estimating and tracking the positions and orientations of the contact points during the robot's interaction with surfaces, we achieve minimal geometric reconstruction necessary for accurate trajectory planning. This comprehensive approach not only facilitates the precise collection of tactile data but also enhances the robot's ability to adapt its movements based on real-time feedback. The resulting pathway, enriched with critical position and normal vector information, serves as a foundational element for the surface reconstruction process, enabling effective application of trajectories across complex surfaces.

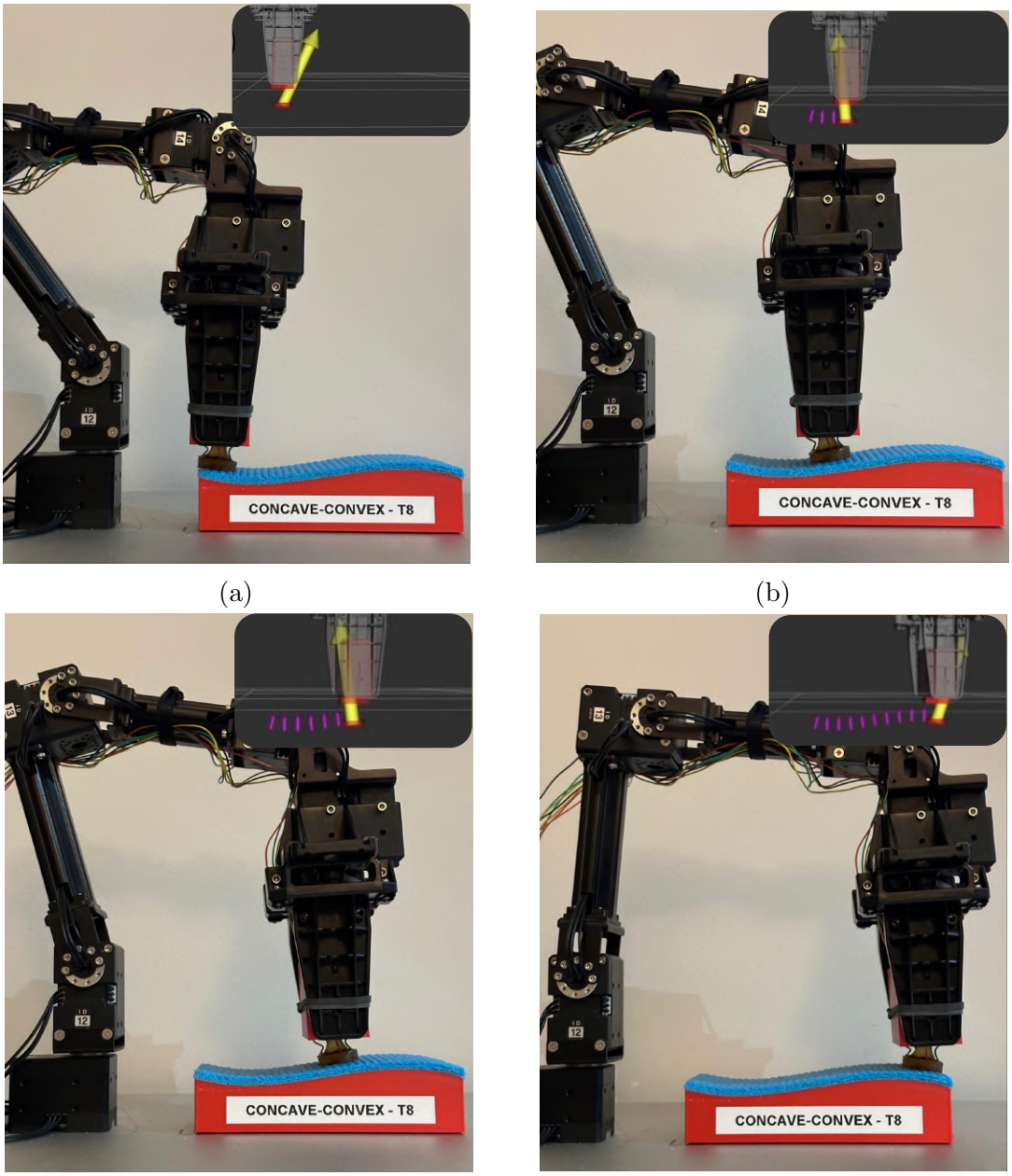

(a) (b)

(c) (d)

Figure 3.6: a-d) Exploratory motion of the robot to detect surface pathway points position and normal vectors

The automated motion of the open manipulator is meticulously designed to systematically collect contact point data and normal vectors from an object's surface, ensuring a high degree of precision and reliability in the measurements. The sequence begins with the end effector of the manipulator oriented perpendicular to the ground. This initial orientation is critical,

as it guarantees a consistent approach angle for each contact measurement, reducing the potential for variability in the data collected.

Starting from an initial position along the x-axis of the object, the end effector is first moved to an intermediate point by adjusting its position along the z-axis. This intermediate point is set at a predetermined height above the object's surface, ensuring that the manipulator can safely begin its approach to the surface without risking premature contact. From this intermediate position, the end effector gradually descends along the z-axis. The descent continues until contact with the object's surface is detected. Upon making contact, the manipulator records the exact position of the contact point, including its x, y, and z coordinates. Additionally, the normal vector at the point of contact is determined and stored. The manipulator also notes the stable marker that defines the orientation at the time of contact, ensuring that all data points are collected with a consistent frame of reference.

Once the contact data has been collected, the end effector retracts to the intermediate point above the surface. This retraction allows the manipulator to prepare for the next measurement without dragging or damaging the surface. Following the retraction, the end effector is moved 1 cm further along the x-axis. This incremental movement ensures that the next contact point will be adjacent to the previous one, facilitating a thorough and systematic profiling of the surface.

The manipulator then repeats the downward approach to the surface, following the same procedure of detecting contact and recording the position and normal vector at each new point. This sequence is repeated iteratively, with the end effector advancing by 1 cm along the x-axis after each contact measurement. This process continues until the entire surface of interest has been profiled.

This automated sequence ensures that each data point is collected consistently and accurately, capturing essential information for surface reconstruction or trajectory planning. The careful approach to contact, systematic data acquisition, and precise control of the manipulator's movements enable the profiling of complex surfaces with a high degree of accuracy.

This method is particularly suitable for applications in robotic sensing, surface analysis, and automated inspection systems, where reliable and precise data collection is paramount.

3.2.2 Trajectory-Based Tactile Data Collection

While gathering data points along a surface path, a trajectory is planned for the robot to navigate across the surface. The end effector and sensor frame are oriented with an offset angle relative to each collected point's orientation. This approach ensures that the robot moves using the edge of the sensor rather than the entire sensor surface. This strategy is adopted to avoid potential issues associated with the sensor's sticky material, which could lead to erratic movements and inaccurate tactile data if the entire sensor surface were used. Moreover, moving with the sensor edge mimics human touch, which typically applies gentle pressure to detect textures accurately without causing damage or undue stress on the sensor. This method not only enhances the reliability of tactile data collection but also reduces the risk of sensor damage and ensures smoother interaction with the surface, thereby improving overall performance and longevity of the robotic system and enhancing the quality of data collection.

For planning and executing the trajectories of the Open Manipulator X robotic arm, I utilized MoveIt. MoveIt is an open-source software framework that provides advanced capabilities for motion planning, manipulation, and control in robotic systems. It features sophisticated motion planning algorithms, an intuitive interface for task specification, and comprehensive simulation and visualization tools. Leveraging MoveIt allowed for precise and efficient trajectory design, validation, and execution, thereby significantly enhancing the efficiency and reliability of the tactile data acquisition process.

In figures (a) to (d) of Figure 3.7, the yellow marker denotes the orientation of the sensor on the surface, showing a distinct angle difference with the normal vector indicated by the small purple marker. The figures in 3.7 capture four stages of the robot's trajectory along the surface, where the sensor engages with the surface using its edge, facilitating the

collection of tactile data. This data integrates inputs from MARG (Magnetic, Angular-Rate, Gravity) and barometer sensors. The MARG sensors provide comprehensive 9-dimensional data, including 3-axis magnetic, angular velocity, and gravity readings, complemented by a barometer reading, summing up to 10 dimensions. These sensory inputs are logged into a rosbag file, a format commonly used in ROS (Robot Operating System), enabling efficient storage and subsequent analysis. This setup ensures detailed capture and storage of sensory information crucial for further research.

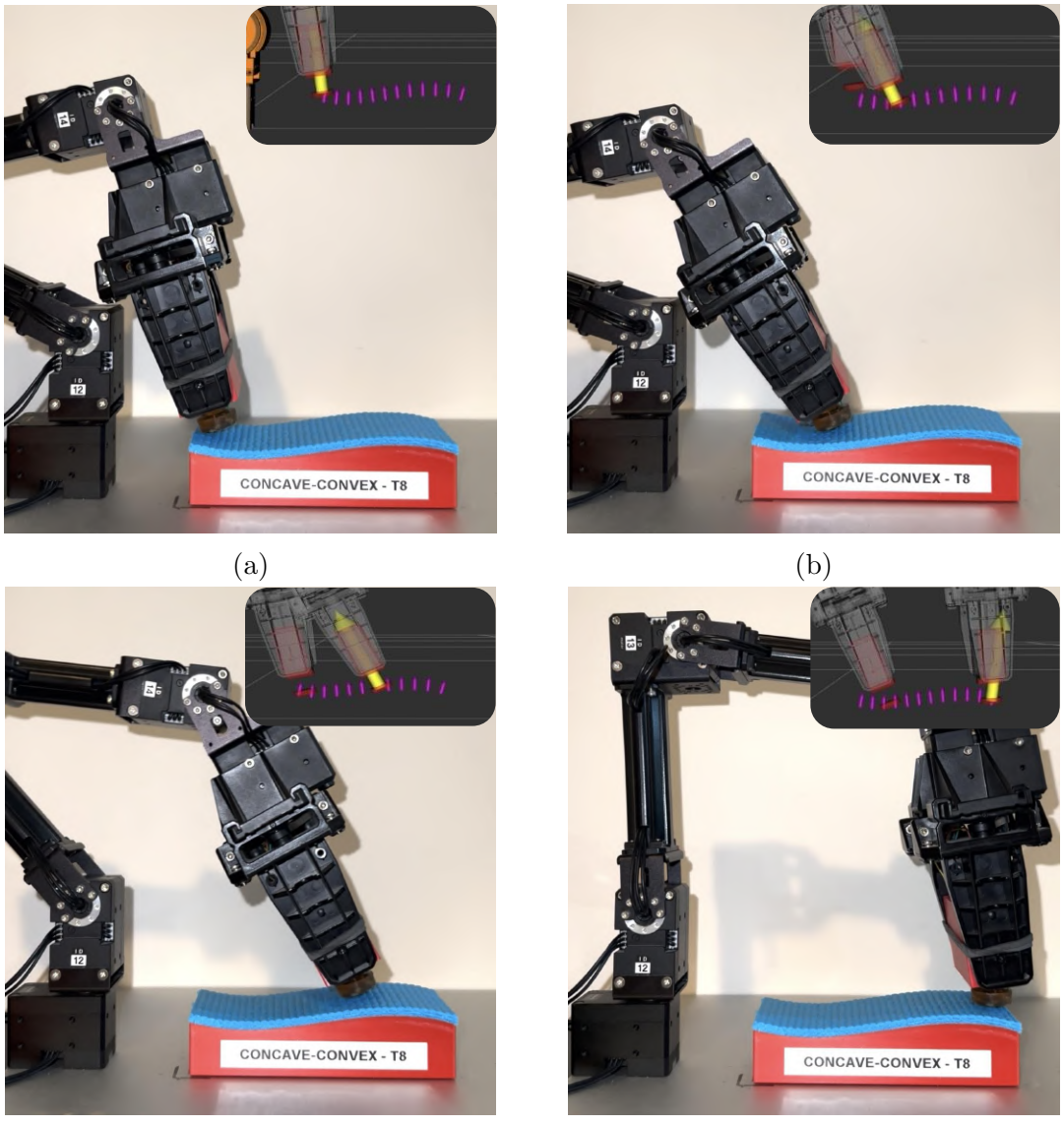

(a) (b) (c) (d)

Figure 3.7: a-d) Trajectory execution of the robot to collect tactile data from the surface texture of the object

3.2.3 Tactile Data Prepossessing

The tactile data collected for this study integrates inputs from MARG (Magnetic, Angular-Rate, Gravity) and barometer sensors, providing a comprehensive 10-dimensional dataset. Specifically, the MARG sensors offer 3-axis magnetic, angular velocity, and gravity readings (ax, ay, az, gx, gy, gz, mx, my, mz), which are complemented by a barometer reading. To ensure the relevance and accuracy of the data, a filtering process is applied to retain only the measurements taken while the robot is in motion on the surface and the sensor is in contact with the object.

We normalize each of the ten variables using the Min-Max scaling method. The normalization is performed using equation 3.10, where min(var) and max(var) represent the minimum and maximum values of the variable, respectively.

$$\text{var}_{\text{norm}} = \frac{\text{var} - \min(\text{var})}{\max(\text{var}) - \min(\text{var})} \tag{3.10}$$

This Min-Max scaling method transforms each variable to a common scale, typically $[0, 1]$, ensuring that all variables contribute equally to the analysis. This approach is particularly useful when the data features have different units or scales, as it preserves the relationships between values while standardizing the range.

One of the critical aims of this research is to emulate the tactile texture classification process as performed by humans. Humans typically do not need to touch the entire surface of an object to recognize its texture. Instead, they often infer the texture from a small section of the object. To closely mimic this human behavior, enhance the perceptual capabilities of robotic tactile texture classification, and optimize the classification process, we adopted a sliding window approach on the dataset with varying window sizes.

The sliding window technique offers several benefits in the context of tactile texture classification. By dividing the dataset into smaller, overlapping segments (windows), local texture features that might be lost when considering the entire dataset as a whole can be captured.

This method not only improves the robustness and accuracy of the classification model by focusing on local patterns and details but also accelerates the classification process by reducing the amount of data processed at any given time. Furthermore, employing different window sizes allows for multi-scale analysis, providing a more comprehensive understanding of the textures.

We applied the sliding window approach to segment the dataset into smaller, overlapping windows. This method emulates the way humans recognize textures by touching only a small section of an object. The sliding window technique involves experimenting with different window sizes to capture various scales of texture features, with an overlap between consecutive windows to ensure continuity and capture transitional features between windows. The benefits of the sliding window approach include capturing fine-grained texture details within each window, ensuring smooth transitions between windows to preserve the temporal continuity of the tactile data, and reducing computational load by processing smaller segments, thereby speeding up the training process.

By adopting this approach, the study aims to enhance the efficiency and accuracy of robotic tactile texture classification, closely mirroring the nuanced and efficient ways in which humans perceive and classify textures. This innovative method promises significant improvements in the field of tactile sensing and robotic perception, providing a robust framework for future developments in robotic texture classification.

3.2.4 Texture Classifiers

In this study, we employed several advanced deep learning architectures to classify tactile textures using time-series data. The models include convolutional neural networks, recurrent neural networks, and a combination of both types.

The One Dimensional Convolutional Neural Network (1D CNN) is employed to efficiently extract spatial features from sequential tactile sensor data. The 1D CNN operates by applying convolutional filters across the time-series input, effectively identifying local patterns

and relationships within a specific window of time. These filters move along the sequence, generating feature maps that capture important characteristics indicative of different textures. For example, variations in pressure, vibration, or other tactile sensor readings can be recognized by the 1D CNN, enabling the model to learn distinct features that distinguish one texture from another.

The Bidirectional Long Short-Term Memory (BiLSTM) model as a recurrent neural network, leverages BiLSTM layers to effectively capture temporal dependencies in both forward and backward directions, enhancing its capability to process and understand sequence data. BiLSTMs are particularly advantageous for tasks like tactile texture classification because they can learn contextual information from the entire sequence, rather than just from past or future states individually. By processing data in both directions, the model gains a more comprehensive understanding of the sequence to accurately interpret complex patterns. The integration of BiLSTM layers helps to capture intricate temporal relationships and dependencies, thereby enhancing its ability to classify textures based on sequential data.

The CNN-LSTM model adeptly integrates one-dimensional Convolutional Neural Networks (CNNs) with bidirectional Long Short-Term Memory (LSTM) networks to enhance the classification of tactile textures. The convolutional layers are employed for their capacity to extract intricate spatial features from tactile sensor readings, effectively capturing local patterns and variations. Following this, bidirectional LSTM layers are utilized to capture temporal dependencies by processing sequences in both forward and backward directions, thereby gaining a comprehensive understanding of the temporal dynamics within the data. This integration of CNN and LSTM components ensures that the model leverages the strengths of both spatial and temporal analysis. The architecture is meticulously designed to handle the complex interplay of spatial and temporal features, making it highly effective for detailed texture classification tasks.

These models are crafted to capture both local and temporal features of tactile data, with the following sections detailing model architectures.

3.2.5 Convolutional-Bidirectional Long Short Term Memory

- **Convolutional-Bidirectional LSTM: Model1**

  As illustrated in Figure 3.8, it begins with two 1D Convolutional layers, the first with 128 filters and the second with 64, both using a kernel size of 3 and ReLU activation for initial feature extraction. These layers are followed by MaxPooling, Dropout (0.1 rate), and Batch Normalization to downsample, regularize, and stabilize the training process. Next, the model incorporates three Bidirectional LSTM layers to handle temporal dependencies, starting with 64 units and progressively reducing to 32 and 16 units, applying Dropout and Batch Normalization to prevent overfitting. The network concludes with a Dense output layer with 12 units and softmax activation, tailored for multi-class classification across the twelve distinct tactile textures. This architecture strategically balances feature extraction, temporal sequence modeling, and regularization to achieve robust tactile texture classification.

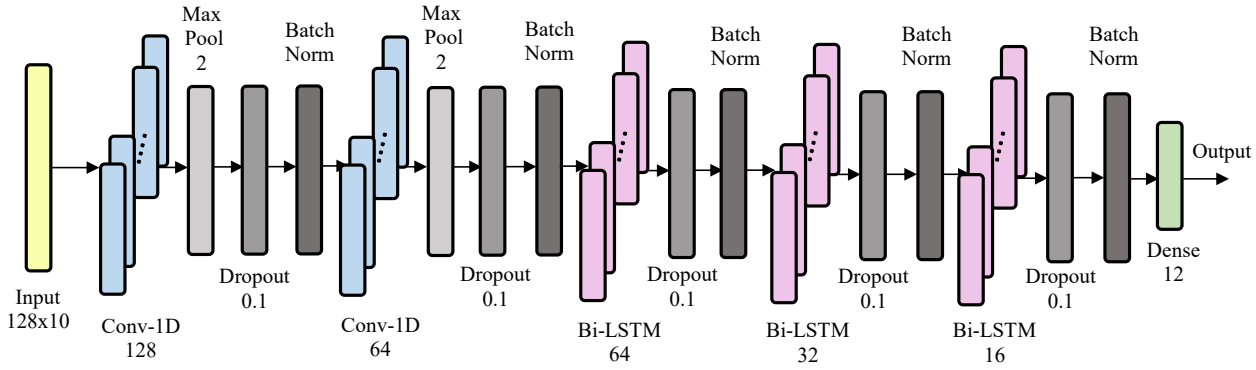

Figure 3.8: First Convolutional-Bidirectional LSTM model architecture

- **Convolutional-Bidirectional LSTM: Model2**

  As can be observed in Fig. 3.9, it initially uses a Conv1D layer with 128 filters and a kernel size of 3, followed by MaxPooling, Dropout (0.1 rate), and Batch Normalization to enhance feature extraction while preventing overfitting and stabilizing training. A second Conv1D layer with 64 filters further refines the feature extraction, accompanied by

similar downsampling and regularization techniques. To capture temporal dependencies, the model incorporates a Bidirectional LSTM layer with 64 units, configured to return sequences, allowing it to analyze data in both forward and backward directions. A second LSTM layer with 32 units follows, enhancing the model's capacity to understand sequential patterns. Each LSTM layer is equipped with Dropout and Batch Normalization to improve generalization and training stability. A Dense layer with 16 units and ReLU activation adds complexity to the learned features, enhancing the model's ability to capture non-linear relationships. Finally, a Dense output layer with 12 units and softmax activation enables multi-class classification, providing a probability distribution across the 12 tactile texture classes for effective texture recognition.

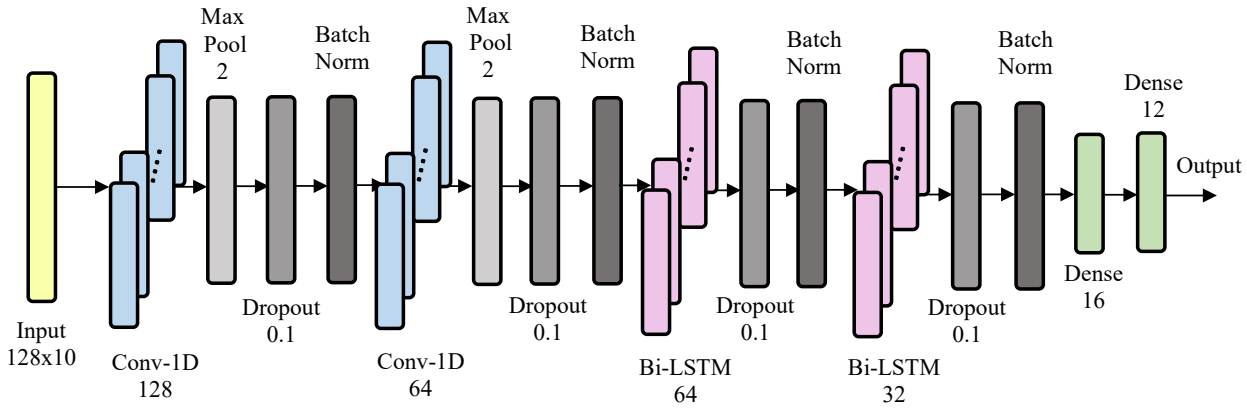

Figure 3.9: Second Convolutional-Bidirectional LSTM model architecture

- **Convolutional-Bidirectional LSTM: Model3**

  As depicted in Fig. 3.10, the architecture begins with two convolutional layers, starting with a block containing 128 filters with a kernel size of 3 and ReLU activation, followed by MaxPooling1D to downsample the data, a Dropout layer (rate 0.5) to prevent overfitting, and Batch Normalization to stabilize training. A second convolutional block with 64 filters further refines these features. After the convolutional layers, the model incorporates three Bidirectional LSTM layers to capture temporal patterns. The first LSTM layer has 64 units, returns sequences for further processing, and is followed by Dropout and Batch

Normalization for enhanced generalization. The second LSTM layer contains 32 units, also returning sequences, while the third layer reduces to 16 units and outputs only the final temporal summary. The model concludes with a Dense output layer with 12 units and softmax activation, which generates probability distributions over twelve tactile texture classes, enabling robust multi-class classification.

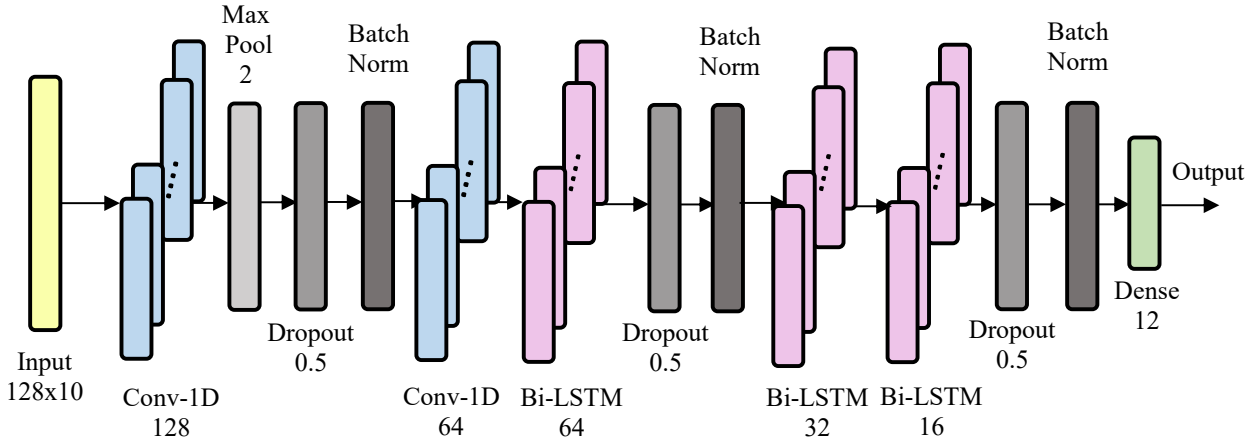

Figure 3.10: Third Convolutional-Bidirectional LSTM model architecture

3.2.6 One Dimensional Convolutional Neural Network

- **1D Convolutional Neural Network: Model1**

  According to Fig. 3.11, the model architecture begins with a series of one-dimensional convolutional layers designed for feature extraction. The first convolutional block consists of a Conv1D layer with 128 filters, a kernel size of 5, and ReLU activation, followed by MaxPooling1D, Dropout regularization with a rate of 0.1, and Batch Normalization to stabilize training. This is followed by a second Conv1D layer with 64 filters, which continues the feature extraction process without additional pooling or regularization. The third convolutional block includes a Conv1D layer with 32 filters, replicating the structure of the first block. The fourth convolutional block, with a Conv1D layer of 16 filters, completes the feature extraction process. The output from the final convolutional block is then flattened into a one-dimensional vector, which is fed into a Dense layer with 12 units

and softmax activation for multi-class classification, providing probability scores across twelve distinct classes.

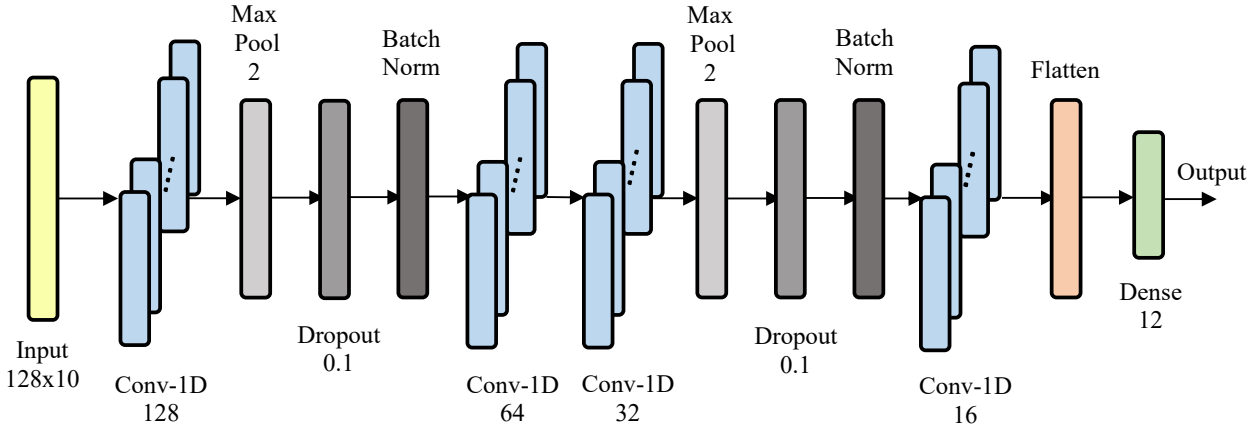

Figure 3.11: First 1D CNN model architecture

- **1D Convolutional Neural Network: Model2**

  As highlighted in Figure 3.12, the model employs a series of 1D convolutional layers for feature extraction. The first convolutional block consists of a Conv1D layer with 128 filters and a kernel size of 5, followed by MaxPooling1D for downsampling, Dropout for regularization, and Batch Normalization. The second block mirrors this structure with 64 filters, continuing the feature extraction process. Both convolutional blocks effectively reduce dimensionality and extract relevant features. After these blocks, the Flatten layer converts the 2D output into a 1D vector. A dense layer with 64 units and ReLU activation then learns complex representations, with additional Dropout and Batch Normalization to mitigate overfitting. The final output layer is a Dense layer with 12 units and softmax activation, classifying the input into one of twelve tactile texture classes.

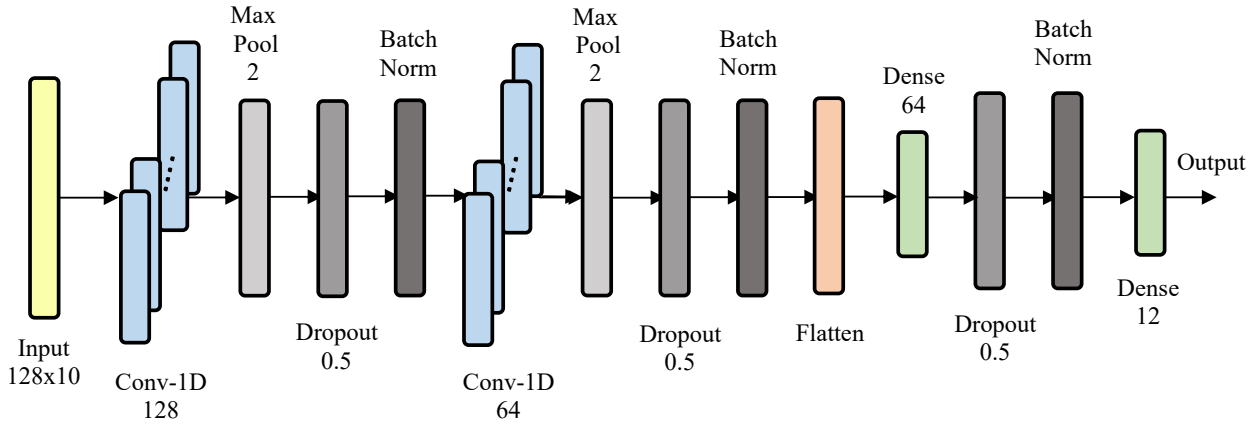

Figure 3.12: Second 1D CNN model architecture

- **1D Convolutional Neural Network: Model3**

  Figure 3.13 demonstrates the model incorporates a series of 1D convolutional layers for hierarchical feature extraction. The initial convolutional block starts with a Conv1D layer that has 128 filters and a kernel size of 5, followed by MaxPooling1D, Dropout regularization with a rate of 0.1, and Batch Normalization to ensure smoother training. Each subsequent block follows a similar structure with Conv1D layers featuring progressively fewer filters: 64, 32, and 16, each followed by MaxPooling1D, Dropout, and Batch Normalization. After feature extraction, the Flatten layer converts the output into a one-dimensional vector. Finally, the dense layer with 12 units and softmax activation performs multi-class classification, providing probabilities for twelve distinct tactile texture classes.

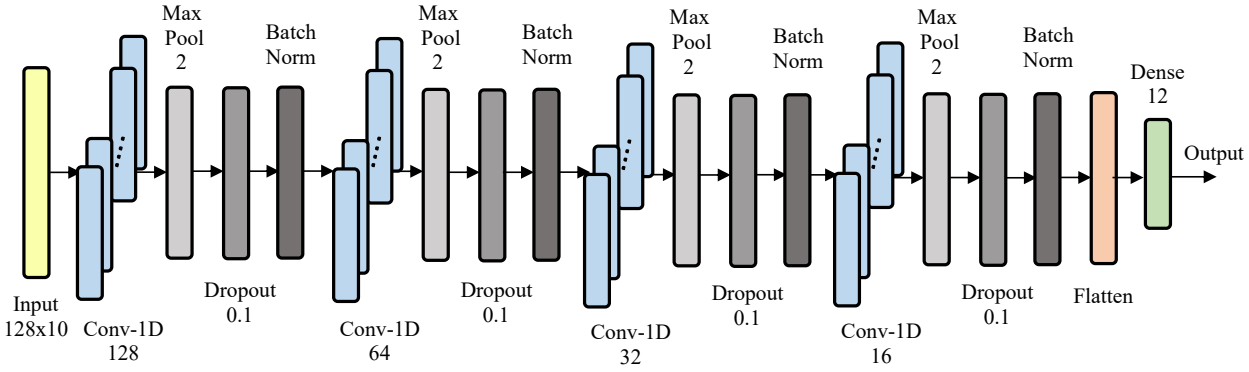

Figure 3.13: Third 1D CNN model architecture

3.2.7 Bidirectional Long Short Term Memory

- **Bidirectional LSTM: Model1**

  As can be seen in Fig. 3.14, the model features BiLSTM layers to capture temporal dependencies in both forward and backward directions. The first BiLSTM layer, with 128 units, returns sequences to preserve temporal information, and is followed by Dropout regularization and Batch Normalization to enhance stability and prevent overfitting. The second BiLSTM layer, with 64 units, mirrors the first in its regularization and normalization processes but outputs a single vector summarizing the entire sequence. A subsequent Dense layer with 32 units and ReLU activation introduces non-linearity, while the final Dense layer with 12 units and softmax activation provides a probability distribution for multi-class classification across twelve tactile texture classes.

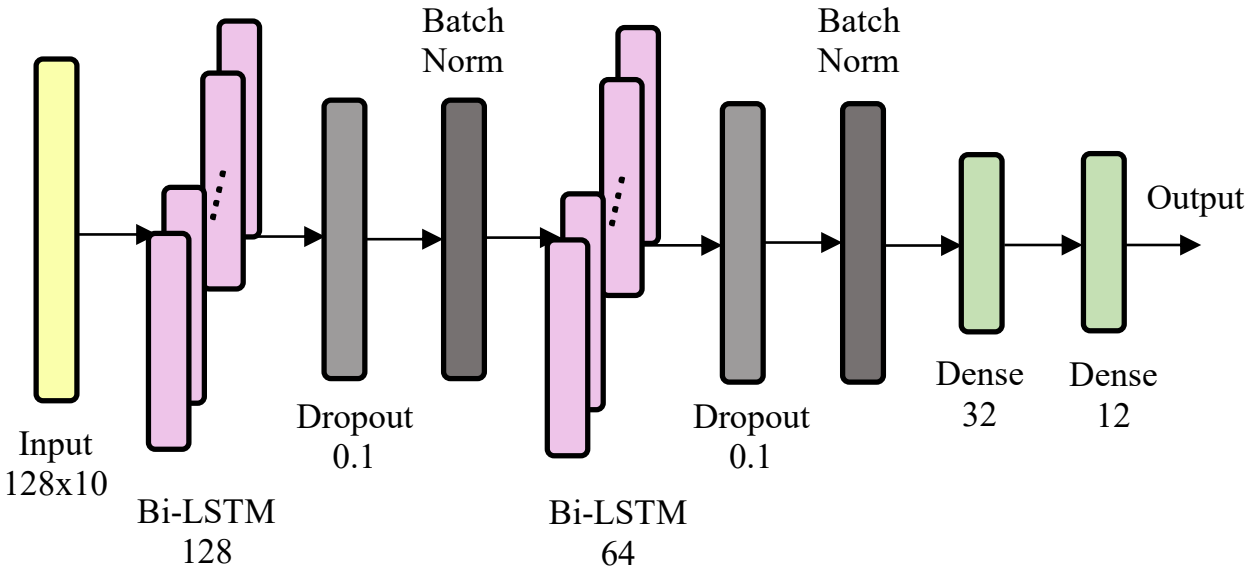

Figure 3.14: First Bidirectional LSTM model architecture

- **Bidirectional LSTM: Model2**

  As illustrated in Figure 3.15, the model uses Bidirectional LSTM layers to capture temporal dependencies from input data. The first Bidirectional LSTM layer, with 128 units, returns sequences and is followed by Dropout (rate of 0.5) and Batch Normalization for

regularization and stability. The second Bidirectional LSTM layer, featuring 64 units, is similar to the first but does not return sequences, instead summarizing the final time step. Following the LSTM layers, a Dense layer with 32 units and ReLU activation learns complex patterns, and the final Dense layer with 12 units and softmax activation performs multi-class classification by outputting probabilities for twelve classes.

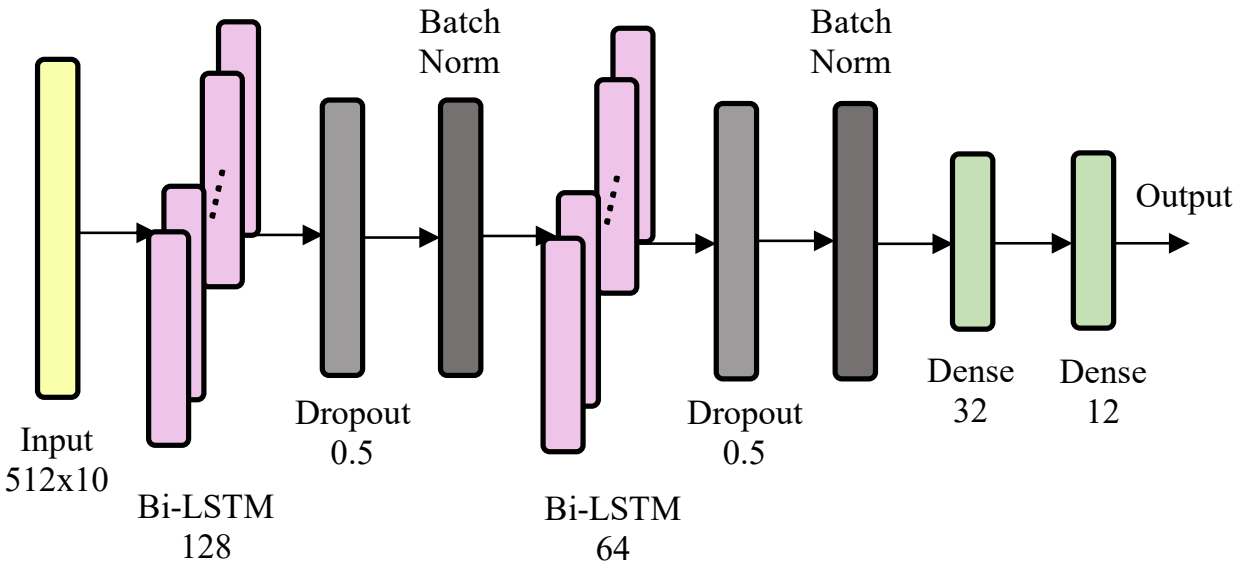

Figure 3.15: Second Bidirectional LSTM model architecture

3.2.8 Textures

For conducting the experiments on tactile data collection and subsequent texture classification, we utilized twelve distinct textures. These textures were specifically chosen and attached to a concave-convex shape to provide a diverse range of tactile sensations (see Figure 3.17). Furthermore, the detailed visual representation and description of these textures are provided in Figure 3.16, offering a clearer view of the surface texture variations and patterns.

This diverse selection of textures ensures a comprehensive evaluation of our classification models, allowing us to rigorously test their ability to discern subtle differences in tactile sensations.

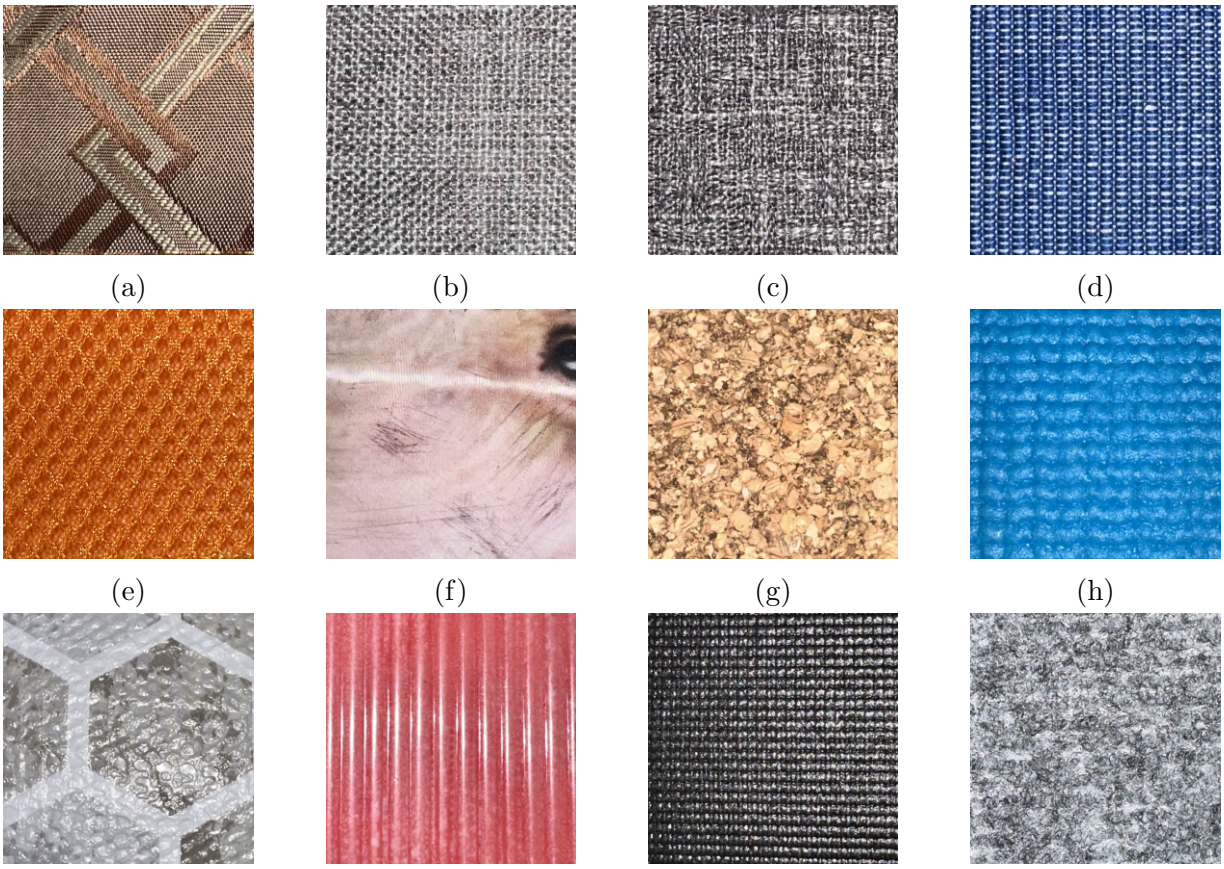

Figure 3.16: The 12 textures used in the experiments. a) brocade fabric; b) open weave cotton; c) tight weave cotton; d) mesh cotton; e) honeycomb fabric; f) embossed plastic; g) wood; h) silicone mesh; i) reptile-patterned leather; j) ridged polymer; k) mesh leather; l) carpet wool.

By affixing these diverse textures to a meticulously designed concave-convex shape, our objective is to authentically replicate a broad spectrum of real-world tactile experiences. This approach aims to significantly enhance the generalizability and robustness of our texture classification methodology. The use of a carefully crafted surface shape ensures that the tactile feedback we collect is representative of a wide variety of textures that one might encounter in real-world scenarios, thus improving the model's applicability and performance across different types of tactile data.

The data collection process was executed with precision, involving the systematic acquisition of tactile data from a range of textures using our advanced robotic setup. Each

texture was carefully and thoroughly sampled to guarantee that the data captured was accurate and reflective of the true tactile properties. This meticulous approach was essential for training and evaluating our classification models effectively. By adhering to a structured and detailed methodology, we established a solid foundation for achieving reliable and precise texture classification outcomes. This rigorous process ensures that our models are well-trained and capable of delivering consistent performance in practical applications.

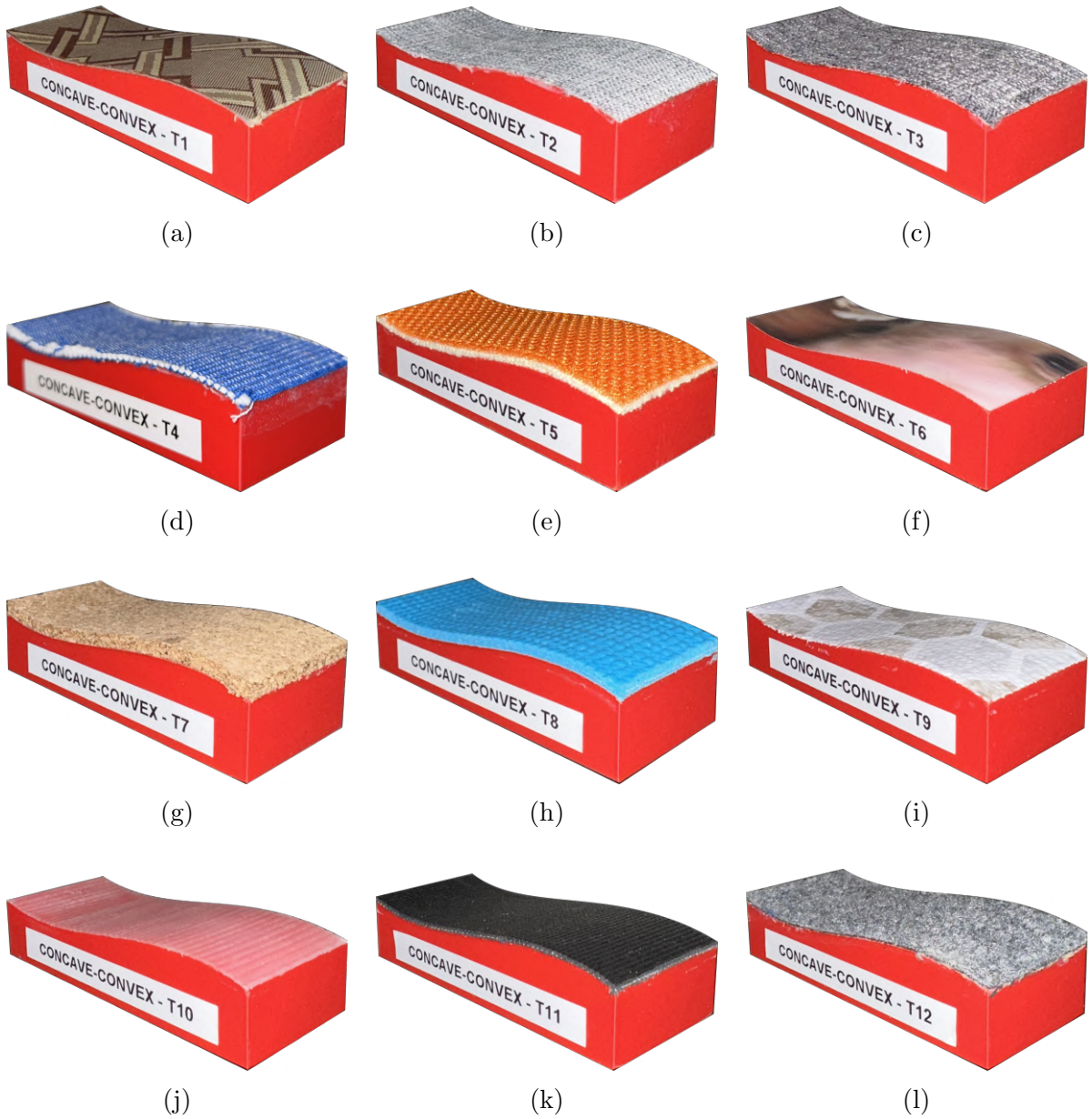

(a) (b) (c)

(d) (e) (f)

(g) (h) (i)

(j) (k) (l)

Figure 3.17: a-l) The 12 textures on the concave-convex object used in the experiments

To ensure a thorough evaluation of our classification models, we extended our analysis by incorporating an additional dataset featuring different textures on an even surface. This approach allowed us to comprehensively assess the models' performance across both uneven and even surfaces, providing a more holistic view of their effectiveness.

The twelve textures used in this supplementary dataset represent a diverse array of materials, including plastic pencil cases, plastic placemats, a cork mat, denim fabrics, felt material, polyester cloth, and a cotton scarf. For detailed descriptions of these textures, please refer to [96].

In our approach, we followed the precedent set by the referenced study, which employed twelve distinct textures for consistency in experimental design. However, whereas their dataset included a number of similar textures, we intentionally selected a broader and more varied range of materials. This strategic choice was made to capture a wider spectrum of tactile experiences, thereby enhancing the models' capacity to differentiate between various surface characteristics. By including a more diverse set of textures, we aimed to better simulate the range of tactile inputs that robots might encounter in real-world scenarios, thereby improving the models' generalizability and robustness.

This careful selection of textures and the comprehensive evaluation across different surface types underscore our commitment to creating a versatile and reliable texture classification system. The broader range of textures not only enriches the dataset but also ensures that our models are well-equipped to handle a wide array of tactile challenges.

Chapter 4

Results and Discussions

In pursuit of the primary objective of this thesis, which is tactile texture classification, we employed two distinct datasets: one for even surfaces and the other for uneven surfaces.

The tactile texture classification task was evaluated on both datasets, encompassing 12 textures on even surfaces and 12 textures on uneven, concave-convex surfaces. This dual-surface approach enabled a rigorous examination of the models' capacity to identify subtle tactile variations across different surface contours, ultimately improving the robustness and generalizability of our texture classification techniques.

The dataset for flat surfaces was sourced from the work of the authors in [96], containing 1200 samples (100 samples for each of the 12 textures), while the dataset for uneven surfaces was meticulously collected during the course of this thesis. This involved performing 25 tactile trajectories across 12 different textures, resulting in 25 samples per texture, for a total of 300 samples.

Classifying the even surface dataset not only ensured that our models were effective for handling various tactile data but also provided a basis for comparison. Given the absence of pre-existing tactile datasets for uneven surfaces, there were no available studies for direct comparison of texture classification on such surfaces.

To address the lack of direct comparison for uneven surface texture classification, we acquired an external dataset of even surfaces. We then trained our models, originally designed for uneven surfaces, using this external even surface dataset. This approach enabled

us to evaluate and compare the performance of our models against those of other researchers who had utilized the same even surface dataset, albeit with different texture classification strategies.

We adopted a sliding window approach on the dataset with varying window sizes to enhance the perceptual capabilities of robotic tactile texture classification and optimize the classification process. This technique involves dividing the dataset into smaller, overlapping windows with a 50% overlap between consecutive windows. This method offers significant advantages, including efficient management of computational time and resources.

By processing smaller segments of data rather than the entire dataset at once, the sliding window approach helps reduce computational load and speeds up both training and evaluation phases. Additionally, this technique closely aligns with the way humans naturally perceive textures, as it enables the model to analyze data in localized segments much like how tactile exploration occurs. This approach not only captures detailed local texture features but also provides a broader understanding of the textures by incorporating overlapping information from adjacent windows. The varying window sizes used in this method allow for multi-scale analysis, further enriching the model's ability to discern subtle differences and enhance overall classification performance.

The characteristics of the datasets utilized in this study, encompassing both even and uneven surfaces, are comprehensively detailed in Table 4.1. Our approach was designed to ensure a rigorous and multifaceted evaluation of our tactile texture classification models, reflecting a variety of real-world conditions.

For the even surface dataset, data collection was performed at a frequency of 350Hz with a velocity of 30mm/s, incorporating 12 distinct textures. Each texture was sampled 100 times, resulting in an initial dataset of 1,200 samples before the application of sliding window techniques. After processing through sliding windows, the dataset's complexity and granularity were further enhanced: a total of 8,399 samples were generated using a 3-second window, while a 6-second window produced 3,599 samples. This allowed the models to

learn from both short-term and extended temporal features, contributing to a more robust classification performance.

Conversely, the uneven surface dataset was gathered at a frequency of 120Hz with a velocity of 15mm/s, featuring the same 12 textures but with 25 samples per texture, totaling 300 samples before the sliding window application. This dataset was analyzed using three distinct window sizes: 128 data points, approximately 1 second; 256 data points, approximately 2 seconds; and 512 data points, approximately 4 seconds. The sliding window approach resulted in 3,962 samples for the 128 data point window, 1,864 samples for the 256 data point window, and 900 samples for the 512 data point window. This varied windowing provided insights into different temporal scales, crucial for capturing diverse texture characteristics and improving the model's classification accuracy.

Both datasets include 10 types of sensor readings: accelerometer (ax, ay, az), gyroscope (gx, gy, gz), magnetometer (mx, my, mz), and barometer (baro). The comprehensive inclusion of these sensors ensures that the models are trained on a wide spectrum of sensory inputs, crucial for distinguishing between subtle differences in textures. To maintain consistency in data analysis, a 50% window overlap was applied across all configurations, enabling seamless integration of temporal information and ensuring continuous and detailed data coverage across the entire dataset. This approach allows for capturing a full range of tactile features and improving the robustness of the texture classification by providing a thorough and nuanced understanding of the sensor data.

Dataset	Frequency	Velocity	Number of Textures	Number of Samples Per Texture	Number of Features	Features	Window Sizes	Window Overlap	Total Number of Samples
Even	350Hz	30mm/s%	12	100	10	ax, ay, az, gx, gy, gz, mx, my, mz, baro	3s 6s	50%	8399 3599
Uneven	120Hz	15mm/s%	12	25	10	ax, ay, az, gx, gy, gz, mx, my, mz, baro	128 (1s) 256 (2s) 512 (4s)	50%	3962 1864 900

Table 4.1: Characteristics of uneven and even surface dataset

This extensive methodology is designed to capture diverse and nuanced tactile information, which serves as a crucial foundation for training and evaluating our texture classification models. The goal is to enhance the models' performance and generalizability, ensuring they are well-equipped to handle a variety of real-world scenarios. By focusing on detailed and varied data collection, our approach aims to improve the models' accuracy and applicability, making them more effective in distinguishing subtle differences between textures in practical applications. This meticulous preparation underscores the importance of having a well-rounded dataset for advancing tactile texture classification research and its practical implementation in robotic systems.

We employed three different model architectures to evaluate their performance on the prepared dataset. The first model is a Convolutional-Bidirectional LSTM model. This model includes convolutional layers to extract spatial features from the tactile data, followed by bidirectional LSTM layers to capture temporal dependencies in both forward and backward directions, enhancing the model's understanding of texture sequences. The second model is a 1D CNN model, which focuses on leveraging convolutional layers to extract features and includes a series of dense layers for the final classification. The third model is a Bidirectional LSTM model, designed to process the entire sequence of tactile data with bidirectional LSTM layers, followed by dense layers for classification.

To rigorously evaluate the performance of the models, we employed a 5-fold stratified cross-validation approach. This technique involves dividing the dataset into five equal parts, ensuring that each fold has a representative distribution of all texture classes. The benefits of this method include providing a more reliable estimate of model performance by training and validating the model on different subsets of the data and mitigating the risk of overfitting by ensuring that the model generalizes well across different data splits.

During training, the model was optimized using the Adamax optimizer with a learning rate set at 0.001, and gradients were clipped to mitigate potential instability issues. Training sessions spanned 250 epochs, with a batch size of 32 chosen to balance computational

efficiency and gradient accuracy.

The evaluation metrics used include accuracy, precision, recall, and F1 score. Accuracy measures the proportion of correctly classified instances over the total instances. Precision is the ratio of true positive predictions to the sum of true positive and false positive predictions, while recall is the ratio of true positive predictions to the sum of true positive and false negative predictions. The F1 score, being the harmonic mean of precision and recall, offers a balance between the two. The final confusion matrix, obtained by summing the confusion matrices of all folds, provides a comprehensive view of the model's performance across the entire validation set. From this matrix, we calculate the overall precision, recall, and F1 score, as well as the performance metrics for each class individually. This detailed analysis ensures a thorough understanding of the model's strengths and areas for improvement.

In conclusion, the combination of advanced model architectures, the sliding window approach for data preparation, and rigorous cross-validation techniques has enabled us to develop robust models for tactile texture classification. These methodologies not only enhance the accuracy and efficiency of the classification process but also bring robotic tactile perception closer to human-like capabilities.

4.1 Tactile Textures on Even Surfaces

4.1.1 Data Preprocessing

For the classification of tactile textures on even surfaces, the dataset used in this work was sourced from a study focusing on tactile texture recognition employing a multi-modal sensing module integrated into a tactile-enabled finger [96]. This dataset includes data collected from 12 different textures commonly encountered in everyday environments, such as plastic pencil cases, placemats, cork, denim fabric, felt, polyester cloth, and cotton scarf.

The data collection process involved exploring each texture with controlled movements, maintaining the finger's position while moving the textures in predefined directions at veloc-

ities of 30 mm/s, 35 mm/s, and 40 mm/s. This approach aimed to capture detailed sensory responses using pressure and MARG (Magnetic, Angular Rate, Gravity) sensors, providing a comprehensive dataset for analyzing and researching texture recognition and robotic manipulation.

We followed a similar approach to the authors in [97], who focused exclusively on the barometer sensor. to compare our model with their results, we performed the same process using both IMU sensors and barometer data. This allowed us to evaluate the performance of our model against theirs and gain insights into the impact of different sensor data on texture classification.

We utilized 1200 samples (corresponding to the 12 textures) collected at a velocity of 30 mm/s. These samples were recorded at a frequency of 350 Hz while exploring the textures. Subsequently, we applied our preprocessing pipeline to these raw samples, which involved converting the Python pickle files to CSV files for each of the 1200 samples.

Our preprocessing pipeline employs an overlapping sliding window approach with a configurable window size, set to overlap by 50% of the window size. This overlap was chosen to prevent excessive similarity among examples, thereby maintaining diversity in the training set and reducing the processing time needed to convert readings into machine-learning-ready data. High overlap thresholds can pose significant challenges in resource-constrained environments.

We experimented with window sizes of 3 and 6 seconds to examine the impact of temporal features on texture classification. These durations were chosen based on the data collection setup: a 3-second window corresponds to 25% of the exploration time, while a 6-second window corresponds to 50%. The following details our model's use of these window sizes.

This approach builds upon the work of the authors in [90], who utilized the same tactile dataset but applied an Active Learning (AL) strategy with a similar window size and overlapping configuration. Our research seeks to extend their methodology by employing the same data and sliding window approach within our own deep learning (DL) models. By

conducting this comparative analysis, we aim to evaluate the performance of our DL models against the established results and further validate their effectiveness using additional data collected from our experiments. This comparative evaluation will ensure the robustness and generalizability of our models across different datasets.

To provide a more complete comparison with existing work, it is important to note that the study referenced experimented with various window sizes, including 1-second, 3-second, 6-second, and 9-second windows. They found that while the 9-second window size improved classification results, this was largely due to capturing nearly all the available data within the 12-second window. The high degree of repetitive data points caused by overlapping windows artificially enhanced classification performance, although this improvement was somewhat misleading as it did not reflect true gains in texture classification accuracy. Conversely, they concluded that a 1-second window was insufficient for distinguishing textures, as it could not extract meaningful features necessary for accurate classification.

Additionally, they tested overlap percentages of 25%, 50%, and 75%, but found that 50% overlap yielded the best results. The 25% overlap was less effective, potentially due to the higher number of window instances leading to increased computational time without significantly improving classification performance. The 75% overlap was avoided because it could result in excessively similar examples, reducing diversity in the training set and increasing processing time, which might pose challenges in resource-constrained environments.

Therefore, we focused on evaluating our models using the best-performing configurations from their study: 3-second and 6-second windows with 50% overlap. This approach allowed for a fair comparison while considering the trade-offs identified in their experiments.

4.1.2 Texture Classification

We evaluated approximately 20 different model architectures to assess their effectiveness in classifying tactile texture data on even surfaces, focusing on various window durations. Our extensive experiments showed that numerous models achieved high classification accuracy,

demonstrating the robustness of our approach across diverse architectures. For each window duration, we selected the three best-performing models to showcase the diversity and strength of the classifiers.

The first model chosen is a straightforward Bidirectional LSTM (BDLSTM), which efficiently processes sequential tactile data by utilizing bidirectional LSTM layers to capture temporal dependencies in both directions. The second model is a 1D Convolutional Neural Network (CNN), which leverages convolutional layers to extract features from the tactile data and uses a series of dense layers for the final classification. The third model is a Convolutional-Bidirectional LSTM (BDLSTM), which combines convolutional layers to extract spatial features from the tactile data with bidirectional LSTM layers to capture temporal dependencies, enhancing the model's ability to classify texture sequences accurately. This selection highlights the capability of our methodology to achieve robust and accurate classification across various model complexities and structures, demonstrating the versatility and effectiveness of different neural network architectures in tactile texture classification.

The following table presents the evaluation metrics, including accuracy, precision, recall, and F1 score, for all models across different window duration. These results provide a comprehensive overview of the performance of each model under varying conditions in the context of tactile texture classification on even surfaces. This data offers valuable insights into their effectiveness and reliability in accurately identifying textures on flat surfaces.

Window Duration	Model	Training Accuracy	Validation Accuracy	Precision	Recall	F1 Score	Highest F1 Score reported in [90]
3 second	BiLSTM	99.23%	**98.6**%	98.7%	98.6%	98.7%	84.2%
	CNN	99.75%	97.5%	97.6%	97.5%	97.6%	
	CNN & BiLSTM	97.04%	96.1%	96.3%	96.1%	96.2%	
6 second	BiLSTM	99.89%	**99.6**%	99.6%	99.6%	99.6%	90.3%
	CNN	99.99%	97.5%	97.5%	97.5%	97.5%	
	CNN & BiLSTM	93.47%	91.8%	92.4%	91.8%	92.1%	

Table 4.2: Performance metrics of models on different window duration

Table 4.2 presents the evaluation metrics for different models using window durations of 3 seconds and 6 seconds. The results clearly indicate that the BiLSTM model outperforms others, achieving the highest evaluation metrics for both window durations. Specifically, for the 6-second window, the BiLSTM model attains a validation accuracy, precision, recall, and F1 score of 99.6%. For the 3-second window, it achieves a validation accuracy of 98.6%, precision of 98.7%, recall of 98.6%, and an F1 score of 98.7%. This demonstrates that despite its simplicity compared to more complex models, the BiLSTM model yields the best performance in our experiments.

In comparison to the Active Learning (AL) approach utilized by the authors in [90], our models show superior performance. The authors reported the highest F1 score of 90.3% for the 6-second window duration and 84.2% for the 3-second window duration, both achieved using an Extra Tree model within their AL framework. Not only does our BiLSTM model surpass these results, but all of our deep learning models exceed the performance metrics reported by the authors (see Table 4.2). This indicates a significant improvement in the effectiveness of our approach. The comparative analysis underscores the robustness and efficacy of our deep learning models, highlighting their potential for superior tactile data classification.

Furthermore, the consistency of the BiLSTM model's performance across different window durations emphasizes its reliability and adaptability. These findings suggest that our models are not only competitive but also potentially more effective than existing AL strategies, offering a promising avenue for future research and application in tactile texture classification.

4.1.2.1 Classification for a Window Duration of 3 Seconds

Bidirectional LSTM Classifier:

This model employs Bidirectional LSTM layers to proficiently capture temporal dependencies in both forward and backward directions, making it particularly well-suited for

tasks involving sequence data, such as tactile texture classification. The use of dropout and batch normalization layers aids in regularization, ensuring stable training, while dense layers facilitate the final classification process, as illustrated in Figure 3.14.

The model demonstrated outstanding performance across all validation folds. Key metrics, including precision, recall, and F1 score, were computed for each class using the aggregated confusion matrix from all folds (see Figure 4.1). The model achieved an overall accuracy of 98.6%, with precision of 98.7%, recall of 98.6%, and F1 scores of 98.7%, underscoring its efficacy in accurately classifying tactile textures across various categories. These results highlight the robustness of the model in handling diverse and complex tactile data.

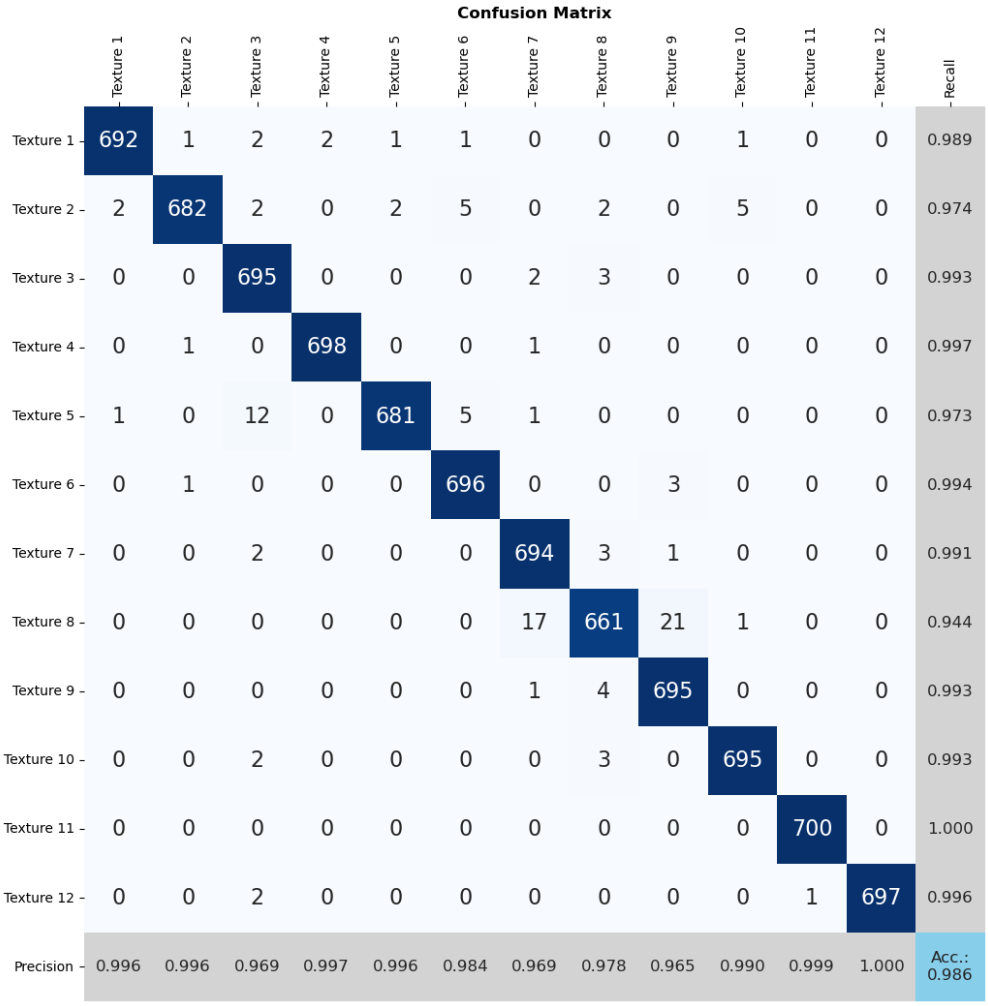

Figure 4.1: Confusion matrix of a BiLSTM classifier for window duration of 3 seconds

1D Convolutional Neural Network Classifier:

Figure 3.13 presents a detailed view of a 1D Convolutional Neural Network (CNN) architecture, meticulously designed for the multi-class classification of tactile texture data. This model is particularly tailored to capture and process the temporal features within the input data, which are crucial for accurately distinguishing between different texture classes. The architecture integrates several key components, including MaxPooling, Dropout, and BatchNormalization layers, each playing a significant role in enhancing the model's learning capacity and generalization capabilities. The MaxPooling layers reduce the dimensionality of the data while preserving important features, the Dropout layers prevent overfitting by randomly deactivating a fraction of neurons during training, and the BatchNormalization layers ensure that the data is normalized within each mini-batch, promoting stable and efficient learning.

Throughout the validation process, this 1D CNN model consistently demonstrated exceptional performance across all validation folds, reflecting its robustness and reliability. The model's effectiveness was evaluated using key metrics such as precision, recall, and F1 score, all of which were computed for each class using the aggregated confusion matrix from all validation folds. The model achieved an impressive overall accuracy of 97.5%, with precision reaching 97.6%, recall at 97.5%, and F1 scores also at 97.6%. These metrics underscore the model's proficiency in accurately classifying a wide range of tactile textures, highlighting its ability to generalize well across diverse data samples and maintain high performance across different texture classes.

To further support these findings, Figure 4.2 provides a comprehensive visualization in the form of a confusion matrix, derived from the validation dataset. This matrix offers a detailed breakdown of the model's classification performance, illustrating its capability to differentiate between various texture classes with high precision and recall metrics for each class. The confusion matrix not only reinforces the overall accuracy and effectiveness of the model but also sheds light on its strengths and potential areas for improvement in

classifying specific texture classes. Collectively, these results affirm the strong performance and reliability of the 1D CNN model in the classification of tactile textures, making it a valuable tool in the field of tactile sensing and robotic perception.

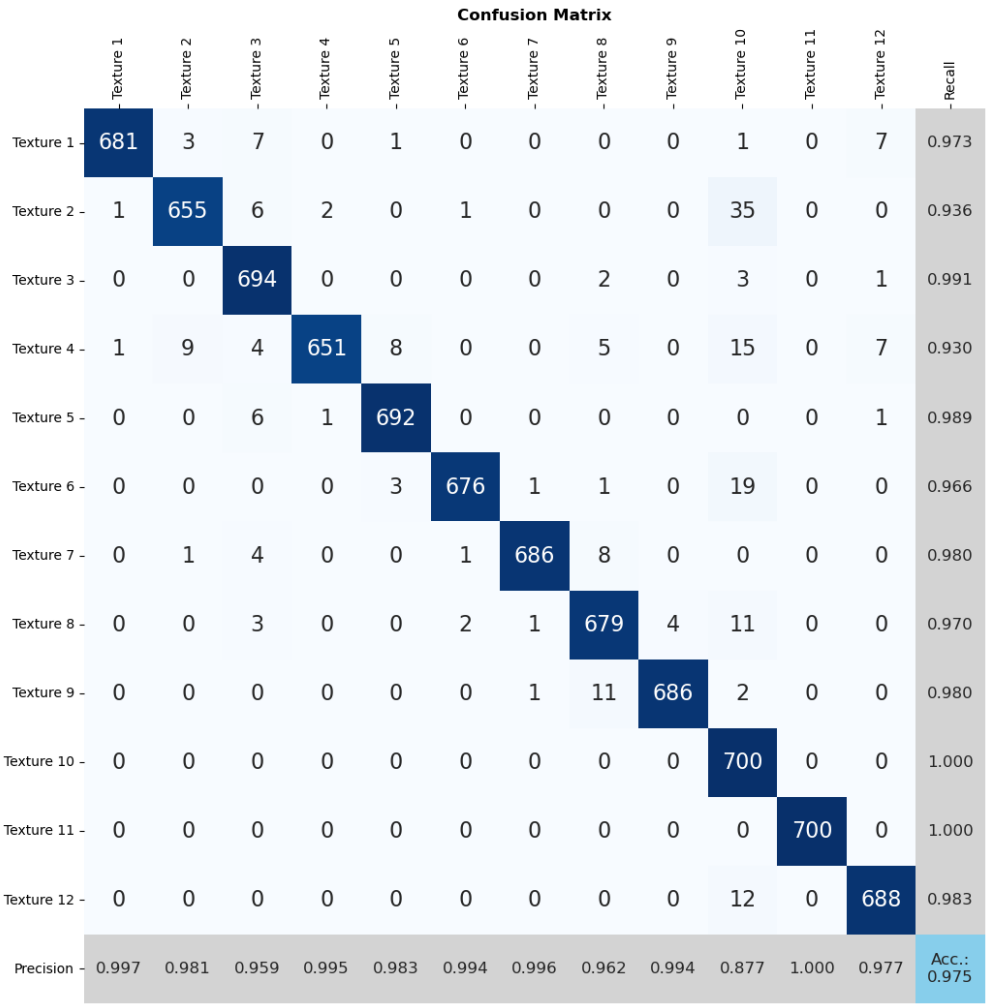

Figure 4.2: Confusion matrix of a 1D CNN classifier for window duration of 3 seconds

Convolutional-Bidirectional LSTM Classifier:

Figure 3.9 showcases a hybrid architecture that combines convolutional layers for feature extraction with bidirectional LSTM (BiLSTM) layers to capture temporal dependencies within the data. The model also incorporates Dropout, batch normalization, and Max-Pooling layers to enhance regularization and refine feature extraction.

The model demonstrated strong performance across all validation folds. Metrics such as

precision, recall, and F1 score were calculated for each class using the aggregated confusion matrix from all folds. The model achieved an overall accuracy of 96.1%, with precision, recall, and F1 scores of 96.3%, 96.1%, and 96.2%, respectively. These results underscore the model's effectiveness in accurately classifying various tactile textures.

Figure 4.3 provides a detailed view of the confusion matrix for the entire validation set, highlighting the model's ability to distinguish between different classes. This figure also presents precision and recall metrics for each class, offering a comprehensive overview of the model's classification accuracy and its capability to differentiate between various tactile textures.

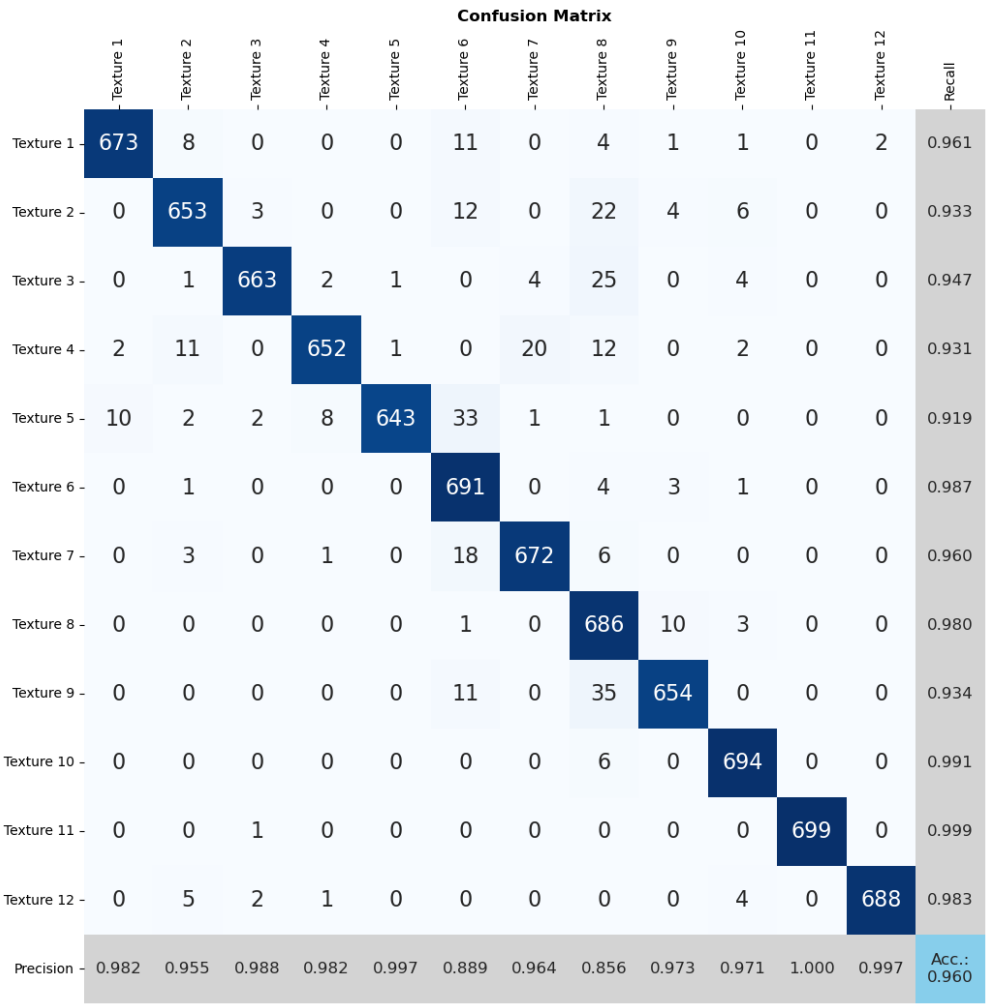

Figure 4.3: Confusion matrix of a Convolutional-Bidirectional LSTM classifier for window duration of 3 seconds

4.1.2.2 Classification for a Window Duration of 6 Seconds

Bidirectional LSTM Classifier:

This model leverages Bidirectional LSTM layers to effectively capture temporal dependencies in both forward and backward directions, making it exceptionally well-suited for sequence data tasks such as tactile texture classification. By processing information in both temporal directions, the model can capture intricate patterns and relationships within the data that might be missed by unidirectional approaches. The integration of dropout and batch normalization layers further enhances the model's performance by providing robust regularization, preventing overfitting, and ensuring stable training across diverse datasets. Dense layers are employed in the final classification stage, translating the extracted temporal features into accurate predictions, as depicted in Figure 3.14.

The model consistently exhibited outstanding performance across all validation folds, reflecting its reliability and precision. Key metrics, including precision, recall, and F1 score, were computed for each class using the aggregated confusion matrix derived from all validation folds. The model achieved an impressive overall accuracy of 99.6%, with precision, recall, and F1 scores also at 99.6%. These results clearly demonstrate the model's exceptional effectiveness in accurately classifying tactile textures across a wide range of categories, highlighting its ability to generalize well across varied data.

Figure 4.4 provides a detailed visualization of the confusion matrix for the entire validation dataset, offering a comprehensive view of the model's classification performance across all texture classes. This figure also includes precision and recall metrics for each class, offering deeper insights into the model's classification accuracy and its ability to distinguish between similar textures with high precision. The overall robustness and high performance of this Bidirectional LSTM model underscore its potential as a powerful tool for advanced tactile texture classification in various applications.

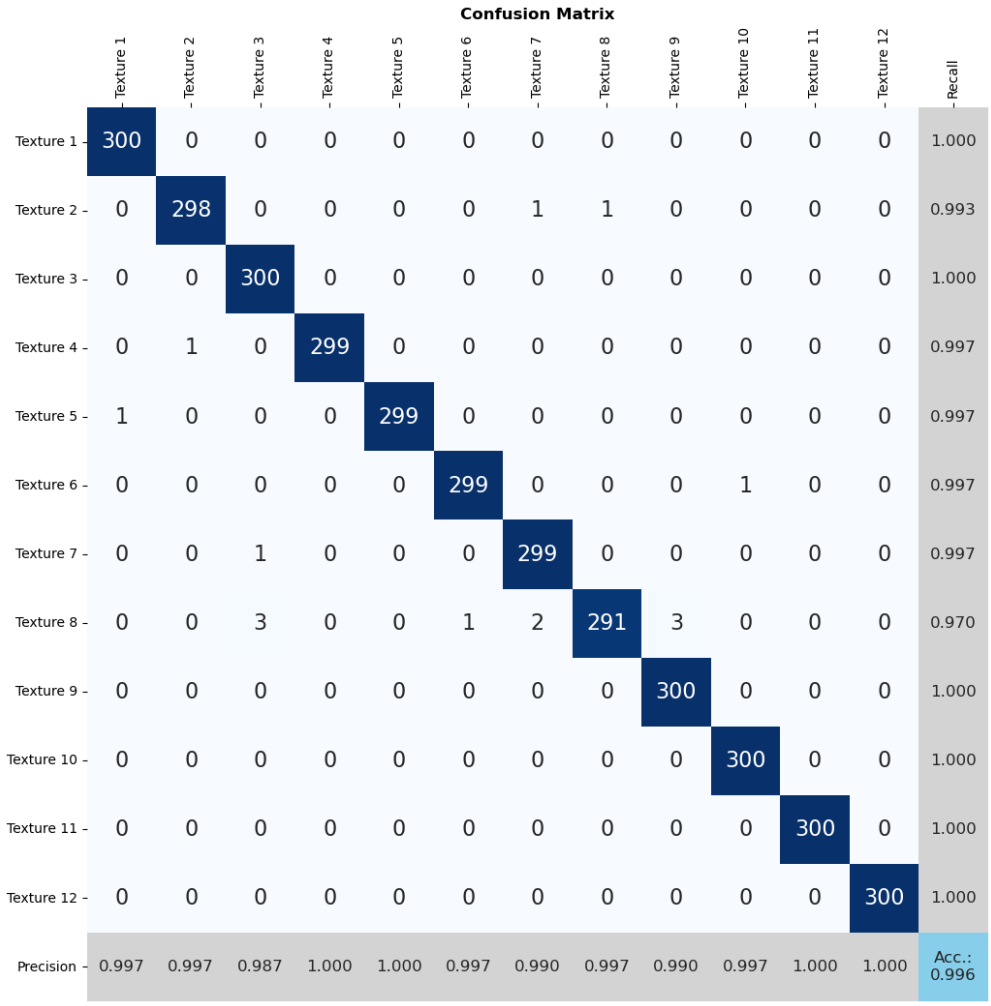

Figure 4.4: Confusion matrix of a BiLSTM classifier for window duration of 6 seconds

1D Convolutional Neural Network Classifier:

The model's architecture was meticulously crafted to capture the temporal dependencies and spatial features inherent in tactile sensor data. It featured sequential layers, integrating 1D Convolutional layers, Max-Pooling, Dropout, and Batch Normalization, culminating in a Dense output layer with softmax activation, as illustrated in Figure 3.11.

Throughout comprehensive cross-validation folds, the model consistently exhibited outstanding performance. Evaluation across all folds indicated an impressive overall accuracy of 97.5%, with precision, recall, and F1 score metrics each at 97.5%. These robust metrics underscore the model's effectiveness in accurately categorizing various tactile textures.

Figure 4.5 presents a detailed confusion matrix for the entire validation dataset, providing a comprehensive view of the model's classification performance across all categories. It also highlights the precision and recall metrics for individual classes, enhancing our understanding of the model's capability to distinguish between different tactile textures.

These results demonstrate the model's ability to effectively capture and classify complex patterns in tactile data, affirming its potential for real-world applications that require precise and reliable texture recognition. Additionally, the model's consistent performance across varied validation sets suggests its robustness and adaptability, making it a valuable asset for deploying in dynamic environments where accurate tactile perception is critical.

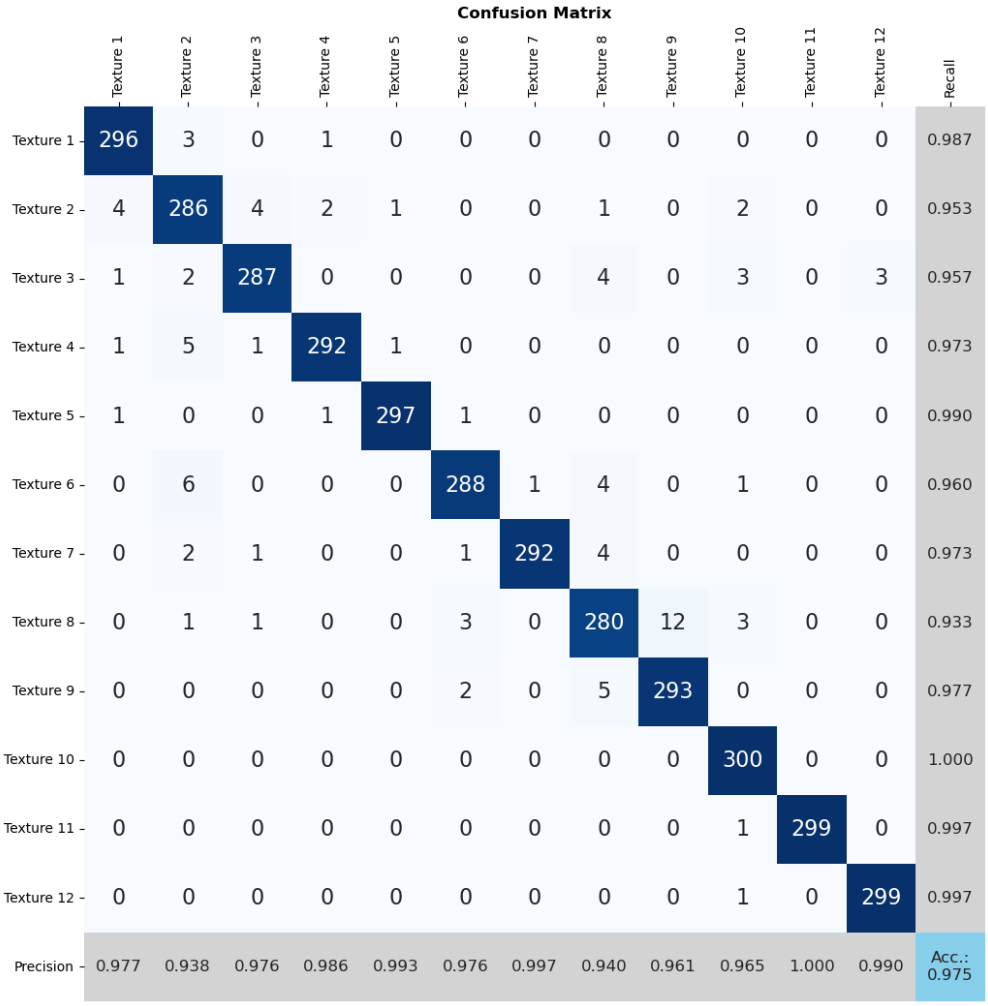

Figure 4.5: Confusion matrix of a 1D CNN classifier for window duration of 6 seconds

Convolutional-Bidirectional LSTM Classifier:

Figure 3.9 illustrates the hybrid architecture, which strategically integrates convolutional layers with bidirectional LSTM (BiLSTM) layers to optimize both spatial and temporal feature extraction from tactile texture data. The convolutional layers serve as a powerful tool for detecting and refining local patterns within the input data, while the BiLSTM layers excel in capturing the sequential dependencies inherent in tactile information. To further enhance the model's stability and generalization capabilities, Dropout, batch normalization, and MaxPooling layers are incorporated. These layers play a crucial role in preventing overfitting, normalizing activations, and downsampling the feature maps to retain the most salient information.

The model's performance was consistently robust across all validation folds, reflecting its capacity to generalize well to unseen data. Key evaluation metrics, including precision, recall, and F1 score, were meticulously calculated for each class using an aggregated confusion matrix derived from all validation folds. The model achieved an overall accuracy of 91.8%, with precision at 92.4%, recall at 91.8%, and F1 scores at 92.1%. These metrics underscore the model's strong capability to accurately classify a diverse range of tactile textures, despite the inherent challenges posed by the complex and varied nature of the input data.

Figure 4.6 provides a detailed overview of the confusion matrix across the entire validation dataset, offering an in-depth look at the model's performance on a per-class basis. This visualization not only illustrates the model's ability to differentiate between texture classes but also highlights the precision and recall achieved for each specific class. Such detailed insights into the model's classification accuracy and discriminatory power are crucial for understanding its strengths and potential areas for improvement, ultimately validating its effectiveness in real-world applications where accurate tactile texture recognition is essential.

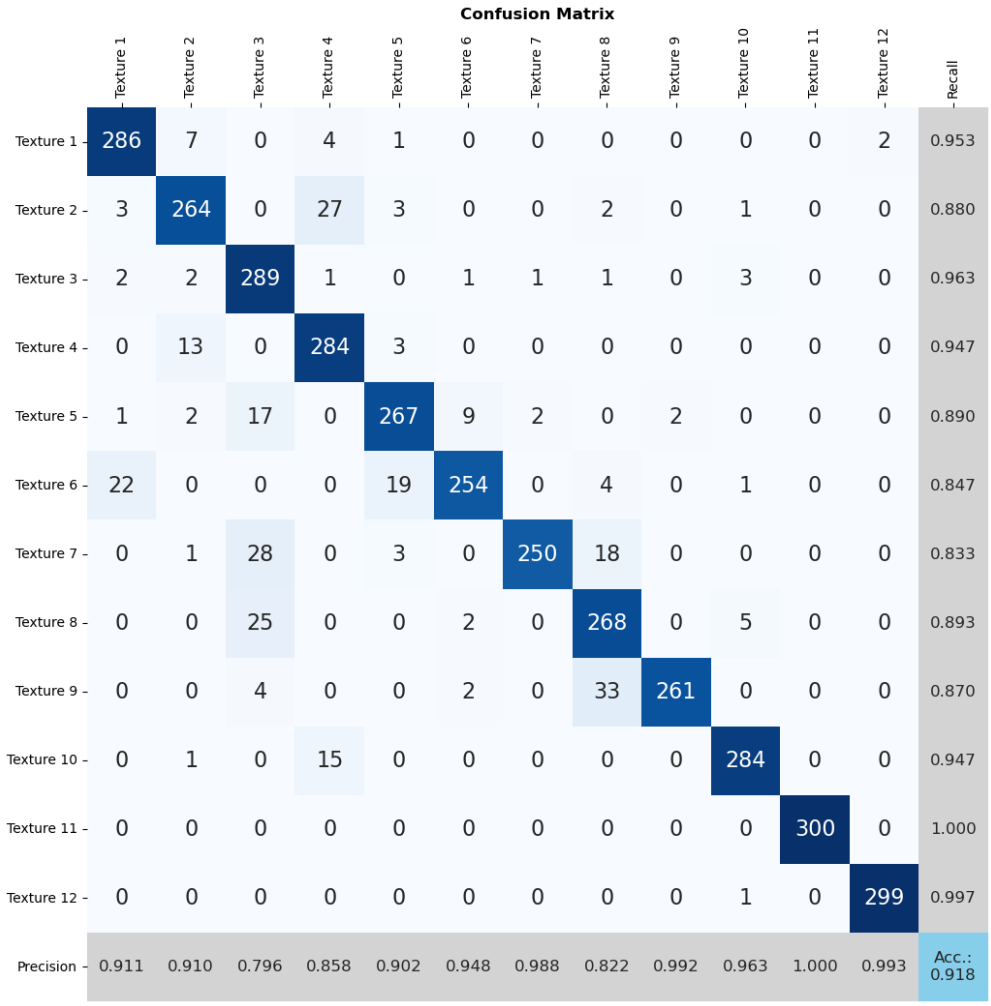

Figure 4.6: Confusion matrix of a Convolutional-Bidirectional LSTM classifier for window duration of 6 seconds

By using identical data and sliding window approaches, For a window duration of 3 seconds, the BiLSTM model achieved the best performance with a validation accuracy of 98.6% and an F1 score of 98.7%. The 1D CNN model followed, with a validation accuracy of 97.5% and an F1 score of 97.6%. The hybrid 1D CNN and BiLSTM model obtained a validation accuracy of 96.1% and an F1 score of 96.2%. For a window duration of 6 seconds, the BiLSTM model again outperformed others, achieving a validation accuracy and F1 score of 99.6%. The 1D CNN model maintained a validation accuracy and F1 score of 97.5%, while the hybrid 1D CNN and BiLSTM model had a validation accuracy of 91.8% and an F1 score of 92.1%. In comparison, the best F1 scores reported in [90] were 90.3% for the 6-

second window duration and 84.2% for the 3-second window duration using an active learning approach. This clearly indicates that not only our top-performing model but all of our models surpass those results and we have ensured a fair comparison with the existing work, thereby validating the robustness and generalizability of our models. The superior performance of our model, as evidenced by the higher evaluation metrics, supports the conclusion that our deep learning approach is well-suited for tactile data analysis. This work paves the way for further exploration and optimization of tactile sensing systems, ultimately enhancing the capabilities of robotic systems in real-world applications.

4.2 Tactile Texture on Uneven Surfaces

4.2.1 Data Collection & Preprocessing

The primary focus of this research is the classification of tactile textures on uneven surfaces. To achieve this, we collected data from an uneven surface with 12 distinct textures, each with a concave-convex shape. This challenging surface geometry aims to mimic real-world conditions more closely, where textures are rarely flat or uniform.

For data acquisition, we utilized a combination of MARG (Magnetic, Angular-Rate, Gravity) and barometer sensors. The MARG sensors provided comprehensive data including 3-axis magnetic, 3-axis angular velocity, and 3-axis gravity readings, totaling 9 dimensions (see Fig. 4.7). Along with one barometer reading (see Fig. 4.8), this made a total of 10 dimensions for our dataset. Tactile data was collected across 25 trajectories for each of the 12 textures, resulting in a total of 300 samples.

For each sample, the pipeline generates a scaled instance using a MinMax scaler, which normalizes the data to a range of 0 to 1 across its 10 dimensions. This scaling ensures that all dimensions contribute equally to the model's training process, preventing dimensions with larger ranges from dominating the learning algorithm. Additionally, MinMax scaling enhances the comparability of the dimensions, which can lead to more insightful visualizations

and more effective pattern recognition during the training process. The resulting scaled data frame, containing the statistical features for each sample, is then used to train the machine learning models.

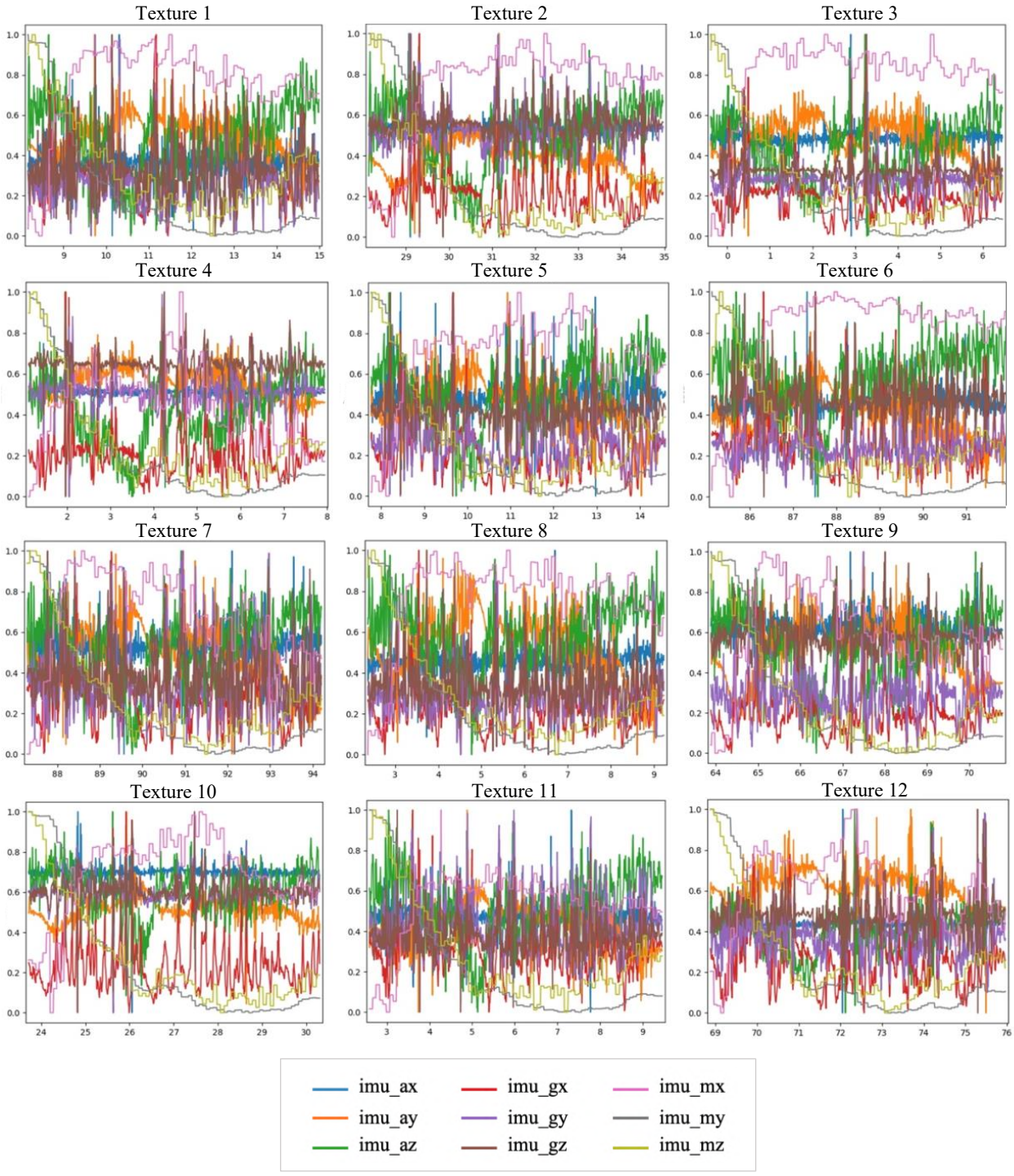

Figure 4.7: Sample of the MARG data for each of the 12 textures

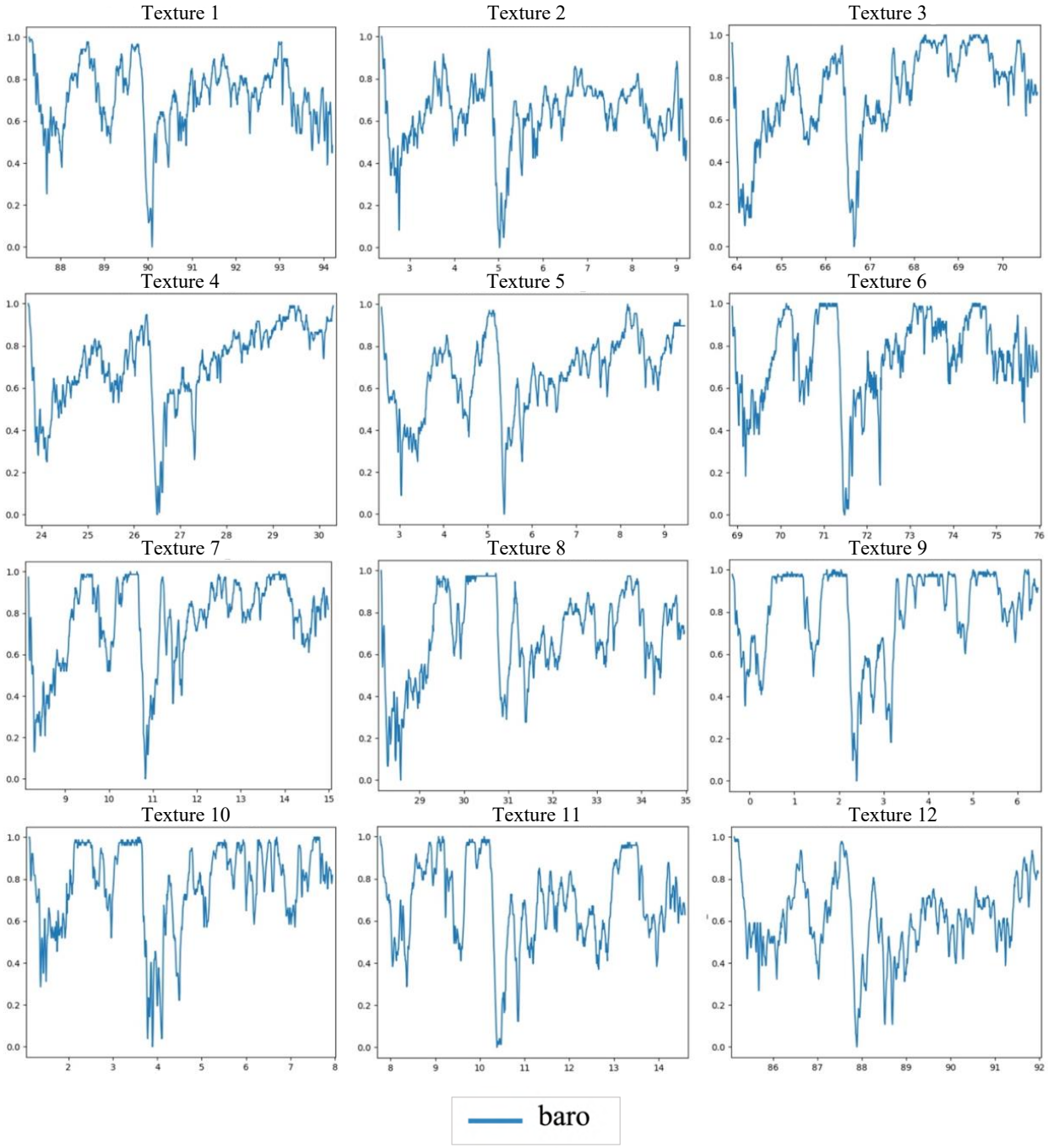

Figure 4.8: Sample of the barometer data for each of the 12 textures

We applied a preprocessing pipeline to these raw samples, which involves using an overlapping sliding window with a configurable window size and an overlap set to 50% of the window size. Higher overlapping thresholds could result in excessively similar examples within the sequence, potentially reducing diversity in the training set and increasing the

processing time required to transform readings into machine-learning-ready examples. This could pose challenges in resource-constrained environments.

We experimented with three window sizes (128, 256, and 512) to explore the impact of temporal features on our texture classification task. This approach generated three datasets: one with a window size of 128 and 50% overlap consisting of 3962 instances, another with a window size of 256 and 50% overlap consisting of 1864 instances, and another with a window size of 512 and 50% overlap consisting of 900 instances.

4.2.2 Texture Classification

In this study, we evaluated nearly 100 different model architectures to determine their effectiveness in classifying tactile texture data on uneven surfaces. Our extensive experimentation demonstrated that a wide range of models achieved high classification accuracy, showcasing the robustness of our approach across various architectures. For each window size, we selected the three best-performing models to highlight the diversity and strength of the classifiers.

The first selected model is a simple Bidirectional LSTM (BDLSTM) model. This model effectively processes the sequential tactile data, leveraging bidirectional LSTM layers to capture temporal dependencies in both directions and providing a strong baseline for texture classification.

The second chosen model is a 1D Convolutional Neural Network (CNN) model in our selection. This model focuses on leveraging convolutional layers to extract features from the tactile data and employs a series of dense layers for the final classification. The 1D CNN model showcases the power of convolutional networks in processing sequential data and demonstrates its effectiveness in texture classification.

Finally, we included a more complex Convolutional-Bidirectional LSTM (BDLSTM) model. This sophisticated architecture combines convolutional layers to extract spatial features from the tactile data with bidirectional LSTM layers to capture temporal dependencies

in both forward and backward directions. This dual approach enhances the model's ability to understand and classify texture sequences accurately.

By selecting these three models, we highlight the versatility and performance of different neural network architectures in tactile texture classification. This selection underscores the capability of our methodology to achieve robust and accurate classification across a variety of model complexities and structures.

The results are summarized in Table 4.3, which details the performance metrics for our models, including 1D Convolutional Neural Networks (CNN), Bidirectional Long Short-Term Memory (BiLSTM) networks, and a hybrid model combining both architectures. The evaluation spans various window sizes: 128, 256, and 512. The metrics reported include accuracy, precision, recall, and F1 score, providing a thorough assessment of each model's effectiveness.

Window Size	Model	Training Accuracy	Validation Accuracy	Precision	Recall	F1 Score
128	CNN & BiLSTM	99.93%	**95.6**%	95.7%	95.6%	95.6%
	CNN	99.92%	94.0%	94.1%	94.1%	94.1%
	BiLSTM	99.97%	90.4%	90.4%	90.4%	90.4%
256	CNN	99.97%	**93.0**%	93.1%	93.1%	93.1%
	CNN & BiLSTM	99.83%	92.5%	92.8%	92.5%	92.6%
	BiLSTM	100%	88.7%	88.9%	88.8%	88.9%
512	CNN	100%	**96.4**%	96.6%	96.4%	96.5%
	CNN & BiLSTM	99.94%	91.1%	91.2%	91.1%	91.2%
	BiLSTM	99.94%	89.0%	89.1%	89.0%	89.0%

Table 4.3: Performance metrics of models on different window sizes

This analysis is instrumental in understanding how well these models perform in accurately identifying textures on uneven surfaces, offering a comprehensive view of their capabilities and strengths. The high validation accuracy, with the highest being 95.6% for a window size of 128, 93.0% for a window size of 256, and 96.4% for a window size of 512, demonstrates the models' proficiency in capturing and classifying intricate tactile patterns.

4.2.2.1 Classification for Window Size of 128

Convolutional-Bidirectional LSTM Classifier:

The model architecture, depicted in Figure 3.8, was composed of sequential layers, incorporating Convolutional Neural Networks(CNN), Max-Pooling, Dropout, Batch Normalization, and Bidirectional Long Short-Term Memory (BiLSTM) layers. It concluded with a Dense output layer utilizing softmax activation. This specific design was selected to efficiently capture both the temporal dependencies and spatial features present in tactile sensor data.

The model consistently demonstrated exceptional performance across all folds. Evaluation metrics, including precision, recall, and F1 score, were computed for each class based on the aggregated confusion matrix from all folds. With an overall accuracy of 95.6%, precision of 95.7%, recall of 95.6%, and F1 score of 95.6%, these results underscore the model's robustness in accurately classifying tactile textures across all classes.

Visual representations in Figure 4.9 illustrated representative learning curves and accuracy trends observed during the training and validation phases. These visual insights provided a clear depiction of the model's progression over epochs, showcasing convergence patterns and performance fluctuations.

Figure 4.10 complements these findings by presenting the confusion matrix for the entire validation dataset, offering a comprehensive view of the model's classification performance across all classes. Additionally, Figure 4.10 delineates precision and recall metrics for each class, further enhancing understanding of the model's discriminatory capabilities. As evident in this figure, the lowest precision is observed for texture 1 at 88.4%, while the highest precision is for texture 10 at 99.1%. In terms of recall, texture 2 has the lowest at 89.6%, whereas texture 4 achieves the highest recall at 100%.

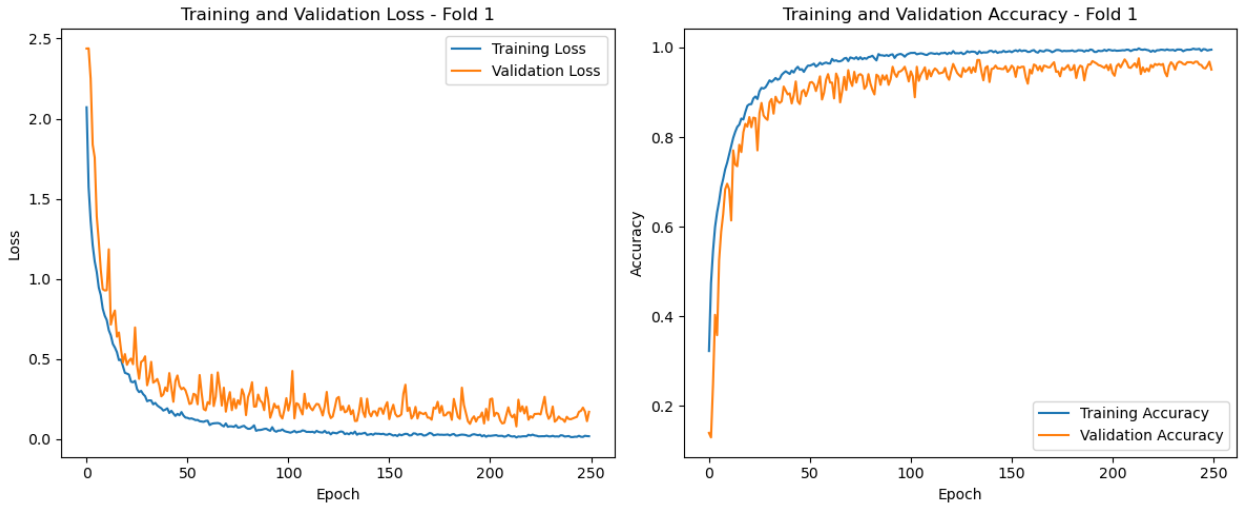

Figure 4.9: Learning and accuracy curves of a Convolutional-Bidirectional LSTM classifier for window size of 128

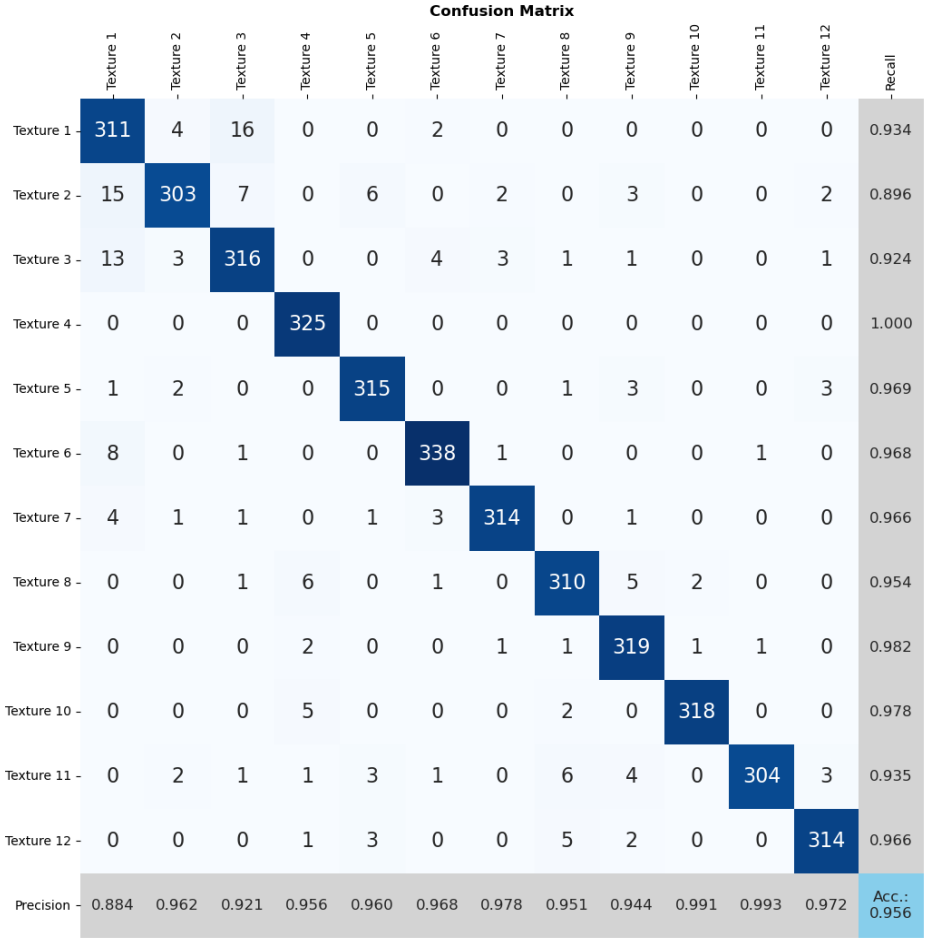

Figure 4.10: Confusion matrix of a Convolutional-Bidirectional LSTM classifier for window size of 128

1D Convolutional Neural Network Classifier:

The model architecture was carefully designed to capture both the temporal dependencies and spatial features inherent in tactile sensor data. It consisted of sequential layers that combined 1D Convolutional, Max-Pooling, Dropout, and Batch Normalization, ultimately concluding with a Dense output layer utilizing softmax activation, as shown in Figure 3.11.

Across rigorous cross-validation folds, the model consistently demonstrated exceptional performance metrics. Evaluation across all folds revealed an impressive overall accuracy of 94.0%, with precision ,recall and F1 score metrics at 94.1%. The model's robust evaluation metrics underscored its efficacy in accurately categorizing tactile textures across diverse classes.

Figure 4.11 visually depicted the model's learning curves and accuracy trends observed during its training and validation phases. These visualizations offered a clear view of how the model's performance evolved over epochs, highlighting patterns of convergence and fluctuations in its effectiveness.

Figure 4.12 provided a detailed confusion matrix for the entire validation dataset, presenting a holistic view of the model's classification performance across all categories. Additionally, it showcased precision and recall metrics for individual classes, enhancing our understanding of the model's ability to distinguish between different tactile textures. As is evident in this figure, the lowest precision is observed for texture 2 at 89.3%, while the highest precision is for texture 6 at 98.5%. In terms of recall, texture 8 has the lowest at 89.8%, whereas texture 4 achieves the highest recall at 99.1%. These findings highlight the model's capacity to effectively capture and classify complex patterns in tactile data, affirming its potential for real-world applications requiring precise and reliable texture recognition.

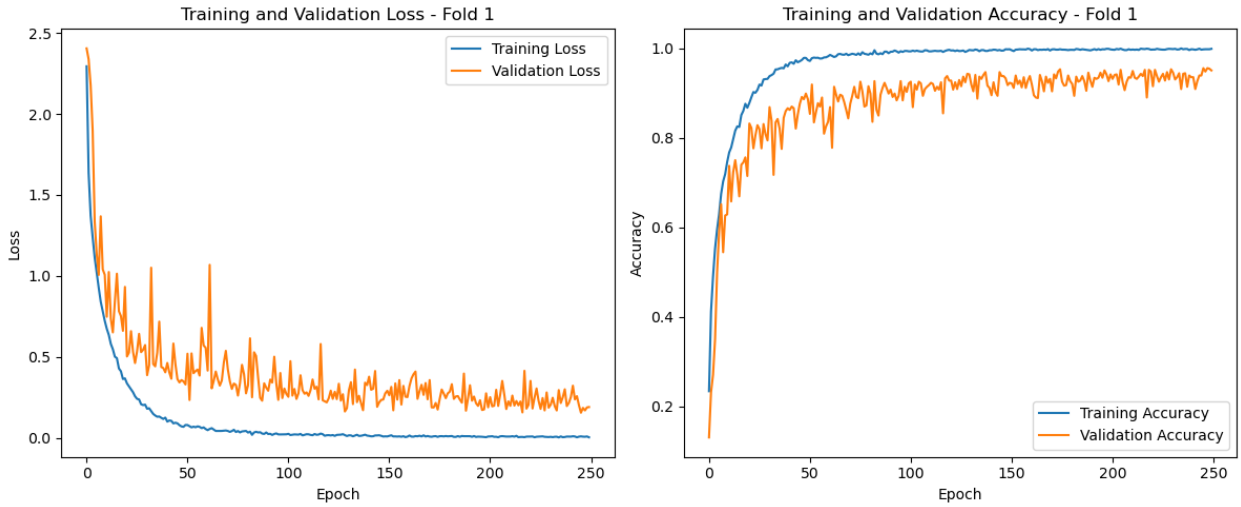

Figure 4.11: Learning and accuracy curves of a 1D CNN classifier for window size of 128

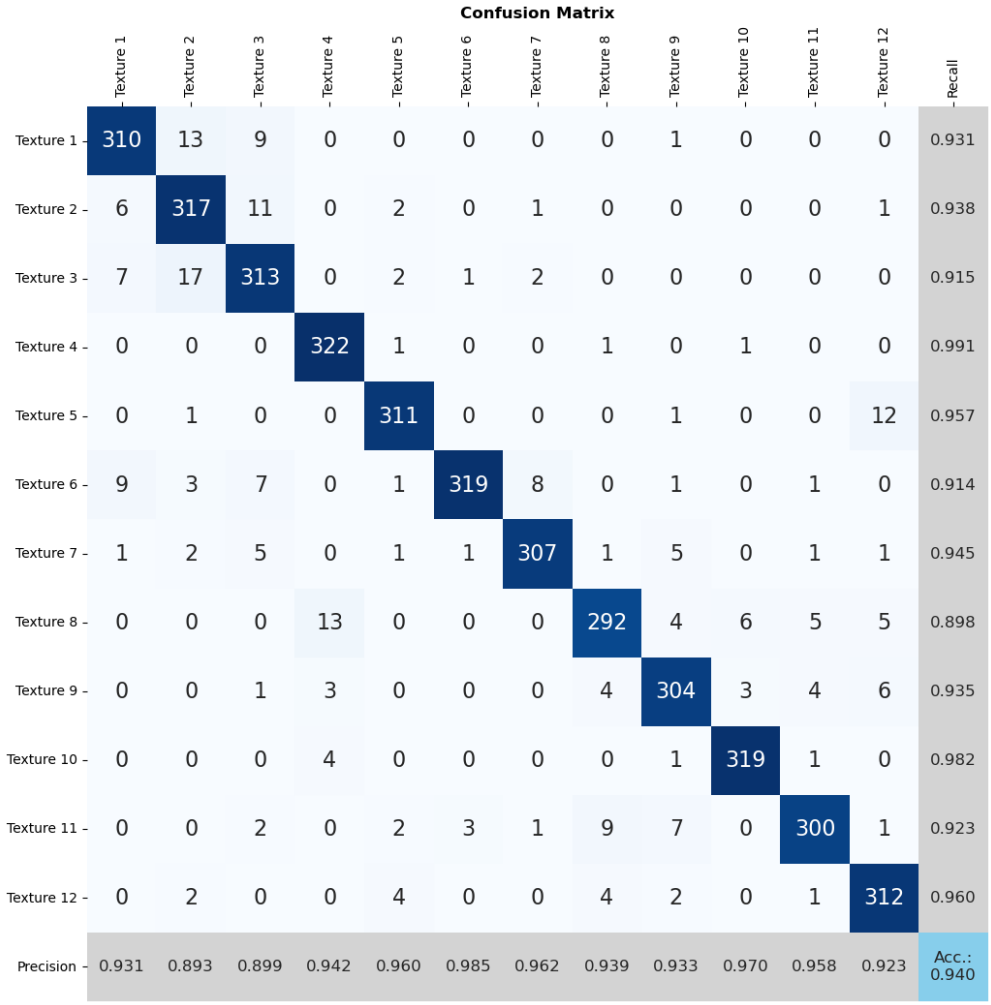

Figure 4.12: Confusion matrix of a 1D CNN classifier for window size of 128

Bidirectional LSTM Classifier:

This model utilizes Bidirectional LSTM layers to adeptly capture temporal dependencies in both directions, making it particularly suitable for tasks involving sequence data like tactile texture classification. The inclusion of dropout and batch normalization layers aids in regularization, ensuring stable training, while dense layers facilitate the final classification process, as depicted in Figure 3.14.

The model showcased excellent performance across all validation folds. Metrics such as precision, recall, and F1 score were calculated for each class, using the combined confusion matrix from all folds. Achieving an overall accuracy of 90.4%, a precision, recall and an F1 score of 90.4%, the results clearly indicate the model's effectiveness in accurately classifying tactile textures across various categories.

Figures 4.13 and 4.14 provide a visual depiction of the model's performance. Figure 4.13 illustrates the learning curves and accuracy trends during training and validation, highlighting the model's progression over epochs and showing patterns of convergence and fluctuations in performance. Figure 4.14 presents the confusion matrix for the entire validation dataset, offering a detailed view of the model's classification performance across all classes. This figure also includes precision and recall metrics for each class, which are crucial for understanding the model's effectiveness and discriminatory abilities in detail. As is evident from this figure, the precision varies significantly among different textures, with texture 2 achieving the lowest precision at 84.4%, and texture 10 reaching the highest precision of 97.5%. Similarly, the recall metrics reveal variability in the model's performance, with texture 3 having the lowest recall at 78.7%, while texture 4 demonstrates the highest recall at 98.5%. These variations highlight the model's strong overall performance while also indicating areas where it may need further improvement. Such detailed insights into precision and recall provide a comprehensive understanding of the model's strengths and limitations in classifying various tactile textures.

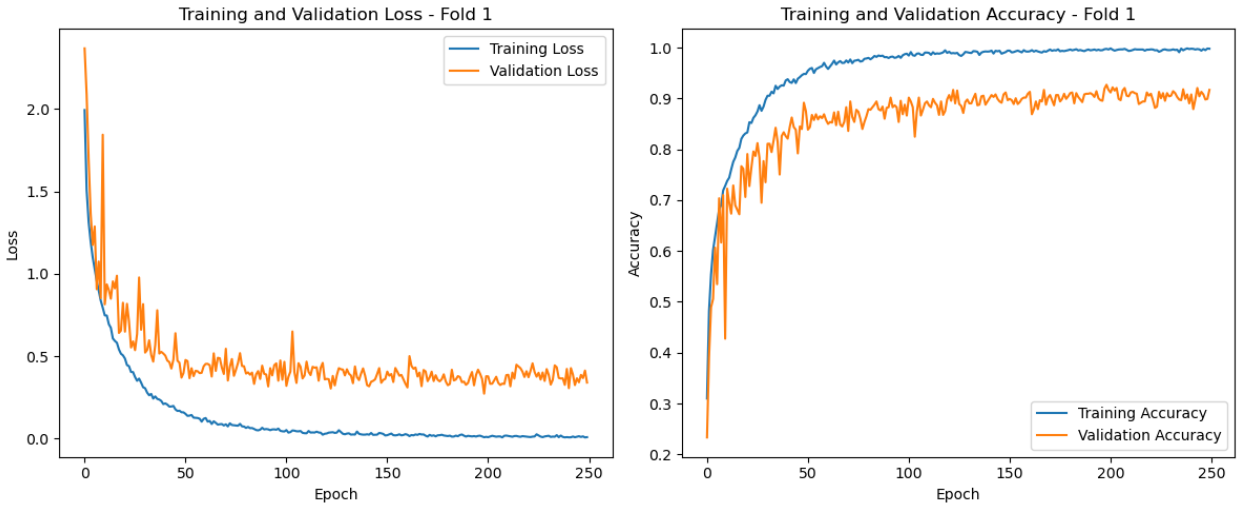

Figure 4.13: Learning and accuracy curves of a BiLSTM classifier for window size of 128

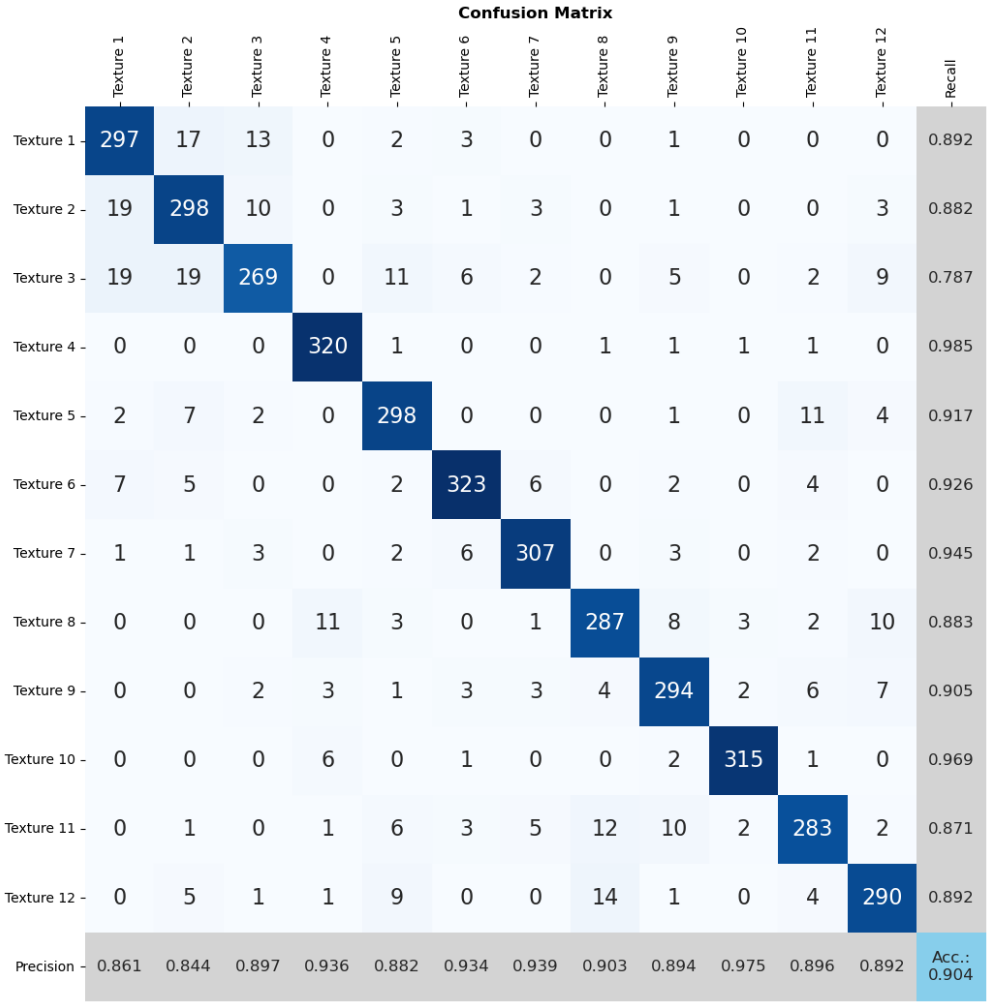

Figure 4.14: Confusion matrix of a BiLSTM classifier for window size of 128

4.2.2.2 Classification for Window Size of 256

1D Convolutional Neural Network Classifier:

This architecture is crafted to efficiently capture and classify intricate patterns within tactile texture data. It utilizes Convolutional Neural Network (CNN) layers for feature extraction, incorporating MaxPooling for dimensionality reduction and Dropout for regularization. Dense layers are employed for final classification tasks, as illustrated in Figure 3.12.

The model exhibited strong performance across all validation folds. Precision, recall, and F1 score metrics were computed for each class using the aggregated confusion matrix from all folds. With an overall accuracy of 93.0%, and precision, recall, and F1 scores of 93.1%, these results demonstrate the model's proficiency in accurately classifying tactile textures across various categories.

Figures 4.15 and 4.16 visually represent the model's performance. Figure 4.15 shows the learning curves and accuracy trends observed during training and validation, highlighting the model's progression over epochs and revealing patterns of convergence and performance fluctuations. Figure 4.16 displays the confusion matrix for the entire validation dataset, providing a detailed view of the model's classification accuracy across all classes. This figure also includes precision and recall metrics for each class, offering deeper insights into the model's discriminatory capabilities. As is evident from this figure, the precision varies among textures, with texture 2 exhibiting the lowest precision at 85.0%, while texture 10 achieves the highest precision of 98.6%. For recall, texture 3 has the lowest value at 86.3%, whereas texture 4 shows the highest recall at 100%. These metrics underscore the model's overall performance while highlighting specific areas of strength and potential improvement in its classification of tactile textures.

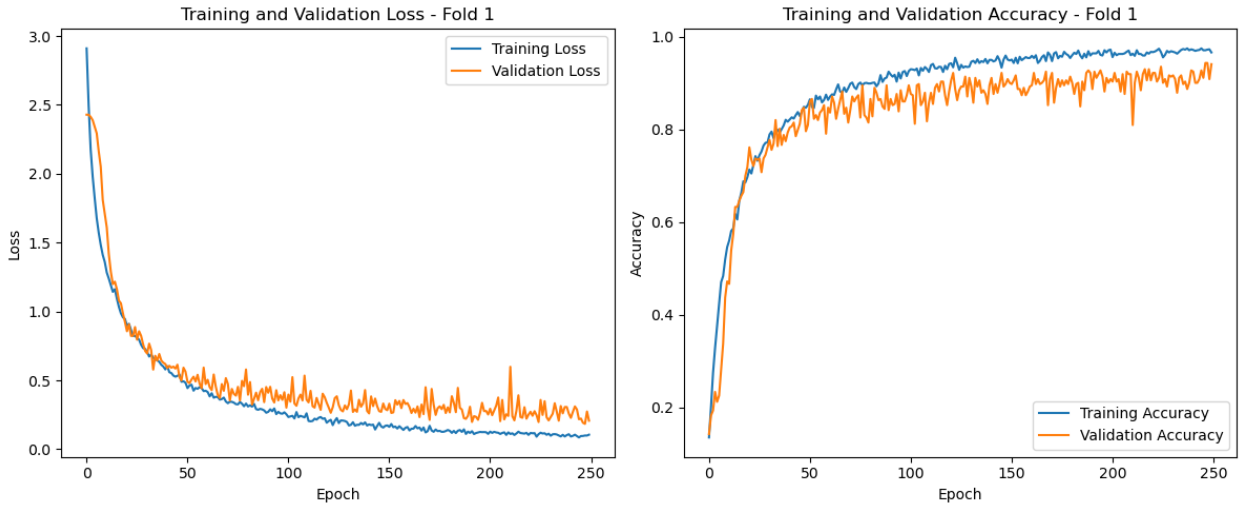

Figure 4.15: Learning and accuracy curves of a 1D CNN classifier for window size of 256

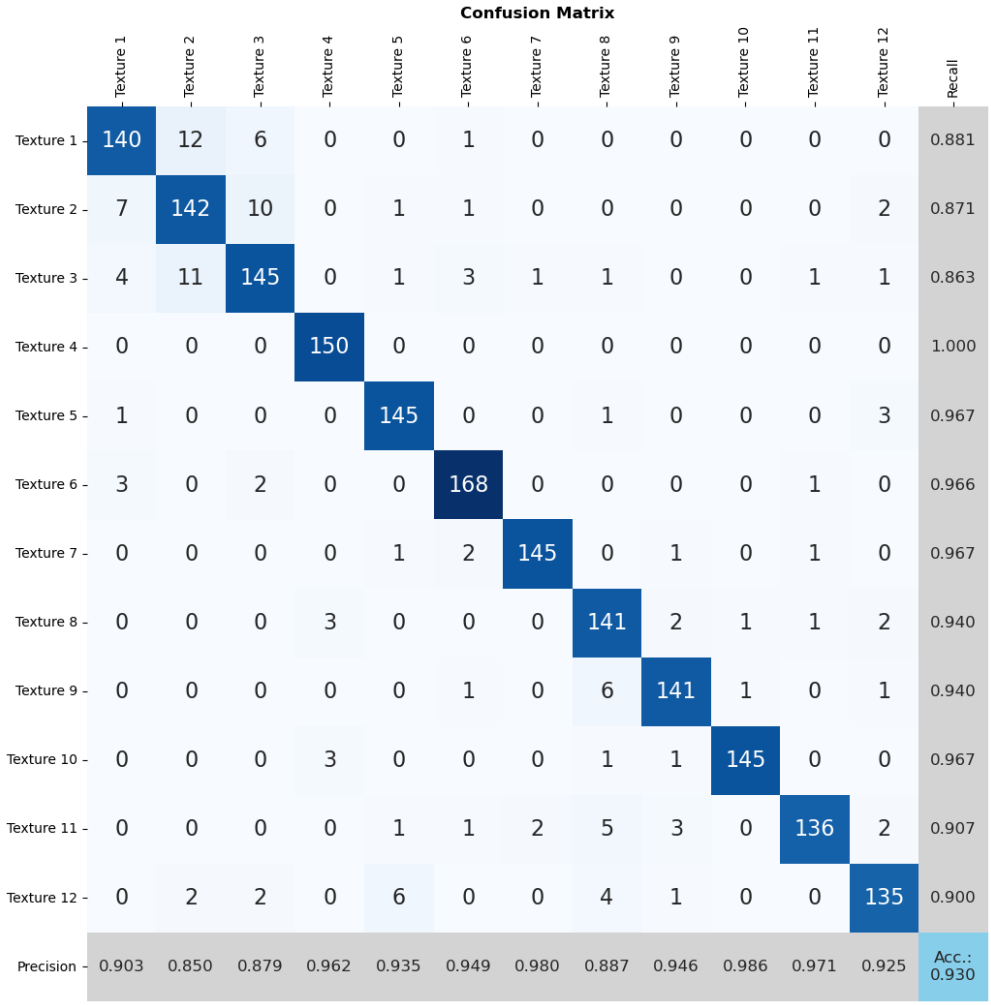

Figure 4.16: Confusion matrix of a 1D CNN classifier for window size of 256

Convolutional-Bidirectional LSTM Classifier:

Figure 3.9 illustrates this hybrid architecture, which effectively integrates convolutional layers for feature extraction with bidirectional LSTM (BiLSTM) layers to capture temporal dependencies in the data. Dropout, batch normalization, and MaxPooling layers are incorporated to enhance regularization and facilitate feature refinement.

The model exhibited strong performance across all validation folds. Precision, recall, and F1 score metrics were computed for each class using the aggregated confusion matrix from all folds. With an overall accuracy of 92.5%, and precision, recall, and F1 scores of 92.8%, 92.5%, and 92.6% respectively, these results demonstrate the model's proficiency in accurately classifying tactile textures across various categories.

Figure 4.17 displays the learning curves and accuracy trends throughout both the training and validation phases. This comprehensive visualization illustrates the model's performance evolution over time, highlighting improvements and stability in accuracy. The curves reflect how the model's accuracy increased as training progressed, indicating effective learning and adaptation. Additionally, the validation accuracy trends offer insights into the model's generalization capability, showcasing its ability to maintain performance on unseen data.

Figure 4.18 provides an insightful look at the confusion matrix for the entire validation set, illustrating how well the model distinguishes between different classes. Additionally, this figure highlights precision and recall for each class, giving a detailed picture of the model's classification accuracy and its ability to discern between different tactile textures. As shown in this figure, the lowest precision is observed for texture 3 at 87.6%, while the highest precision is achieved by texture 7 at 99.2%. For recall, the lowest is for texture 11 at 87.3%, and the highest is for texture 4 at 100%.

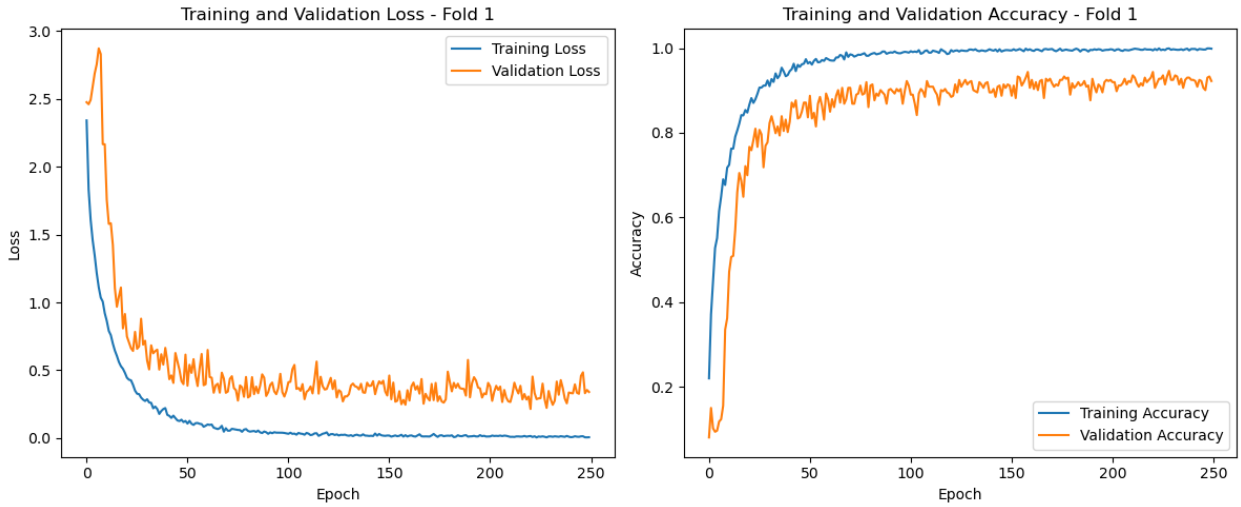

Figure 4.17: Learning and accuracy curves of a Convolutional-Bidirectional LSTM classifier for window size of 256

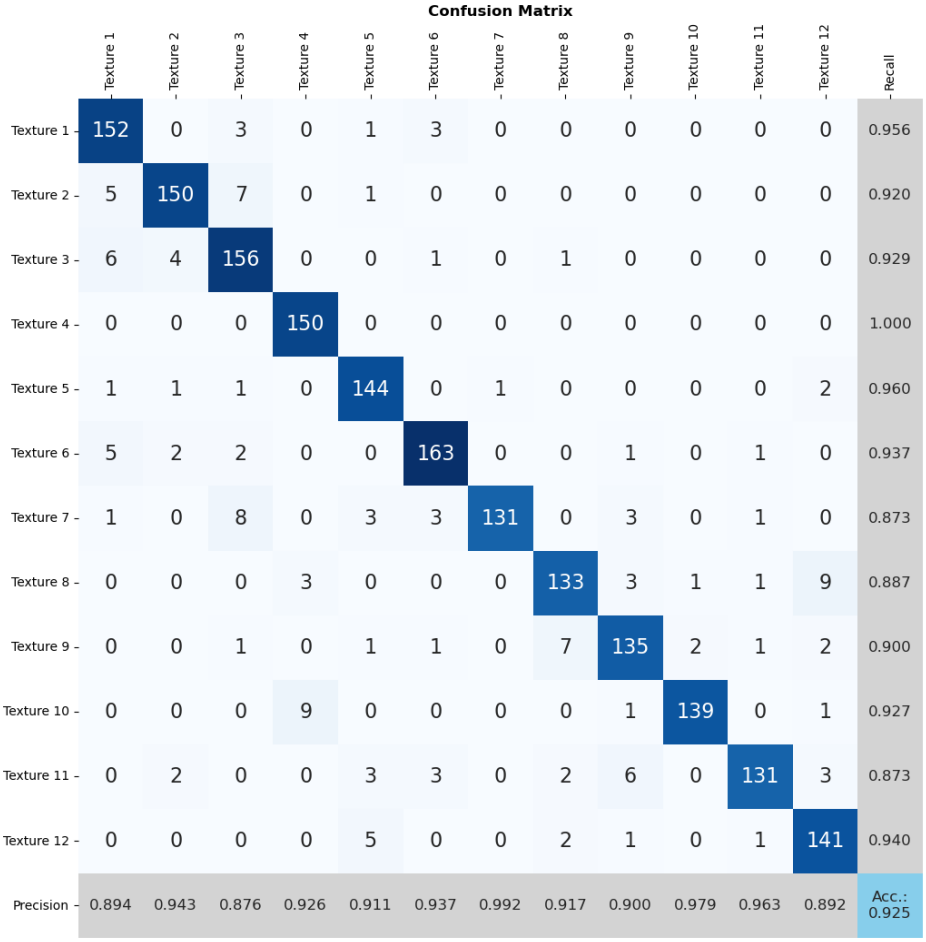

Figure 4.18: Confusion matrix of a Convolutional-Bidirectional LSTM classifier for window size of 256

Bidirectional LSTM Classifier:

This model architecture leverages the strengths of Bidirectional LSTM layers to capture temporal dependencies in the data from both directions. The inclusion of dropout and batch normalization layers helps in preventing overfitting and stabilizing training, ensuring robust performance, as illustrated in Figure 3.14.

The model demonstrated commendable performance across all validation folds. Precision, recall, and F1 score metrics were evaluated for each class using the aggregated confusion matrix from all folds. The model achieved an overall accuracy of 88.7%, with precision, recall, and F1 scores of 88.9%, 88.8%, and 88.9%, respectively. These results affirm the model's ability to accurately classify a diverse range of tactile textures.

Figures 4.19 and 4.20 provide a comprehensive visualization of the model's performance. Figure 4.19 illustrates the learning curves and accuracy trends observed during both the training and validation phases. This figure provides a comprehensive view of the model's performance evolution over time, highlighting consistent improvements and the stability of the learning process. It showcases how the model's accuracy and loss metrics fluctuate during training, offering insights into the convergence behavior and the overall effectiveness of the training strategy. The curves reveal a steady progression in performance, reflecting the model's ability to learn and adapt to the data effectively throughout the training process. Meanwhile, Figure 4.20 presents a detailed confusion matrix for the entire validation dataset, showcasing the model's capability to distinguish between different classes. Additionally, this figure offers class-specific precision and recall metrics, providing deeper insights into the model's classification performance and its effectiveness in identifying various tactile textures. As is evident in this figure, the lowest precision is observed for texture 1 at 80%, while the highest precision is achieved for texture 10 at 97.3%. For recall, the lowest is recorded for texture 2 at 81.6%, with the highest recall found for texture 4 at 98%.

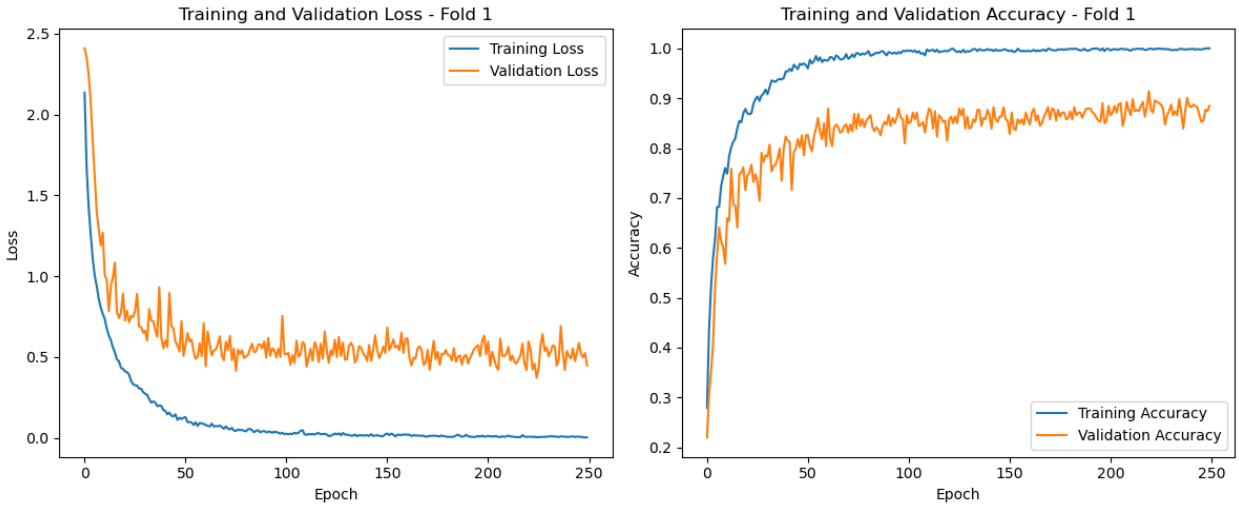

Figure 4.19: Learning and accuracy curves of a BiLSTM classifier for window size of 256

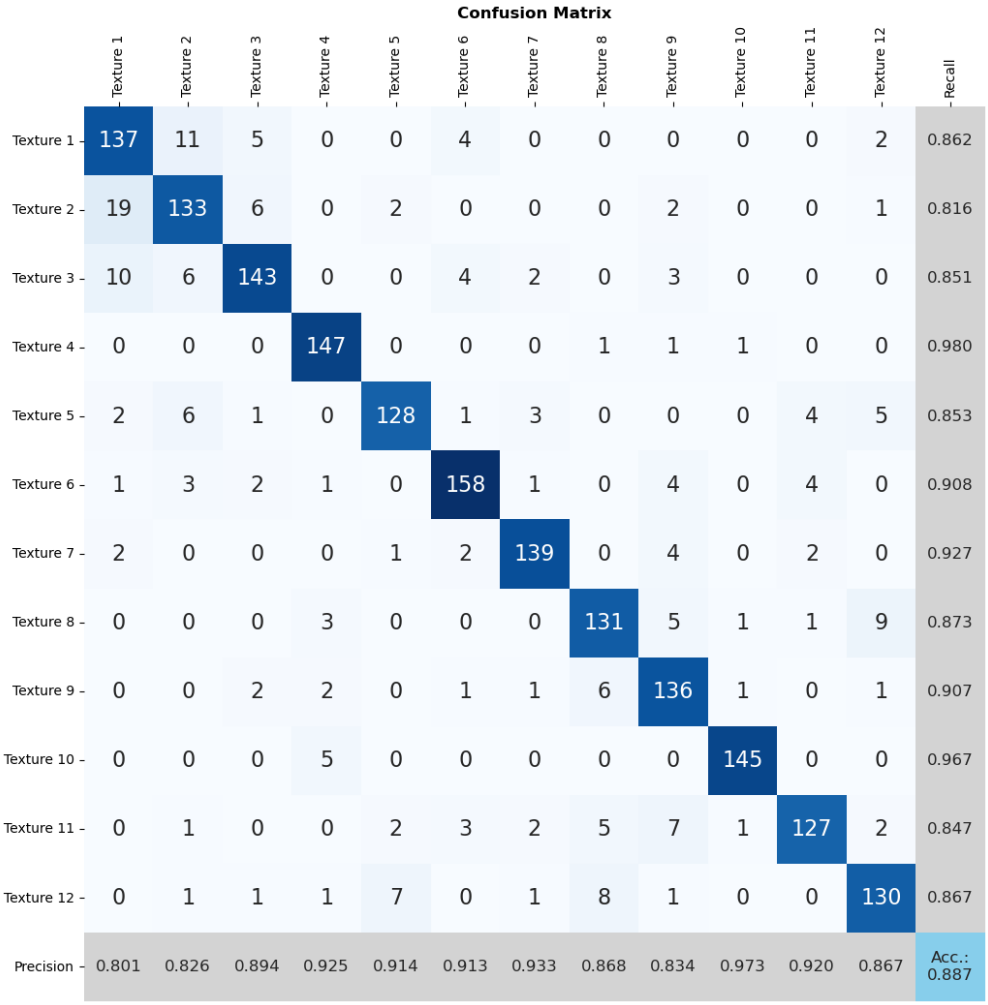

Figure 4.20: Confusion matrix of a BiLSTM classifier for window size of 256

4.2.2.3 Classification for Window Size of 512

1D Convolutional Neural Network Classifier:

Figure 3.13 illustrates this model, which employs a 1D Convolutional Neural Network (CNN) architecture for multi-class classification of tactile texture data. The design is tailored to adeptly capture and process temporal features from the input data, crucial for precise differentiation between various texture classes. Incorporating MaxPooling, Dropout, and BatchNormalization layers enhances its capability to effectively learn and generalize patterns.

The model exhibited strong performance across all validation folds, demonstrating robust metrics for precision, recall, and F1 score derived from an aggregated confusion matrix. It achieved an overall accuracy of 96.4%, showcasing its proficiency in classifying diverse tactile textures with precision of 96.6%, recall of 96.4%, and F1 scores at 96.5%.

Visual insights provided by Figure 4.21 reveal dynamic learning curves and accuracy trends observed during both training and validation phases, highlighting the model's consistent improvement and stability over time.

Figure 4.22 complements these findings with a comprehensive confusion matrix tailored to the validation dataset. This visualization underscores the model's effectiveness in distinguishing between various texture classes, supplemented by detailed precision and recall metrics for each class. As is evident in this figure, the lowest precision is observed for texture 2 at 84.5%, while the highest precision is achieved for textures 9 and 10, both at 100%. For recall, the lowest is recorded for texture 3 at 92%, with the highest recall found for textures 7 and 4, both at 100%. These insights collectively affirm the model's robust classification performance across tactile textures.

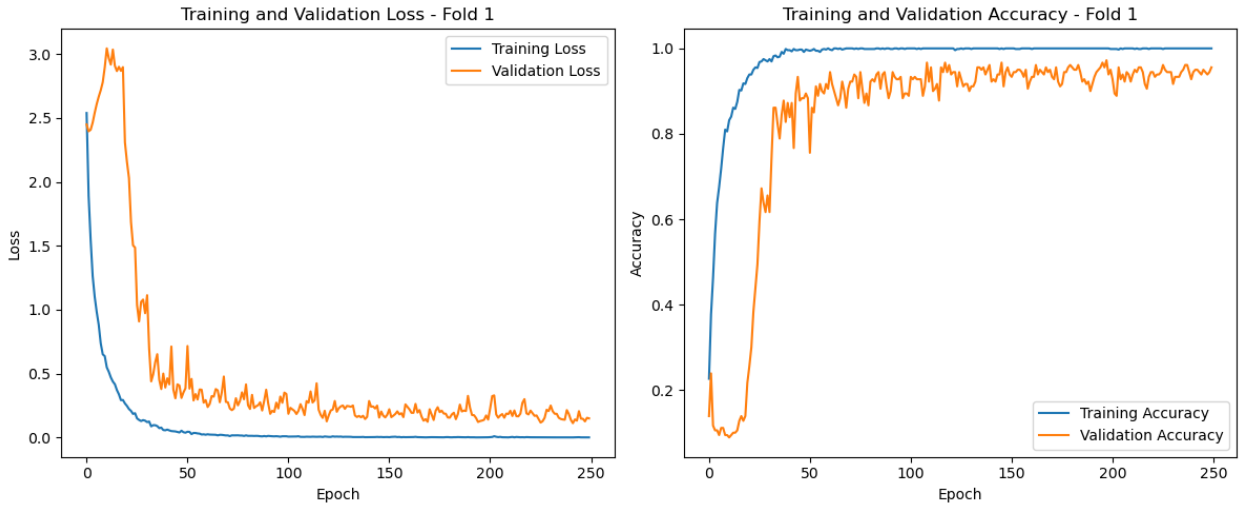

Figure 4.21: Learning and accuracy curves of a 1D CNN classifier for window size of 512

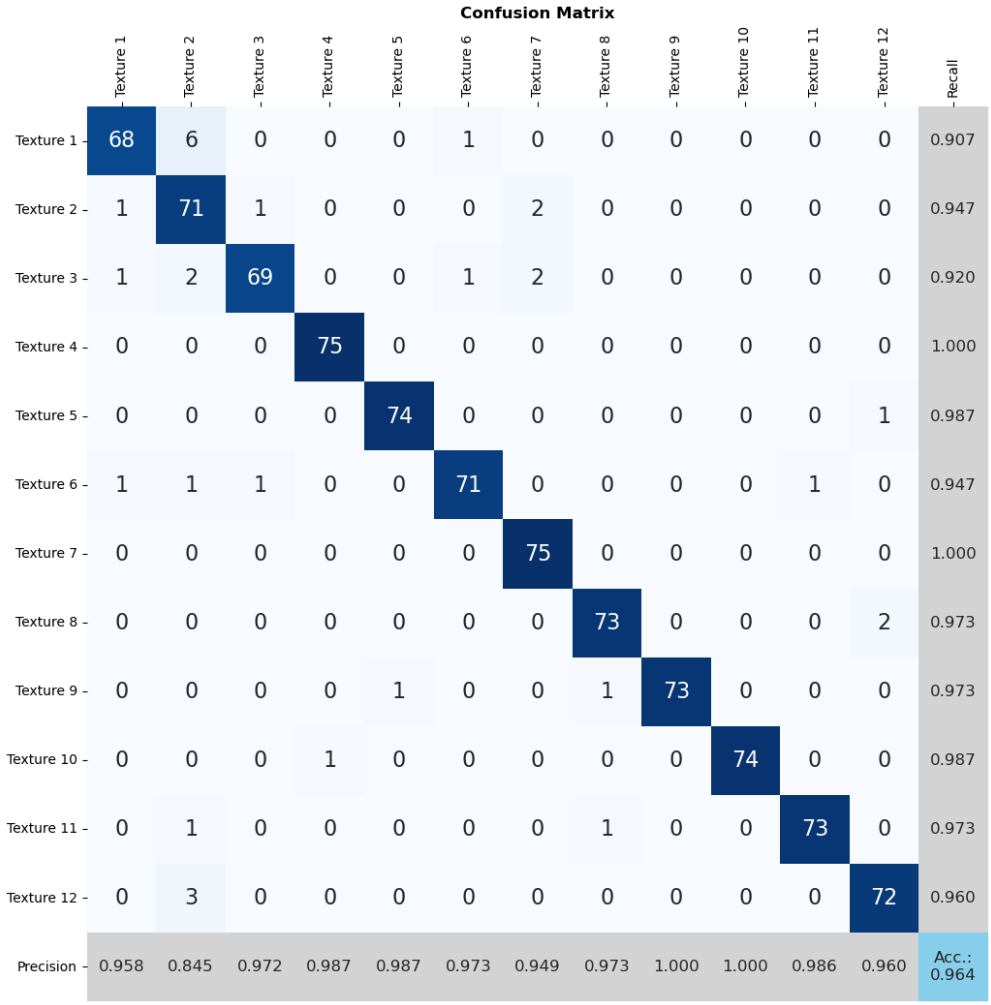

Figure 4.22: Confusion matrix of a 1D CNN classifier for window size of 512

Convolutional-Bidirectional LSTM Classifier:

Figure 3.10 illustrates this model, which utilizes a hybrid architecture combining 1D Convolutional Neural Networks (CNN) with Bidirectional Long Short-Term Memory (BiLSTM) networks for multi-class texture classification. This approach synergistically leverages CNNs for spatial feature extraction and BiLSTMs for capturing temporal dependencies in the input data. The incorporation of Dropout, BatchNormalization, and MaxPooling layers enhances its ability to effectively process and classify complex patterns.

The model gracefully excelled across all validation folds, revealing its prowess in intricate tactile texture classification. With an overall validation accuracy soaring at 91.1%, it confidently navigated the nuances of each texture class, achieving precision, recall, and an F1 score of 91.2%, 91.2%, and 91.2%, respectively.

In the saga of training and validation, Figure 4.23 unveils the model's evolution—its learning curves tracing a tale of perseverance and growth, weaving through epochs with unwavering stability and progress.

Meanwhile, in Figure 4.24, the narrative shifts to a visual symphony of the model's discernment. Each pixel of the confusion matrix paints a portrait of its ability to untangle the threads of texture classification, with precision and recall metrics adorning each class, illuminating the model's keen eye for detail and accuracy. As is evident in this figure, the lowest precision is observed for texture 8 at 82.5%, while the highest precision is achieved for texture 10 at 98.6%. For recall, the lowest is recorded for texture 11 at 80%, with the highest recall found for texture 10 and texture 4 at 97.3%.

Together, these visual epics encapsulate the model's journey—its triumphs etched in accuracy metrics and visualized through the artistry of learning curves and confusion matrices.

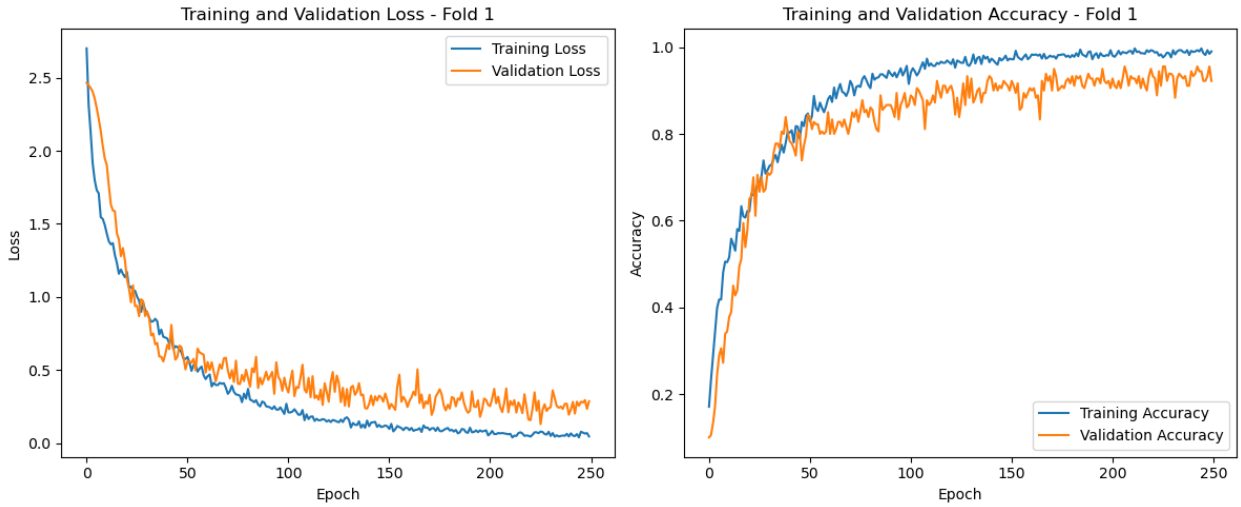

Figure 4.23: Learning and accuracy curves of a Convolutional-Bidirectional LSTM classifier for window size of 512

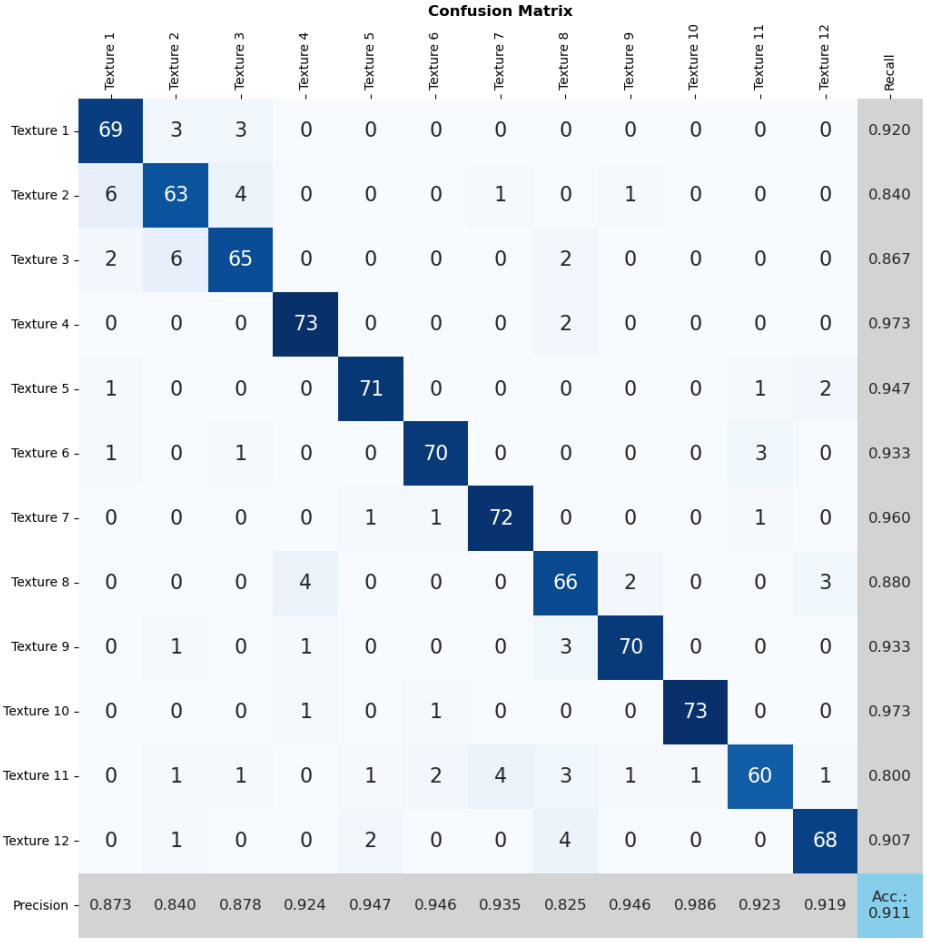

Figure 4.24: Confusion matrix of a Convolutional-Bidirectional LSTM classifier for window size of 512

Bidirectional LSTM Classifier:

This model employs a Bidirectional Long Short-Term Memory (BiLSTM) architecture for texture classification. Bidirectional LSTMs effectively capture dependencies in both forward and backward directions in sequential data. The inclusion of Dropout and Batch Normalization layers enhances the model's robustness and stability, as depicted in Figure 3.15.

The model demonstrated exceptional performance across all validation folds, showcasing its capability in intricate tactile texture classification. Achieving an overall validation accuracy of 89.0%, it effectively navigated the complexities of each texture class with precision, recall, and an F1 score of 89.1%, 89.0%, and 89.0%, respectively

During the training and validation phases, Figure 4.25 provides insights into the model's progression—an evolution depicted through its learning curves, marking steady growth and stability across epochs.

Figure 4.26, on the other hand, visually represents the model's discernment capabilities through a comprehensive confusion matrix. This matrix illustrates the model's proficiency in distinguishing between various texture classes, with each cell providing insights into the model's classification accuracy. Complementing this, precision and recall metrics for each class are highlighted, offering a detailed view of the model's performance.

As evident in this figure, the lowest precision is observed for texture 8, with a value of 82.3%, while the highest precision is achieved for texture 10 at 98.6%. When examining recall, texture 11 shows the lowest value at 80%, whereas texture 7 attains the highest recall of 97.3%. These figures provide a nuanced understanding of the model's strengths and limitations, demonstrating its robust overall performance while also pinpointing specific areas where the model excels or could be further refined.

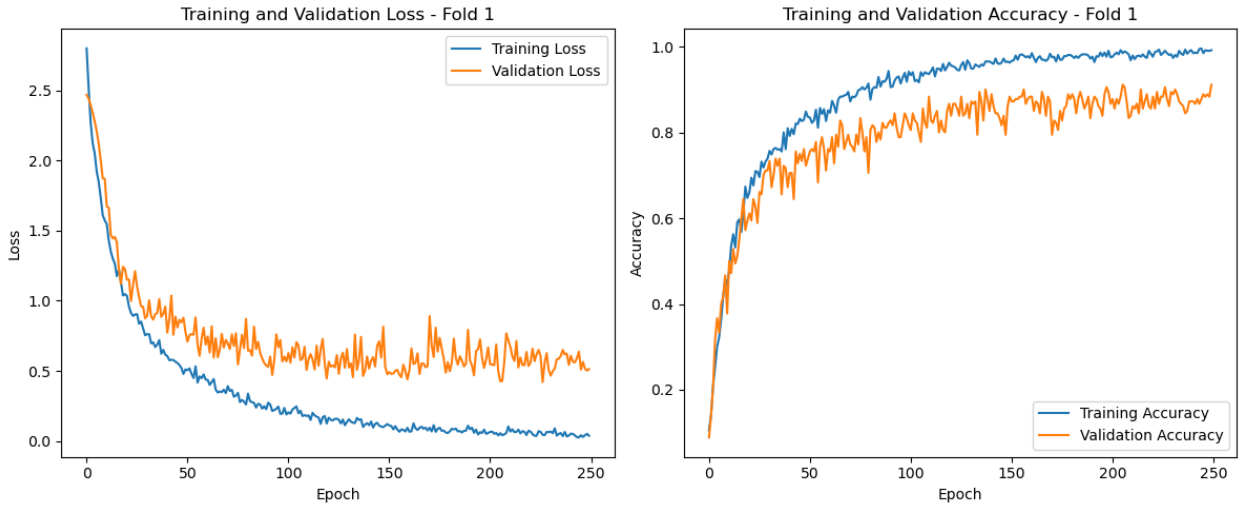

Figure 4.25: Learning and accuracy curves of a BiLSTM classifier for window size of 512

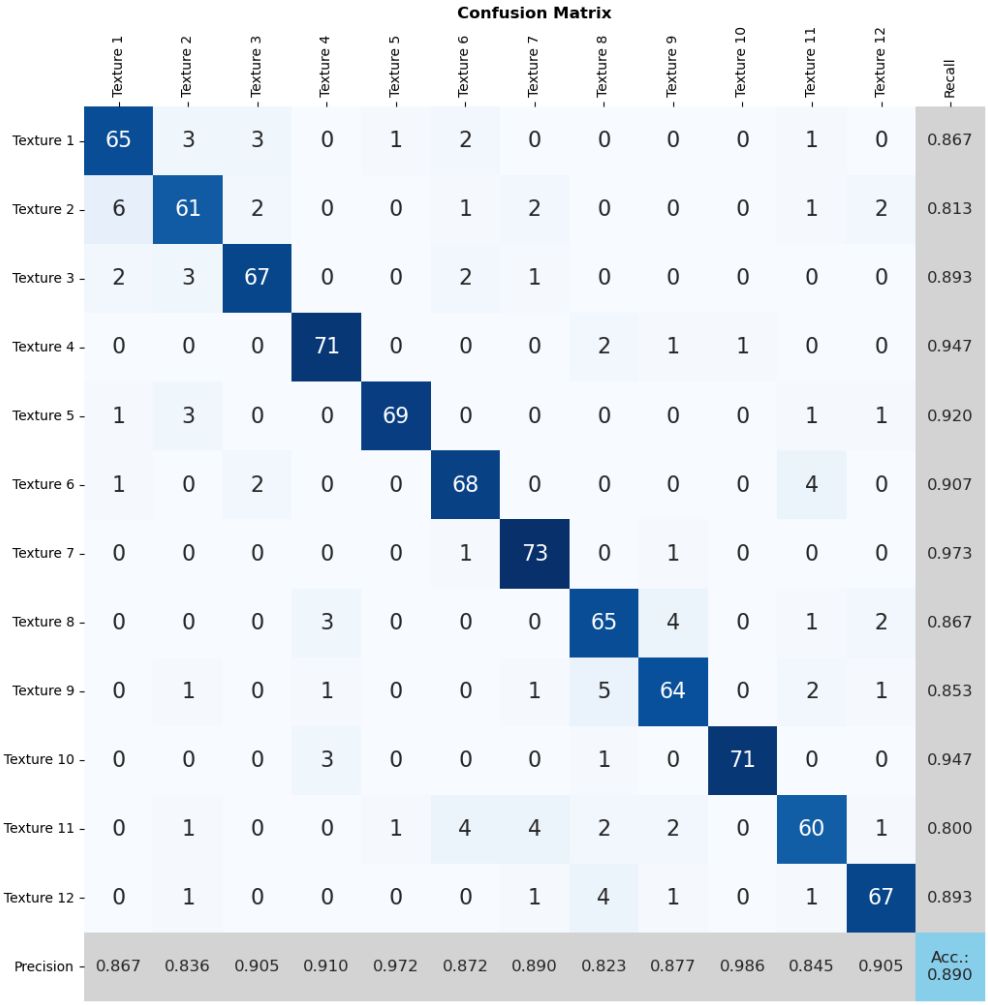

Figure 4.26: Confusion matrix of a BiLSTM classifier for window size of 512

In our study, we evaluated the performance of three different models—CNN, BiLSTM, and a hybrid CNN & BiLSTM model—across three distinct window sizes for tactile texture classification on uneven surfaces. The validation accuracy results demonstrate that the CNN model generally performs best across the different window sizes, achieving a peak validation accuracy of 96.4% with a window size of 512. The hybrid CNN & BiLSTM model exhibited its strongest performance with a validation accuracy of 95.6% using a window size of 128, whereas the BiLSTM model showed the highest accuracy of 90.4% with a window size of 128.

Specifically, for the window size of 256, the CNN model achieved a validation accuracy of 93.0%, outperforming the hybrid CNN & BiLSTM model with 92.5% and the BiLSTM model with 88.7%. For the window size of 512, the CNN model achieved the highest accuracy at 96.4%, followed by the hybrid CNN & BiLSTM model at 91.1% and the BiLSTM model at 89.0%. These findings underscore the effectiveness of the CNN model in handling the classification task across different window sizes, with the hybrid model also demonstrating competitive performance (see Table 4.3).

Given the absence of existing literature on tactile texture classification for uneven surfaces, we could not benchmark our results against other studies. Therefore, while our findings highlight the efficacy of the models employed, further research and comparative analysis would be valuable for contextualizing these results within the broader scope of tactile texture classification advancements.

Chapter 5

Conclusion

In this thesis, we have made significant strides in advancing tactile perception in robotics, with a specific emphasis on texture recognition on uneven surfaces through deep learning techniques. This research addresses critical gaps in the existing literature, particularly the challenges associated with collecting and processing tactile data on uneven surfaces—an area that has been largely overlooked.

To address these challenges, we developed and implemented a comprehensive strategy for tactile data collection, which was rigorously tested in both simulated and real-world environments to ensure robustness and reliability. Our approach includes a novel method for blind surface reconstruction, aimed at enhancing the collection of tactile data along pathways on uneven surfaces. Additionally, we introduced a robust texture classification method for uneven surfaces by integrating kinematic data from a robotic manipulator with an IMU sensor. Through a series of controlled experiments, our methodologies demonstrated effective tactile texture classification across twelve different textures printed on curved surfaces

The first main achievement was the development of a novel approach for blind surface reconstruction on uneven surfaces. This approach enables robotic systems to acquire tactile data from surfaces where traditional vision-based methods might fail. The reconstruction process is achieved by collecting contact points, along with their corresponding position and normal vectors, as the robot explores the surface. These points act as waypoints for generating exploratory trajectories, ensuring comprehensive coverage and data collection.

This method facilitates tactile data acquisition on complex surfaces, a task that has not been fully explored in previous research.

The second major accomplishment was the validation of this approach through the design of a simulation environment that closely mirrors real-world conditions. This simulation was crucial for testing and refining strategies before deploying them in a physical robot, providing significant advantages in terms of cost, safety, and time efficiency. The absence of similar simulation tools in the existing literature highlights the novelty and importance of this work, setting a new standard for tactile sensing research.

The third key advancement was the establishment of the first tactile texture dataset specifically for uneven surfaces. While previous studies have focused predominantly on even surfaces, this work pioneers the creation of a dataset that captures the complexities of uneven textures. The dataset was generated using a combination of MARG (Magnetic, Angular-Rate, Gravity) and barometer sensors, providing a rich set of features for subsequent analysis. A meticulous preprocessing pipeline, involving sliding windows and MinMax scaling, was employed to ensure the data was ready for machine learning applications. The sliding window method segments the dataset into overlapping windows, facilitating multi-scale analysis while efficiently managing computational resources. Furthermore, the sliding window approach mimics human tactile exploration, where textures are discerned through sequential touches, providing a more refined understanding of surface characteristics. This dataset represents a significant resource for future research in tactile texture classification and addresses a previously unexplored area in the field.

The fourth significant result involved conducting texture classification on a separate dataset from even surfaces, sourced from an alternative study. This approach enabled us to evaluate and compare the performance of our classification models on both surface types separately. We applied several deep learning models, including 1D Convolutional Neural Networks (CNNs), Bidirectional Long Short-Term Memory (BiLSTM) networks, and a hybrid of these architectures, to analyze time-series data for texture classification. For uneven

surfaces, our models achieved an average accuracy, precision, and recall of 92.3%, 92.4%, and 92.3%, respectively. In comparison, for even surfaces, the metrics improved substantially, with average values of 96.9%, 97.0%, and 97.0%, respectively. This demonstrates the efficacy of our approach and the advantages of using advanced deep learning techniques for accurate texture classification across different surface types.

For even surfaces, we conducted a comparison with the work of [90], which utilized an active learning (AL) approach. Our models consistently outperformed their results. Specifically, our best model, the BiLSTM, achieved a validation accuracy of 98.6% and an F1 score of 98.7% for the 3-second window, compared to their best F1 score of 84.2% using AL. Similarly, for the 6-second window, our BiLSTM model reached a validation accuracy and F1 score of 99.6%, significantly surpassing their best F1 score of 90.3%. These findings demonstrate that not only our top-performing models but also all our models delivered superior performance compared to their best results, underscoring the robustness and effectiveness of our approach.

Several challenges were encountered during trajectory execution. The manipulator's limitation of four degrees of freedom restricted its ability to follow the orientation markers in all directions, necessitating a straightforward pathway for experimental validation. Additionally, the sensory module risked getting stuck in surface gaps during exploratory movement, spectacularly due to the relatively large radius of the sensor's circular part and its adhesive material. To mitigate this, the trajectory was performed using the sensor's edge, ensuring a smoother and safer operation that prevented damage to both the manipulator and the sensor. To address these challenges, simulated environments were utilized to ensure reliable surface reconstruction and trajectory planning before real-world deployment. This preliminary validation in a controlled setting facilitated the development of robust methods for surface exploration.

Future research should explore several avenues to enhance tactile texture classification and robotic perception. Employing manipulators with additional degrees of freedom could

significantly improve access to all surface points during trajectory execution, allowing for more comprehensive data collection, particularly in complex environments. Additionally, smaller tactile modules could be incorporated to facilitate exploration of intricate concavities and finer surface features, providing a more detailed understanding of diverse textures.

To advance the field further, expanding the dataset by including a broader range of textures and increasing the number of trajectories per texture would yield a larger sample size for each texture class, ultimately enhancing the robustness and accuracy of classification models. Moreover, incorporating a variety of uneven surface geometries, beyond the single concave-convex shape used in the current study, would enable the development of datasets applicable to both texture and shape recognition tasks. This would make the data more versatile and representative of real-world scenarios.

Focusing on the most impactful features among the ten different sensor dimensions is another critical area for future research. By identifying and prioritizing these features, the performance of texture classification models could be optimized for greater efficiency and effectiveness. Additionally, experimenting with alternative models and surface reconstruction methodologies for uneven surfaces could lead to new insights and improved performance. Training on various model architectures, such as advanced neural networks or hybrid approaches, would further refine classification accuracy and adaptability.

n conclusion, this thesis presents a novel methodology for tactile texture classification, with a focus on uneven surfaces. This research marks a significant advancement in the field, introducing innovative techniques for analyzing and understanding complex surface textures. The findings hold great promise for improving robotic navigation and interaction in diverse environments. Additionally, the dataset developed in this study could serve as a valuable resource for further research, providing a foundation for future advancements. Building upon this work, future efforts could pave the way for more sophisticated and efficient robotic systems, further enhancing their tactile perception capabilities.

Bibliography

[1] Félix Ingrand and Malik Ghallab. "Deliberation for autonomous robots: A survey". In: *Artificial Intelligence* 247 (2017), pp. 10–44.

[2] Debasmita Mukherjee et al. "A survey of robot learning strategies for human-robot collaboration in industrial settings". In: *Robotics and Computer-Integrated Manufacturing* 73 (2022), p. 102231.

[3] Sandra Robla-Gómez et al. "Working together: A review on safe human-robot collaboration in industrial environments". In: *Ieee Access* 5 (2017), pp. 26754–26773.

[4] Weidong Li et al. "Safe human–robot collaboration for industrial settings: a survey". In: *Journal of Intelligent Manufacturing* (2023), pp. 1–27.

[5] Yutaka Yamamoto et al. "Optical sensing for robot perception and localization". In: *IEEE Workshop on Advanced Robotics and its Social Impacts, 2005.* IEEE. 2005, pp. 14–17.

[6] Hengyu Guo et al. "A highly sensitive, self-powered triboelectric auditory sensor for social robotics and hearing aids". In: *Science robotics* 3.20 (2018), eaat2516.

[7] Huaping Liu, Fuchun Sun, et al. *Robotic tactile perception and understanding*. Springer, 2018.

[8] Ziwei Xia et al. "A review on sensory perception for dexterous robotic manipulation". In: *International Journal of Advanced Robotic Systems* 19.2 (2022), p. 17298806221095974.

[9] Shan Luo et al. "Robotic tactile perception of object properties: A review". In: *Mechatronics* 48 (2017), pp. 54–67.

[10] Sida Yang et al. "Multi-source vision perception for human-robot collaboration in manufacturing". In: *2018 ieee 15th international conference on networking, sensing and control (icnsc)*. IEEE. 2018, pp. 1–6.

[11] Shiyao Huang and Hao Wu. "Texture recognition based on perception data from a bionic tactile sensor". In: *Sensors* 21.15 (2021), p. 5224.

[12] Bin Fang et al. "A dual-modal vision-based tactile sensor for robotic hand grasping". In: *2018 IEEE International Conference on Robotics and Automation (ICRA)*. IEEE. 2018, pp. 4740–4745.

[13] Timo Markert et al. “Fingertip 6-axis force/torque sensing for texture recognition in robotic manipulation”. In: *2021 26th IEEE International Conference on Emerging Technologies and Factory Automation (ETFA)*. IEEE. 2021, pp. 1–8.

[14] Mike Lambeta et al. “Digit: A novel design for a low-cost compact high-resolution tactile sensor with application to in-hand manipulation”. In: *IEEE Robotics and Automation Letters* 5.3 (2020), pp. 3838–3845.

[15] Jung-Hwan Yang, Seong-Yong Kim, and Soo-Chul Lim. “Effects of sensing tactile arrays, shear force, and proprioception of robot on texture recognition”. In: *Sensors* 23.6 (2023), p. 3201.

[16] Samuel Rispal, Axay K Rana, and Vincent Duchaine. “Textures recognition through tactile exploration for robotic applications”. In: *2017 3rd International Conference on Control, Automation and Robotics (ICCAR)*. IEEE. 2017, pp. 121–128.

[17] Haoran Zheng et al. “DotView: A low-cost compact tactile sensor for pressure, shear, and torsion estimation”. In: *IEEE Robotics and Automation Letters* 8.2 (2023), pp. 880–887.

[18] Daehwan Choi et al. “A highly sensitive tactile sensor using a pyramid-plug structure for detecting pressure, shear force, and torsion”. In: *Advanced Materials Technologies* 4.3 (2019), p. 1800284.

[19] Thiago Eustaquio Alves De Oliveira, Ana-Maria Cretu, and Emil M Petriu. “Multimodal bio-inspired tactile sensing module”. In: *IEEE Sensors Journal* 17.11 (2017), pp. 3231–3243.

[20] Peter Kampmann and Frank Kirchner. “Integration of fiber-optic sensor arrays into a multi-modal tactile sensor processing system for robotic end-effectors”. In: *sensors* 14.4 (2014), pp. 6854–6876.

[21] Pinhas Ben-Tzvi and Paul Moubarak. “A Mechatronic Perspective on Robotic Arms and End-Effectors”. In: *Edited by Ganesh R. Naik* (2011), p. 1.

[22] Shengshun Duan, Qiongfeng Shi, and Jun Wu. “Multimodal Sensors and ML-Based Data Fusion for Advanced Robots”. In: *Advanced Intelligent Systems* 4.12 (2022), p. 2200213.

[23] Pengwen Xiong et al. “A novel tactile sensor with multimodal vision and tactile units for multifunctional robot interaction”. In: *Robotica* (2024), pp. 1–16.

[24] Thiago Eustaquio Alves de Oliveira et al. “Tactile profile classification using a multimodal MEMs-based sensing module”. In: *Proceedings*. Vol. 1. 2. MDPI. 2016, p. 27.

[25] Thiago Eustaquio Alves de Oliveira et al. "Data-driven analysis of kinaesthetic and tactile information for shape classification". In: *2015 IEEE International Conference on Computational Intelligence and Virtual Environments for Measurement Systems and Applications (CIVEMSA)*. IEEE. 2015, pp. 1–5.

[26] Ana-Maria Cretu et al. "Computational intelligence and mechatronics solutions for robotic tactile object recognition". In: *2015 IEEE 9th international symposium on intelligent signal processing (WISP) proceedings*. IEEE. 2015, pp. 1–6.

[27] Thomas Thurner et al. "Tactile sensor solution with MEMS pressure sensors in industrial robotics". In: *e & i Elektrotechnik und Informationstechnik* 140.6 (2023), pp. 541–550.

[28] Allison M Okamura, Maja J Matarić, and Henrik I Christensen. "Medical and healthcare robotics". In: *IEEE Robotics & Automation Magazine* 17.3 (2010), pp. 26–37.

[29] Bruno Monteiro Rocha Lima et al. "Heart rate detection using a multimodal tactile sensor and a z-score based peak detection algorithm". In: *CMBES proceedings* 42 (2019).

[30] Bruno Monteiro Rocha Lima et al. "Heart Rate Detection Using a Miniaturized Multimodal Tactile Sensor". In: *2019 IEEE International Symposium on Medical Measurements and Applications (MeMeA)*. 2019, pp. 1–6. DOI: 10.1109/MeMeA.2019.8802209.

[31] Markus Fritzsche, Norbert Elkmann, and Erik Schulenburg. "Tactile sensing: A key technology for safe physical human robot interaction". In: *Proceedings of the 6th International Conference on Human-robot Interaction*. 2011, pp. 139–140.

[32] Thiago Eustaquio Alves de Oliveira, Ana-Maria Cretu, and Emil M Petriu. "Multimodal bio-inspired tactile sensing module for surface characterization". In: *Sensors* 17.6 (2017), p. 1187.

[33] Ravinder S Dahiya and Maurizio Valle. *Robotic tactile sensing: technologies and system*. Vol. 1. Springer, 2013.

[34] Li Sun et al. "Recognising the clothing categories from free-configuration using gaussian-process-based interactive perception". In: *2016 IEEE international conference on robotics and automation (ICRA)*. IEEE. 2016, pp. 2464–2470.

[35] Wenzhen Yuan et al. "Connecting look and feel: Associating the visual and tactile properties of physical materials". In: *Proceedings of the IEEE conference on computer vision and pattern recognition*. 2017, pp. 5580–5588.

[36] Wentuo Yang et al. "Multifunctional soft robotic finger based on a nanoscale flexible temperature–pressure tactile sensor for material recognition". In: *ACS Applied Materials & Interfaces* 13.46 (2021), pp. 55756–55765.

[37] Snehal Dikhale et al. "Visuotactile 6d pose estimation of an in-hand object using vision and tactile sensor data". In: *IEEE Robotics and Automation Letters* 7.2 (2022), pp. 2148–2155.

[38] Guozhen Li and Rong Zhu. "A multisensory tactile system for robotic hands to recognize objects". In: *Advanced Materials Technologies* 4.11 (2019), p. 1900602.

[39] Naoto Komeno and Takamitsu Matsubara. "Tactile perception based on injected vibration in soft sensor". In: *IEEE Robotics and Automation Letters* 6.3 (2021), pp. 5365–5372.

[40] Rebecca P Khurshid et al. "Effects of grip-force, contact, and acceleration feedback on a teleoperated pick-and-place task". In: *IEEE transactions on haptics* 10.1 (2016), pp. 40–53.

[41] Angelica I Aviles et al. "Towards retrieving force feedback in robotic-assisted surgery: A supervised neuro-recurrent-vision approach". In: *IEEE transactions on haptics* 10.3 (2016), pp. 431–443.

[42] Maurizio Maisto et al. "Evaluation of wearable haptic systems for the fingers in augmented reality applications". In: *IEEE transactions on haptics* 10.4 (2017), pp. 511–522.

[43] Siyuan Dong et al. "Tactile-rl for insertion: Generalization to objects of unknown geometry". In: *2021 IEEE International Conference on Robotics and Automation (ICRA)*. IEEE. 2021, pp. 6437–6443.

[44] Viral Rasik Galaiya et al. "Exploring Tactile Temporal Features for Object Pose Estimation during Robotic Manipulation". In: *Sensors* 23.9 (2023). ISSN: 1424-8220. DOI: 10.3390/s23094535. URL: https://www.mdpi.com/1424-8220/23/9/4535.

[45] Vinicius Prado da Fonseca, Thiago Eustaquio Alves de Oliveira, and Emil M. Petriu. "Estimating the Orientation of Objects from Tactile Sensing Data Using Machine Learning Methods and Visual Frames of Reference". In: *Sensors* 19.10 (2019). ISSN: 1424-8220. DOI: 10.3390/s19102285. URL: https://www.mdpi.com/1424-8220/19/10/2285.

[46] Susan J Lederman and Roberta L Klatzky. "Hand movements: A window into haptic object recognition". In: *Cognitive psychology* 19.3 (1987), pp. 342–368.

[47] Vinicius Prado da Fonseca et al. “Tactile object recognition in early phases of grasping using underactuated robotic hands”. In: *Intelligent Service Robotics* 15.4 (2022), pp. 513–525.

[48] Qiang Li et al. “A review of tactile information: Perception and action through touch”. In: *IEEE Transactions on Robotics* 36.6 (2020), pp. 1619–1634.

[49] Francois R Hogan et al. “Tactile regrasp: Grasp adjustments via simulated tactile transformations”. In: *2018 IEEE/RSJ International Conference on Intelligent Robots and Systems (IROS)*. IEEE. 2018, pp. 2963–2970.

[50] Yevgen Chebotar et al. “Self-supervised regrasping using spatio-temporal tactile features and reinforcement learning”. In: *2016 IEEE/RSJ International Conference on Intelligent Robots and Systems (IROS)*. IEEE. 2016, pp. 1960–1966.

[51] Herke Van Hoof et al. “Stable reinforcement learning with autoencoders for tactile and visual data”. In: *2016 IEEE/RSJ international conference on intelligent robots and systems (IROS)*. IEEE. 2016, pp. 3928–3934.

[52] Nathan F Lepora et al. “From pixels to percepts: Highly robust edge perception and contour following using deep learning and an optical biomimetic tactile sensor”. In: *IEEE Robotics and Automation Letters* 4.2 (2019), pp. 2101–2107.

[53] Vinicius Prado da Fonseca et al. “In-Hand Telemanipulation Using a Robotic Hand and Biology-Inspired Haptic Sensing”. In: *2019 IEEE International Symposium on Medical Measurements and Applications (MeMeA)*. 2019, pp. 1–6. DOI: 10.1109/MeMeA.2019.8802139.

[54] Jeffrey Mahler et al. “Dex-net 2.0: Deep learning to plan robust grasps with synthetic point clouds and analytic grasp metrics”. In: *arXiv preprint arXiv:1703.09312* (2017).

[55] Hongzhuo Liang et al. “Pointnetgpd: Detecting grasp configurations from point sets”. In: *2019 International Conference on Robotics and Automation (ICRA)*. IEEE. 2019, pp. 3629–3635.

[56] Xinchen Yan et al. “Learning 6-dof grasping interaction via deep 3d geometry-aware representations”. In: *Proceedings of IEEE International Conference on Robotics and Automation (ICRA 2018)*. 2018.

[57] Naveen Kuppuswamy et al. “Fast model-based contact patch and pose estimation for highly deformable dense-geometry tactile sensors”. In: *IEEE Robotics and Automation Letters* 5.2 (2019), pp. 1811–1818.

[58] Marco Costanzo, Giuseppe De Maria, and Ciro Natale. "Dual-arm in-hand manipulation with parallel grippers using tactile feedback". In: *2021 20th International Conference on Advanced Robotics (ICAR)*. IEEE. 2021, pp. 942–947.

[59] GertWillem Romer et al. "Alternative grippers for the assistive robotic manipulator (ARM)". In: *9th International Conference on Rehabilitation Robotics, 2005. ICORR 2005.* IEEE. 2005, pp. 473–476.

[60] Raunaq Bhirangi et al. "All the Feels: A dexterous hand with large-area tactile sensing". In: *IEEE Robotics and Automation Letters* (2023).

[61] Haruhisa Kawasaki, Tsuneo Komatsu, and Kazunao Uchiyama. "Dexterous anthropomorphic robot hand with distributed tactile sensor: Gifu hand II". In: *IEEE/ASME transactions on mechatronics* 7.3 (2002), pp. 296–303.

[62] Kuo Liu et al. "Dexterous robotic hand with humanoid finger structure and large coverage tactile sensing ability for Human-Robot Interactions". In: *2022 IEEE International Conference on Robotics and Biomimetics (ROBIO)*. IEEE. 2022, pp. 531–536.

[63] Josie Hughes et al. "Soft manipulators and grippers: A review". In: *Frontiers in Robotics and AI* 3 (2016), p. 69.

[64] Dhruba Jyoti Sut and Prabhu Sethuramalingam. "Soft Manipulator for Soft Robotic Applications: a Review". In: *Journal of Intelligent & Robotic Systems* 108.1 (2023), p. 10.

[65] Seunghun Jeon et al. "Learning whole-body manipulation for quadrupedal robot". In: *IEEE Robotics and Automation Letters* 9.1 (2023), pp. 699–706.

[66] Yamin Li, Yong Wang, and Dianhong Wang. "Multiple RGB-D sensor-based 3-D reconstruction and localization of indoor environment for mini MAV". In: *Computers & Electrical Engineering* 70 (2018), pp. 509–524.

[67] Wenqiang Xu et al. "Visual-tactile sensing for in-hand object reconstruction". In: *Proceedings of the IEEE/CVF Conference on Computer Vision and Pattern Recognition*. 2023, pp. 8803–8812.

[68] Xie Zongwu, Zhu Zhaojie, and Liu Yechao. "3-D Object Reconstruction Using Tactile Sensing for Multi-fingered Hand". In: *2018 10th International Conference on Intelligent Human-Machine Systems and Cybernetics (IHMSC)*. Vol. 1. IEEE. 2018, pp. 209–212.

[69] Junyuan Lu, Zeyu Wan, and Yu Zhang. "Tac2Structure: Object Surface Reconstruction Only Through Multi Times Touch". In: *IEEE Robotics and Automation Letters* 8.3 (2023), pp. 1391–1398.

[70] Sebastian Schramm et al. “Combining modern 3D reconstruction and thermal imaging: Generation of large-scale 3D thermograms in real-time”. In: *Quantitative InfraRed Thermography Journal* 19.5 (2022), pp. 295–311.

[71] Martin Meier et al. “A probabilistic approach to tactile shape reconstruction”. In: *IEEE Transactions on Robotics* 27.3 (2011), pp. 630–635.

[72] Luiz C. S. Ramos et al. “Haptic Bio-Inspired Sensor Calibration For Surface Reconstruction”. In: *IECON 2019 - 45th Annual Conference of the IEEE Industrial Electronics Society*. Vol. 1. 2019, pp. 663–668. DOI: 10.1109/IECON.2019.8927545.

[73] Thiago Eustaquio Alves de Oliveira et al. “End-Effector Approach Flexibilization in a Surface Approximation Task Using a Bioinspired Tactile Sensing Module”. In: *2019 IEEE International Symposium on Robotic and Sensors Environments (ROSE)*. 2019, pp. 1–6. DOI: 10.1109/ROSE.2019.8790433.

[74] Laurent Y. E. Ramos Cheret, Vinicius Prado Da Fonseca, and Thiago E. Alves de Oliveira. “Leveraging Compliant Tactile Perception for Haptic Blind Surface Reconstruction”. In: *2024 IEEE International Conference on Robotics and Automation (ICRA)*. 2024, pp. 17139–17145. DOI: 10.1109/ICRA57147.2024.10610162.

[75] Rajat Sharma et al. “Point cloud upsampling and normal estimation using deep learning for robust surface reconstruction”. In: *arXiv preprint arXiv:2102.13391* (2021).

[76] Youngji Kim, Jinyong Jeong, and Ayoung Kim. “Stereo camera localization in 3d lidar maps”. In: *2018 IEEE/RSJ International Conference on Intelligent Robots and Systems (IROS)*. IEEE. 2018, pp. 1–9.

[77] Miaohui Wang, Wuyuan Xie, and Maolin Cui. “Surface reconstruction with unconnected normal maps: An efficient mesh-based approach”. In: *Proceedings of the 28th ACM International Conference on Multimedia*. 2020, pp. 2617–2625.

[78] David Bonneau, Paul-Mark DiFrancesco, and D Jean Hutchinson. “Surface reconstruction for three-dimensional rockfall volumetric analysis”. In: *ISPRS International Journal of Geo-Information* 8.12 (2019), p. 548.

[79] Mateusz Michalkiewicz et al. “Implicit surface representations as layers in neural networks”. In: *Proceedings of the IEEE/CVF International Conference on Computer Vision*. 2019, pp. 4743–4752.

[80] Anis Farshian et al. “Deep-Learning-Based 3-D Surface Reconstruction—A Survey”. In: *Proceedings of the IEEE* (2023).

[81] Edward Smith et al. “Active 3D shape reconstruction from vision and touch”. In: *Advances in Neural Information Processing Systems* 34 (2021), pp. 16064–16078.

[82] Thiago Eustaquio Alves de Oliveira, Ana-Maria Cretu, and Emil M. Petriu. "Multimodal Bio-Inspired Tactile Sensing Module". In: *IEEE Sensors Journal* 17.11 (2017), pp. 3231–3243. DOI: 10.1109/JSEN.2017.2690898.

[83] Mauro Comi et al. "Snap-it, Tap-it, Splat-it: Tactile-Informed 3D Gaussian Splatting for Reconstructing Challenging Surfaces". In: *arXiv preprint arXiv:2403.20275* (2024).

[84] Bruno Monteiro Rocha Lima et al. "Dynamic Tactile Exploration for Texture Classification using a Miniaturized Multi-modal Tactile Sensor and Machine Learning". In: *2020 IEEE International Systems Conference (SysCon)*. 2020, pp. 1–7. DOI: 10.1109/SysCon47679.2020.9275871.

[85] Bruno Monteiro Rocha Lima, Thiago Eustaquio Alves de Oliveira, and Vinicius Prado da Fonseca. "Classification of Textures using a Tactile-Enabled Finger in Dynamic Exploration Tasks". In: *2021 IEEE Sensors*. 2021, pp. 1–4. DOI: 10.1109/SENSORS47087.2021.9639755.

[86] Liguo Qin et al. "Fingerprint-inspired biomimetic tactile sensors for the surface texture recognition". In: *Sensors and Actuators A: Physical* 371 (2024), p. 115275.

[87] Juan M Gandarias, Alfonso J Garcia-Cerezo, and Jesus M Gomez-de Gabriel. "CNN-based methods for object recognition with high-resolution tactile sensors". In: *IEEE Sensors Journal* 19.16 (2019), pp. 6872–6882.

[88] Ujjawal Dixit et al. "Texture classification using convolutional neural network optimized with whale optimization algorithm". In: *SN Applied Sciences* 1.6 (2019), p. 655.

[89] Ozan Özdenizci et al. "EEG-based texture roughness classification in active tactile exploration with invariant representation learning networks". In: *Biomedical signal processing and control* 67 (2021), p. 102507.

[90] Shemonto Das, Vinicius Prado da Fonseca, and Amilcar Soares. "Active learning strategies for robotic tactile texture recognition tasks". In: *Frontiers in Robotics and AI* 11 (2024), p. 1281060.

[91] Philip Maus et al. "The Impact of Data Augmentation on Tactile-Based Object Classification Using Deep Learning Approach". In: *IEEE Sensors Journal* 22.14 (2022), pp. 14574–14583.

[92] Robotis. *Robotis Open Manipulator-X*. https://emanual.robotis.com/docs/en/platform/openmanipulator_x/overview/. [Online; accessed 15-July-2024].

[93] Thiago Eustaquio Alves de Oliveira and Vinicius Prado da Fonseca. "BioIn-Tacto: A compliant multi-modal tactile sensing module for robotic tasks". In: *HardwareX* 16 (2023), e00478.

[94] Open Robotics. *Robot Operating System (ROS)*. `https://www.ros.org/`. [Online; accessed 15-July-2024].

[95] PJRC. *Teensy: A Complete USB-based Microcontroller Development System*. `https://www.pjrc.com/teensy/`. [Online; accessed 15-July-2024].

[96] Bruno Monteiro Rocha Lima et al. "A multimodal tactile dataset for dynamic texture classification". In: *Data in Brief* 50 (2023), p. 109590.

[97] Shemonto Das. "An Active Learning Framework with a Class Balancing Strategy for Time Series Classification". In: *arXiv preprint arXiv:2405.12122* (2024).